MONTHLY NOTICES

OF THE

ROYAL ASTRONOMICAL SOCIETY.

VOL. LXXXI. JUNE 10, 1921. No. 8

Professor A. S. EDDINGTON, F.R.S., PRESIDENT, in the Chair.

Edward Osborne Fountain, B.A., M.D., Crossley House, Ruislip, Uxbridge,

was balloted for and duly elected a Fellow of the Society.

Antonio Abetti, Professor of Astronomy and Director of the Arcetri Observatory, Florence;

Heber D. Curtis, Director of the Allegheny Observatory, University of Pittsburgh, Pennsylvania, U.S.A.;

Ejnar Hertzsprung, Chief Assistant, Observatory, Leiden, Holland; and

Georges Lecointe, Director of the Royal Observatory of Belgium, Uccle, Belgium,

were balloted for and duly elected Associates of the Society.

The following candidates were proposed for election as Fellows of the Society, the names of the proposers from personal knowledge being appended:—

Capt. Dudley S. A. Cosby, D.L. for Queen's County, Stradbally Hall, Queen's County, Ireland (proposed by G. P. B. Hallowes);

Christopher Clive Langton Gregory, M.A., D.I.C., Chief Assistant, Helwan Observatory, "Melville," Parkstone, Dorset (proposed by J. H. Reynolds); and

Ernest W. F. Keevil, Broomfield, Abbots Langley, Herts (proposed by A. E. Conrady).

Sixty-four presents were announced as having been received since the last Meeting, including, amongst others:—

Salomons (Sir David L.): Breguet (1747–1823), presented by the author.

Seasonal Changes occurring in certain Lunar Craters.
By William H. Pickering, Assoc.R.A.S. (Plates 12, 13.)

The craters that we shall consider here are Conon, Aristillus, and Eratosthenes. They are all situated near the centre of the moon's disk, and are therefore not subject to librational change. The changes that we shall investigate are mainly of the size, shape, and position of both bright and dark markings. Changes of brightness and of darkness have also been recorded. The bright markings we shall refer to simply as snow, making no distinctions as to possible fog or frost.

In fig. 1 are shown four drawings of Conon and the region to the north-east of it. Conon measures 13 by 15 miles in diameter. Under each drawing is given the date, the age of the moon, the corresponding colongitude, and the quality of the seeing on the Standard Scale, where for an 11-inch aperture 12 is perfect. Conon is shown at the top, and just to the east of it in the first drawing we see a crooked line of patches of snow lying along the crest of the ridge of Bradley. In the second drawing three of these patches have united; in the third they have begun to melt, and in the fourth have almost completely disappeared, but farther to the east a conspicuous patch of snow has formed. At colongitude 20° a small bright patch of snow always appears near the centre of the region represented in the drawings. The next night, as shown in the first drawing, three others have appeared one after the other to the left of it. These soon unite to form a bright patch, widest at first at the right, later at the left. The right-hand end then begins to disappear, breaking up into separate patches. These changes occur with very considerable uniformity at the same colongitude, lunation after lunation.

Fig. 2 shows two drawings of Conon on a somewhat larger scale. On the first at colongitude 20° a rill is seen crossing the floor. On it are situated two craterlets, shown to be such, since their interior shadows are on the left, as is the case with Conon itself. The next night the lower or more northerly craterlet has enlarged very slightly, and the shadow has shifted to the right-hand side, indicating thereby that the hollow has changed to a mound. This mound rapidly enlarges, and in the second drawing is seen to have reached the centre of the rim of the crater. Immediately to the south of it a dark patch or "plat" has developed, whose duration is unusually short, barely exceeding a day. We can hardly doubt that this enlarged white area is simply a cloud or fog upon the crater floor.

Fig. 1.

1920 Jan. 30, 10^d, $34^\circ 8$, 12. | 1919 Oct. 6, 13^d, $64^\circ 0$. | 1920 Feb. 5, 16^d, $107^\circ 7$, 8. | 1920 Feb. 10, 21^d, $171^\circ 2$, 8, 11.

CONON.

Fig. 2.

1920 Mar. 28, 9^d, $19^\circ 8$, 12. | 1920 Feb. 2, 13^d, $69^\circ 6$, 8.

CONON.

Fig. 3.

27°. | 52°.

ARISTILLUS.

Digitized by the Internet Archive
in 2026

https://archive.org/details/monthly-notices-of-the-royal-astronomical-society_1921-06-10_81_8

Fig. 4.

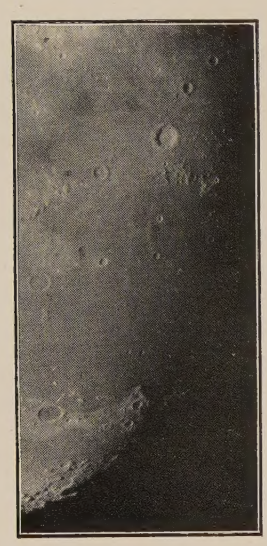

Fig. 5.

20°. 70°.

110°. 150°.

ERATOSTHENES.

In fig. 3 are shown two drawings of Aristillus—the first at colongitude 27°, the second at 52°. These are exactly as they were drawn at the telescope, and have not been smoothed down or finished at all. The diameter of this crater is 34 miles. In the north-west sector on the wall are shown two narrow divergent canals or "runs," quite close together within the crater rim, but farther apart outside. At only four observatories has it been possible hitherto to separate the inner sections—Jamaica, Lowell, Mount Wilson, and at M. Jarry-Desloges' Observatory. Observers at other locations are known to have tried unsuccessfully. It will thus be seen that they form a rather delicate test of planetary definition. In the second drawing the runs have broadened and enlarged within the crater rim, and are no longer separable. New and more difficult runs have developed immediately to the north of them, while large dark "fields" are shown farther to the north, which are wholly invisible as such, earlier and later in the lunation. At the extreme north is shown a shallow hexagonal crater whose floor presents no detail at first. At 20° four parallel bright streaks appear upon it. At 52° a network of fine bright lines is shown nearly equi-spaced, and at right angles to one another. Position angles show that their average deviation does not exceed one degree.

Since the divergent runs first mentioned are invisible at both sunrise and sunset on the moon, and are most marked at midday or midsummer, that is to say when the sun is on their meridian, it is quite impossible that they should be cracks. They can therefore only be a surface discoloration of some sort. The northern one is absolutely straight for 12 miles, and then it divides in two. The southern one is also straight for the same distance, except where it crosses the crater rim. When first visible their maximum width is only 300 feet, but in a few days they broaden to 1500, and then later the inner ones unite. The outer fields do not develop until after the divergent runs or canals have formed.

Of the two photographs shown in fig. 4, one represents Copernicus near the terminator, and Eratosthenes slightly to the left and below it. It is there shown located at the end of the chain of the Apennines. In this view the two craters resemble one another so closely, that with a telescope having so small a field of view that only one of them could be seen at a time, an inexperienced observer might readily mistake one for the other. The other photograph was taken at about the time of full moon, when no shadows were visible. Copernicus, it will be noticed, has turned white with snow, and is very brilliant. Eratosthenes, on the other hand, has turned dark in part, from vegetation, and now no longer resembles Copernicus.

Fig. 5 represents four views of Eratosthenes. They were drawn at colongitudes 20°, 70°, 110°, and 150°. The rim of the crater is in all cases represented by a dotted line, and two of the central peaks by small dotted circles. In the lower right-hand quadrant, filling a considerable portion of the floor, may be traced

the darkened figure of what vaguely resembles an inverted bird, with its wings spread, flying away from the central peaks. The head and beak are conspicuous. I have adopted this name merely for convenience of description. In the second view, taken four days later, the bird has changed into something resembling a fox or squirrel. In the third view it has changed into a diamond-shaped figure with a long handle. In the fourth it resembles a letter N, the handle having mostly vanished. These figures are repeated at every lunation with but slight change. Thus the diamond is sometimes replaced by a pentagon. The fox also is liable to some variation.

Full moon always occurs at colongitude $90° \pm 7°$. From then until the sun reaches the meridian of the crater, or until 101°, shadows are impossible. This marking is visible throughout this interval, and therefore cannot be due to shadows. Moreover, between 70° and 110° any shadow would be very narrow, and clearly incompetent to produce the broad dark areas shown in the second and third views. Indeed, quite apart from the impossibility of their being caused by shadows, it is difficult to conceive, given the change in the direction of the light, what conformation of the ground could give the changes noted in these four views.

Other changes are also observed outside of the upper portion of the crater rim. The large dark formation shown in the second view I have called the crab. The changes visible along the crater rim during the interval occurring between the times when it and the first view was taken can be better seen in the drawings than described. This line is supposed to form the inside boundary of the claws of the crab. As the lunation progresses the head appears to advance down the inner wall of the crater, and the claws curve inward. This is well shown in fig. 6, which was drawn at about the time of full moon. The central peak is shown at P. The question at once arose, When the curvature appears, do the head H and the claw C really advance towards the central peak, or does the arm A retreat from it? Micrometric measurements showed that all three features were in motion down hill, the arm outside of the rim, the head and claw inside of it. The maximum distance travelled by the head and claw was 3 miles, and by the arm 2.

We now come to the runs or canals. These are well shown in the upper portions of the four views in fig. 5. Several plats or lakes are also shown in the same region in the first, second, and last views. In general these are not identical with one another. We may compare the apparent size of these formations with those visible on the planet Mars, if we consider that at an average apparition the apparent size of the planet is about half the diameter of the crater. The runs change materially in the course of the lunation, and while some of them can always be counted on to appear at their proper time, others seem to be very unreliable.

Two of the most conspicuous ones have been named Cross and Main. They are well shown in the second view of fig. 5. Each

measures about 6 miles or 5″ in length by 1″ in width. The former leaves the southern claw of the crab in a nearly perpendicular direction, passing immediately through a large but rather faint plat. The latter lies next to the southern arm and is parallel to it. These two runs can be recognised in all four of the views. While in the third one their inclination to one another is seen to be about 60°, in the first and last it is found to be nearer 90°. This was confirmed in many sketches, but it was impossible to determine certainly from them which run shifted. Position angles were then secured with regard to the azimuth of the moon's axis, and the results are shown in fig. 7, where the abscissæ give the colongitude and approximate age of the moon, and the ordinates, the azimuths. The heavy vertical

Fig. 6.

line indicates the colongitude where the sun crosses the meridian of the crater, that is its noon, or midsummer. The broken lines indicate the results for different lunations, each line being marked with the initial of the corresponding month.

It will be seen at once from the figure that the azimuth of Cross varies but little, remaining throughout the duration of the observations at about 130°. Main, on the other hand, starts at azimuth 50°, following the upper line, or lunation of 1919 October. It drops gradually until colongitude 90°, then suddenly for 10° more, to a minimum at 100°, after which it slowly rises to the end of the lunation. In other words, the run swings back and forth something like a pendulum. We further notice that the sudden drop begins in 1920 February as far back as colongitude 70°, so that the swing varies distinctly during different lunations, the season being appreciably more advanced during the latter month. It will be seen that observations on three successive nights

between colongitudes 64° and 90° indicate that the October results cannot be far wrong. Observations on three successive nights between colongitude 83° and 106° confirm the February results. Moreover, it is impossible that an error of 20° in position angle should be made in the case of a clearly defined narrow dark marking 5″ in length.

During the sudden drop the position angle changes by 14° in the course of twenty-four hours, or more than 1° in two hours. This implied that the change could be detected during a long

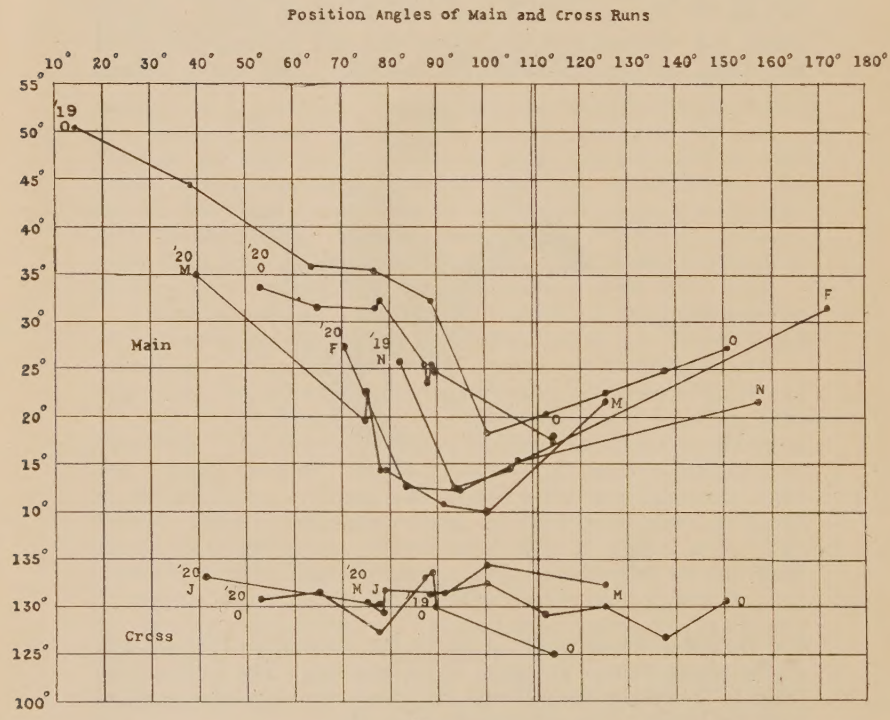

Fig. 7.

watch on a single night, and in March 1920, as shown in the figure, four observations made within seven hours actually showed a drop of about 7°. We can thus actually watch the effect of life, if such it is, as it slowly moves across the surface of the moon.

In studying the varying azimuths of this run the question naturally arose as to which end was stationary and which end moved. The answer was readily given by the micrometer. The south-western end moves first, away from the central peaks, at first slowly and later more rapidly, until the minimum azimuth is reached. Then the north-eastern end begins to move in the same direction, thus increasing the azimuth. As a whole the run moves

up hill, and in the opposite direction to which a shadow would travel, supposing that a dark marking visible at full moon could be due to a shadow. That is to say the dark run moves towards the setting sun.

The maximum linear speed observed is 132 feet per hour, and the run travels through a distance slightly exceeding its own width. It thus appears that the lunar runs, like the canals on Mars, slowly shift over the surface. Since this surface discoloration changes its place it cannot be mineral, and it consequently appears that the most reasonable explanation is that life exists upon both planets. In beginning this investigation it had been hoped that it would lead to some satisfactory explanation of many of the smaller canals on Mars, but on the contrary it appears hitherto only to have added to our difficulties. What might be possible on the moon appears very improbable in the case of Mars, and *vice versa*. This very fact, however, only adds to its interest. We find here a living world, lying at our very doors, whose life is wholly unlike anything found upon our own planet,—a world which the astronomical profession in general, for the last fifty years, has utterly and systematically neglected and ignored.

Finally, it must be pointed out that in this paper stress is laid on the facts, not on the explanation of them. Also that all explanations appear improbable, but it is believed that that of vegetation is less so than any other that has heretofore been suggested.

1921 *May* 13.

The Spectrum of φ Cassiopeiæ in Relation to those of α Cygni and γ Cygni. By Major William J. S. Lockyer, M.A., Ph.D., and D. L. Edwards, A.R.C.S., D.I.C. (Plate 14.)

In the "Catalogue of 470 of the Brighter Stars," published by Sir Norman Lockyer in 1902, the spectrum of only one star, namely, η Leonis, was found to resemble the spectrum of α Cygni (A2*p*), which may be regarded as typical of the giant A stars. More recent work at the Norman Lockyer Observatory, at which 1150 more spectra have been secured, has resulted in the finding of only three more stars of this type, namely, μ Orionis, 13 Monocerotis, and 9 Persei. It seems probable that this dearth of A to F stars of ascending temperature may be due to the comparatively short time taken by stars to pass through this stage of their evolution, so that it is of great importance to obtain as much detailed information as possible regarding the spectra of the few stars about this type which are available. This class of star is also characteristic of novæ in the earlier stages of their careers, so that any type of spectrum which resembles the α Cygni type, especially if it is slightly higher or lower in temperature, may prove useful for comparison with novæ.

During the routine work at this observatory of photographing and classifying stellar spectra, the spectrum of ϕ Cassiopeiæ (R.A. $1^h\ 13^m{\cdot}8$, Dec. $+57^\circ\ 42'$ mag. 5·25, class F5*p*) was secured, and this was found to approximate to that of α Cygni, but with certain marked differences indicating a lower stage of temperature or ionisation. In fact, the spectrum of this star could be well placed at an intermediate position between α Cygni (A2*p*) and γ Cygni (F8*p*) (also a giant and of lower temperature than α Cygni), thus placing it in the class Fo according to the Harvard notation.

The wave-lengths, intensities, and origins of the lines in the spectra of α Cygni and γ Cygni have been published in full by Lockyer and Baxandall in an earlier publication * entitled "The Spectrum of γ Cygni," so no useful purpose would be served by repeating these and presenting a comparison table of wave-lengths and intensities of ϕ Cassiopeiæ.

It is therefore considered sufficient to describe the main differences between these stars. A general idea of the changes in the intensities of the individual lines can be gathered from the accompanying plate showing the three types of spectra (Plate 14, Nos. 1–4). The photographs in this plate were taken with the McClean telescope, which consists of a Grubb 12-inch refractor having an objective prism of 12 inches aperture and 20° angle, the scale of the spectra being 21·4 mm. between H_β and H_δ.

Chief Differences between α Cygni and ϕ Cassiopeiæ.

The most striking difference which is observed in passing from the spectrum of α Cygni to that of ϕ Cassiopeiæ is a general strengthening of the enhanced lines of titanium. This strengthening is very pronounced, and practically all the more important of the Ti^+ lines (*e.g.* λλ4572·2, 4468·7, 4374·9, 4367·9) are affected. The Si^+ double at λλ4128·1, 4131·1 also appears to be slightly strengthened. This is probably due in part to the presence of the iron lines at λλ4128·0 and 4132·2, which occur very close to the Si^+ pair; but there is little doubt that the silicium lines are present and nearly as strong as in α Cygni. The presence of the above mentioned iron lines is rendered more probable by the fact that several other iron lines are slightly strengthened—notably those at λλ4046·0, 4063·8, and 4071·9. This strengthening, however, is not so pronounced as in the case of the Ti^+ lines and is by no means general, the majority of the Fe lines being unaffected. The hydrogen lines are very slightly weaker in ϕ Cassiopeiæ, and the lines of Mg^+ (λ4481) and Fe^+ (*e g.* λ4233) are decidedly weaker. Sr^+ (λλ4078, 4215), however, together with the arc lines of iron, calcium, scandium, and nickel, are found to be slightly strengthened in the spectrum of ϕ Cassiopeiæ, while helium and Si^+III are apparently absent.

* *Phil. Trans. R.S.*, ser. A, 201, 205–222.

Chief Differences between ϕ Cassiopeiæ and γ Cygni.

In passing from the spectrum of ϕ Cassiopeiæ to that of γ Cygni, the chief change observed is a very considerable strengthening of the arc lines of iron. A very large proportion of all the lines which were noted as being "stronger" or "very much stronger" in γ Cygni were identified as iron lines, most of the remainder being due to Ti^+. The Si^+ lines, which were very strong both in α Cygni and ϕ Cassiopeiæ, have practically disappeared in γ Cygni. Among the less prominent changes which were observed may be mentioned a weakening of the lines of H, Mg^+, Fe^+, and Sr^+, and a strengthening in the case of the arc lines of calcium, nickel, and scandium.

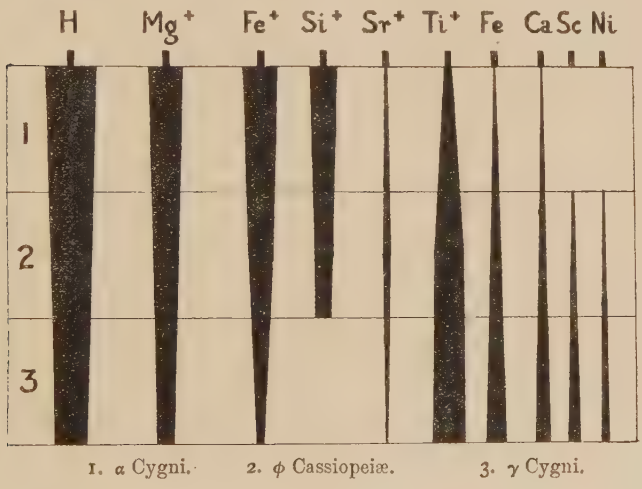

FIG. 1.

An examination of fig. 1 shows diagrammatically the sequences of changes which hydrogen and some of the enhanced-metallic and metallic elements pass through as indicated by the relative width of the spectral lines. The first four elements on the left become more pronounced as the temperature rises from γ to α Cygni, and the last five on the right behave in an opposite manner. Sr^+ shows its maximum in the ϕ Cassiopeiæ stage.

The differences between the spectra of α and γ Cygni which have been obtained are almost entirely in harmony with the conclusions drawn by Lockyer and Baxandall, namely, that "the present detailed investigation of the γ Cygni spectrum confirms this result (viz. the enhanced lines of the various metals attained a maximum intensity at varying levels of the stellar temperature sequence), the enhanced lines of strontium, scandium, and titanium being at their strongest in γ Cygni and much stronger than in α Cygni, while in the latter spectrum the enhanced

lines of iron, chromium, and magnesium attain their maximum intensity."

In this investigation the Cr^+ lines seem to be of about the same intensities in all three spectra, and while some of these lines suggest an increase of intensity from γ to α Cygni, others indicate a decrease. The peculiarity of the spectrum of ϕ Cassiopeiæ is that not only does it endorse the changes in the intensities of the lines of the metals and ionised-metals as one passes from γ Cygni to α Cygni, but it presents a stage where the lines of Sr^+ are at their maximum intensity.

To find out if there were any other stars the spectra of which approximated to ϕ Cassiopeiæ more than to α or γ Cygni, an examination was made of all the stellar spectra which had been secured at this observatory. Search was also made among the valuable series of original negatives of stellar spectra taken by the late Frank McClean, F.R.S. The result of this was that the following stars were found to be almost exact replicas of ϕ Cassiopeiæ:—

TABLE I.

Star.	1900. R.A.	1900. Dec.	Mag.	Spectral Type. Harv. Revd.	Henry Draper.	Adams and Joy. Mt. Wilson.	Abs. Vis. Mag.
	h m	° ′					
ϕ Cassiopeiæ	1 13·8	+57 42	5·25	G	F5*p*		
ϵ Aurigæ	4 54·8	+43 40	3·4–4·1	F5*p*	F5*p*	F5*p*	+1·0
α Leporis	5 28·3	−17 54	2·69	F	Fo	F4*p*	−1·5
α Carinæ	6 21·7	−52 38	0·86	F	Fo		
θ Scorpii	17 30·1	−42 56	2·04	F			
ι Scorpii	17 40·6	−40 5	3·14	F5*p*			
34 Draconis	17 56·9	+72 1	5·54	F	...	F4	
45 Draconis	18 30·9	+56 58	4·95	F8*p*			

The columns under the general heading "Spectral Type" give the classifications of the spectra according to *Harvard College Annals*, vol. **50** (Harvard Revised); *Harvard College Annals*, vols. **91–94** (Henry Draper); and *The Astrophysical Journal*, vol. **53** (Adams and Joy, Mount Wilson).

Three of the stars in the above list (viz. ϵ Aurigæ, ϕ Cassiopeiæ, and ι Scorpii) are classed as "peculiar" by the Harvard observers, and in the notes which are appended it is remarked in each case that the lines are very narrow, and in their intensities resemble those of δ Canis Majoris. The spectrum of the latter star, however, appears to resemble more closely that of γ Cygni. The greater prominence of the metallic lines and the weakening of the more characteristic lines of ϕ Cassiopeiæ show that δ Canis Majoris is nearer to the γ Cygni than to the ϕ Cassiopeiæ stage.

The stars in the following table were found to be very similar to ϕ Cassiopeiæ, but showed a larger number of lines typical of

the γ Cygni spectrum. They are therefore probably at a slightly lower temperature, and represent a stage intermediate between γ Cygni and φ Cassiopeiæ. It will be noticed that two Cepheid variables are included in this table. Several negatives of each of these stars have been examined and the spectra found to vary quite appreciably, in some cases being almost identical with φ Cassiopeiæ and in others being more like γ Cygni. It therefore seems probable that the cepheids have a spectrum of the φ Cassiopeiæ type when at maximum brightness, and of the γ Cygni type when at minimum.

TABLE II.

Star	1900. R.A.	1900. Dec.	Mag.	Spectral Type. Harv. Revd.	Henry Draper.	Adams and Joy, Mt. Wilson.	Abs. Vis. Mag.
	h m	° ′					
α Persei	3 17·2	+49 30	1·90	F5	F5	F5	−2·1
ο Leonis	9 35·8	+10 21	3·80	F5*p*	F5 / A3	F4*p*	+1·3
χ Leonis	10 59·9	+ 7 53	4·66	F	Fo	F5	+0·6
89 Herculis	17 51·4	+25 4	5·48	F			
π Sagittarii	19 3·8	−21 11	3·02	F2	...	F4*p*	−0·8
ν Aquilæ	19 21·4	+ 0 9	4·86	A8			
η Aquilæ	19 47·4	+ 0 45	var.	G	...	F9	−2·0
δ Cephei	22 25·4	+57 54	var.	G	...	Go	−0·7

In the last column of the above two tables are given the absolute magnitudes of the stars for which reliable parallaxes are available. It will be noticed that these all lie very closely round a mean absolute magnitude of −0·5, and therefore, according to Professor Russell, should be classed as giants. The distinction in magnitude between giants and dwarfs, according to Russell, begins to be well defined for stars of spectral type below Fo; for F5 stars the average absolute magnitude for giants is 0·0, while for dwarfs it is about +4·0. The Cepheid variables are known from other considerations to be giant stars, so that the evidence which is available from other sources all tends to confirm our spectroscopic evidence for placing these stars among those ascending in temperature.

It will be noticed that the spectra of the stars given in the tables above vary, according to the Harvard classification, from the type Fo to F8*p*, excluding the two stars at the bottom of Table II. This is hardly what might have been expected, since it might reasonably be supposed that stars which, in one system of classification, are grouped together and found to be nearly identical, would at least appear very close together in any other scheme of classification. Such large differences (amounting to nearly a whole division on the Harvard scale) as have been found even among the few stars which have already been examined, are certainly rather

unexpected. The spectra as classified at Mount Wilson, however, seem to be much more consistent. Those for which we have any record are all classed as F4 or F5, so that the Mount Wilson observers are in agreement with us in grouping these stars together.

On the other hand, since the average Harvard classification of stars like φ Cassiopeiæ appears to be about Fo, it would naturally be expected that a great number of Fo stars would fall into this group. Up to the present, however, among all the Fo stars which have been examined, only four have shown sufficient resemblance to φ Cassiopeiæ and α Carinæ to be included in the same group.

In his "Catalogue of 470 of the Brighter Stars," Lockyer published the chief criteria of the spectra of α Cygni and α Ursæ Minoris. As the spectrum of the latter star is similar to γ Cygni, these criteria may be usefully repeated here to compare with those now obtained for the intermediate stage represented by φ Cassiopeiæ.

α Cygni.

Predominant:—H, Ca^+, Mg^+, Fe^+, Si^+II, Ti^+, Cr^+.

Fainter:—Ni^+, SiI, V^+, Mn^+, Sr^+, Fe, He, Si^+III, Ast.

φ Cassiopeiæ.

Predominant:—H, Ca^+, Ti^+, Mg^+, Fe^+, Si^+II, Ca, Cr^+.

Fainter:—Fe, Mn. Other ionised-metals and metals.

α Ursæ Minoris.

Predominant:—Ca^+, Ti^+, H, Mg^+, Fe^+; are lines of Ca, Fe, Mn, SiI.

Fainter:—The other ionised-metals and metals occurring in α Canis Majoris.

Chief Differences between φ Cassiopeiæ and Stars of Descending Temperature.

Spectroscopic distinctions between stars at the same temperature level (*i.e.* having the same general type of spectrum) were first pointed out by Sir Norman Lockyer. The two chief differences lie in the relative fineness of the hydrogen lines and the greater strength of the enhanced lines in stars of rising temperature (giants). These differences are well brought out in the case of φ Cassiopeiæ and corresponding stars of descending temperature (dwarfs). The hydrogen lines in φ Cassiopeiæ and other stars of this group are decidedly sharper than those on the descending side —of which α Canis Minoris may be taken as an example, since it is regarded as "a typical F5 star" on the Harvard system. The enhanced metallic lines are much more pronounced in the

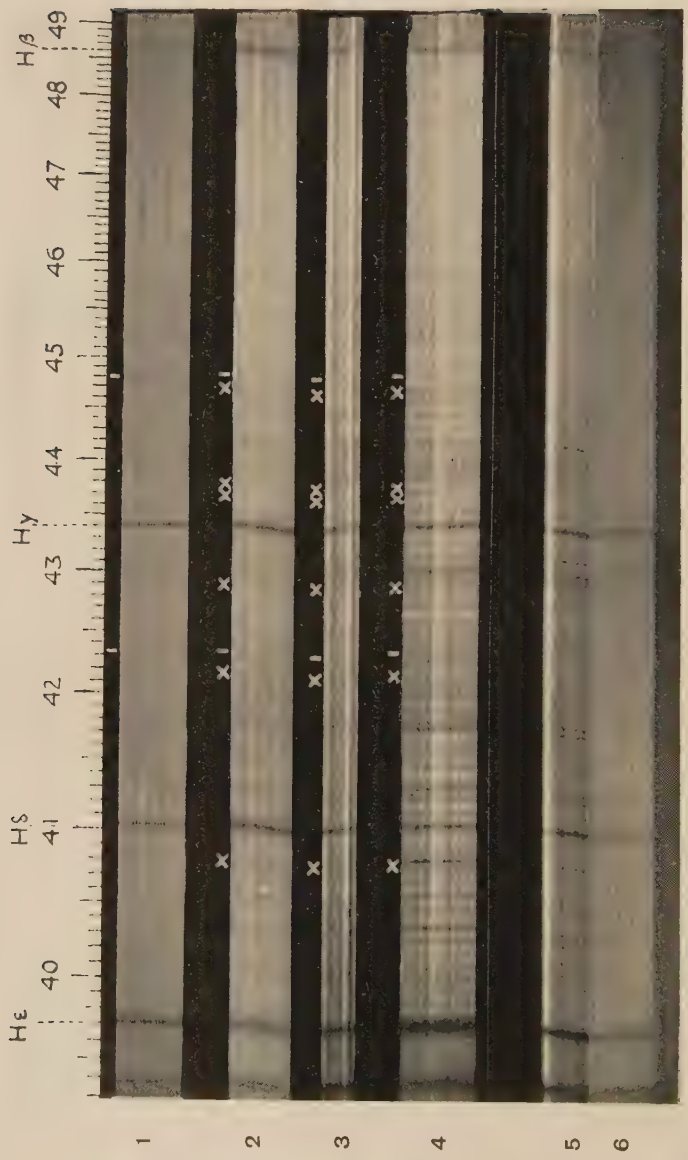

1. 11 Cygni. 2. α Leporis. 3. φ Cassiopeiæ. 4. γ Cygni. 5. ε Aurigæ. (Giant). 6. α Can. Min. (Dwarf).

ϕ Cassiopeiæ group. Among the more conspicuous examples of these may be mentioned the lines of Fe^+ at λλ4233·3, 4178·9, 4173·5, the Sr^+ line at λ4215·7, and the Si^+ double at λλ4128·1, 4131·4. Many other enhanced lines are noticeably stronger in the ϕ Cassiopeiæ group, including the majority of the Ti^+ lines.

Description of Plate 14.

(Enlargements 7 times.)

The photographs (Nos. 1–4) are intended to illustrate the intermediate position of α Leporis (2) and ϕ Cassiopeiæ (3) between the γ Cygni (4) and α Cygni (1) groups.

A few of the more prominent intensity changes in the spectral lines are indicated by white dots and crosses. The short white *lines* denote lines which become stronger, and the white *crosses* lines which become weaker, in passing from γ Cygni to α Cygni respectively.

Photographs Nos. 5 and 6 illustrate the differences between a giant (No. 5, ϵ Aurigæ) and a dwarf star (No. 6, α Canis Minoris).

Further Notes on the Displacements of the Absorption Lines in the Spectrum of Nova Geminorum (2) *in March* 1912. By W. H. Wright, Assoc.R.A.S. (Plates 15, 16.)

In the January number of this Journal I communicated some measures of the hydrogen absorption lines in the spectrum of *Nova Geminorum* (2) which appeared to indicate a departure from the simple rule of proportionality that is usually assumed to express the relation between the displacements of lines in a nova spectrum and their wave-lengths. The paper was published partly as a caution against the unqualified acceptance, at the present time, of the law of proportionality, but principally for the purpose of communicating what were believed to be observations of immediate interest in relation to the interpretation of spectral displacements in the novæ in terms of the Doppler effect, which had been so strongly emphasised in Colonel Stratton's advance notice of the results of his investigation of the spectrum of *Nova Geminorum*. Except for the fulfilment of this major purpose I should not have ventured to appropriate the considerable amount of space required to record the details of the observations.

In a note following mine Colonel Stratton questions the suitability of observations of the hydrogen lines to the purpose of deriving the displacement law, and while he confirms, on one of the dates referred to by me and within the limited range of wave-length available to him, the departure of the displacements from strict proportionality, he finds that on another occasion the proportional law was observed, and he implies, or states, that the

failure of the law on the dates of my observations was due to a broadening, toward the violet, of the lower lines of the hydrogen series.

As the record of a plea for an open view respecting the novæ my paper may be considered to have served its purpose, and I should not in the circumstances seek to continue a discussion which, if prolonged, might take on some of the aspects of a controversy, were it not that silence on my part might be construed as acquiescence in Stratton's views respecting my observations, which would in that case, I think, lose whatever of value attaches to them. As it is, I feel that some effort should be made to remove them from the shadow of his rather adverse criticism, and this note has been prepared for that purpose. Its publication may, however, require justification from another standpoint. Measurements of the spectrum of *Nova Aquilæ* (3) will be available in the future which will undoubtedly afford a better basis for the study of line displacement than is provided by the observations of the star in Gemini or of any other nova, and it might therefore seem useless to devote time and space to the discussion of such observations as these. On the other hand, it will be valuable in future comparative studies to know to just what degree each object contributes to the total of our knowledge. I shall, therefore, without further apology, endeavour to make a little clearer than I appear to have done in my first note the extent of the disturbance (if we agree to call it that) of the hydrogen lines on 1912 March 23.

As a first step it will be necessary to subject Stratton's criticisms to a rather close examination. I may here interpolate the observation that in his comments he suggests a number of sources of error against which an observer of but little experience might be assumed to be on his guard, at least to the extent of recognising them. This will necessitate a longer and more detailed discussion than I should otherwise have thought necessary. Stratton regards as "unfortunate" the basing of conclusions respecting the displacement relation on the hydrogen absorption lines, and part of this note will necessarily be devoted to a consideration of the relative value, for the purpose in view, of these lines in the one case, and of the rest of the absorption lines in the other. In support of his objection to their use Stratton advances a number of arguments which, for systematic discussion, will be quoted separately.

1. That "these lines are parts of very complex bands containing several bright maxima as well as the absorption components. The exact portion of the band which is taken as the absorption line depends in part on the exposure of the plate, and may vary for purely photographic reasons from line to line."

This might be urged with some force against improperly made observations of the lines of absorption II.* which border the

* It should perhaps be pointed out that the notation used by Stratton is different from that adopted in my earlier paper, thus his components II. and III. were referred to by me as I. and II. In the present note Stratton's system will be adopted.

brighter part of the emission bands. As an objection to the III. lines, which serve in effect as the basis of my discussion, it can hardly be seriously entertained, because the wings reaching from the emission bands toward these lines were extremely faint at the times the observations were made. But in what respect are the hydrogen lines of absorption II. inferior for purposes of measurement to any of the other lines of the spectrum? Colonel Stratton's objection could be urged against those of iron and titanium, which are also accompanied by emission bands. The iron emission bands are perhaps brighter with respect to absorption than is the case for hydrogen, while with titanium the reverse is true, and yet, as Stratton has shown, this does not serve in general to introduce a systematic difference between the iron and titanium lines. The inference is that the effect of the emission band on the position of the close dark line is small, and in any event the argument may not be directed at the hydrogen lines to the exclusion of others.

2. "Irradiation from the very bright emission band of Hα would tend to displace the measured δλ of the accompanying absorption towards the violet."

Although this is a particular case of (1) above, it requires especial mention, because the Hα line, on account of its distance from the other members of the series, has great weight in determining the parameters of the equations. This will be appreciated on glancing at the figure on p. 195 of my former note, or fig. 2 of the present one. Stratton has, in his discussion, ignored the measures of this line, presumably for the reason above cited. In view of the description contained in footnote (h) at the bottom of p. 193 of my other note, I am somewhat at a loss to understand

Fig. 1.—Sketch Curve of Intensity for Hα Absorption III. and Emission Band.

his comment, apparently the description was overlooked or misunderstood, and I have therefore prepared, with the aid of a microphotometer, the approximate intensity sketch shown in fig. 1, which is supplementary to that description.* The dark Hα III. is 19 angstroms from the bright edge of the emission band, and the faint wing or extension referred to as reaching toward it is scarcely brighter than the continuous spectrum which borders the violet edge of the dark line. In fact, one must look carefully to see the wing at all. The line is clear and definite

* The sketch does not show the suspected dark band Hα II., bordering the brighter part of the band, whose presence is doubtful.

and, except for the low dispersion in that region, is quite as suitable for measurement as any line in the series. The wave-length is given only to the nearest unit because of the low dispersion, which also serves to render uncertain the width of the line. The measured width is a little over 5 angstroms. I should perhaps state that the plate is correctly exposed and that it is impossible to consider seriously the suggestion that the measured position of the absorption line is affected by irradiation.

I may make the further comment that Colonel Stratton's rejection of Hα is somewhat surprising in view of the fact that he appears to have approved its use for the purpose of establishing the law of direct proportionality. In his discussion of results secured elsewhere than at Cambridge he states: "The greater range of spectrum (up to Hα) available on the Mount Wilson plates confirms the fact that the displacement of dark lines varies directly as the wave-length, λ." *

Now an examination of the observations referred to discloses reference to only three dark lines within the extended range. The first of these, at 5577, has not, so far as I know, been identified; the second, at 5581 (displaced D_1–D_2), does not check with the law of proportionality; and the third is Hα II. the line actually used for the purposes referred to.† I can only interpret the foregoing excerpt as at once an admission that the extended range is necessary to the proof of the law of proportionality, and an acceptance of the competency of the Hα absorption line to supply the proof. It will be recalled that Hα II. borders the brighter part of the band and is therefore much more subject to disturbance by irradiation than Hα III., which lies at a considerable distance. If the former, which is favourable to the law of direct proportionality, is acceptable, it is not clear why the more easily measurable Hα III., which suggests another relation, is not at least equally so.

3. "Further, for the hydrogen series beyond Hη the absorption components of one line are superimposed on the neighbouring radiation bands of hydrogen; the position of the measured absorption lines may be affected by this, especially as the maxima and the absorption lines are not as a rule symmetrical about their centres. We may get an absorption line from one source coinciding with a bright maximum from another; *e.g.* Hκ absorption II. at 3741·0 coincides with maximum II. from Hλ. The sources of these two parts of the spectra are probably separate in the nova. We may have a superposition of bright and dark effects in the spectrum as distinct from ordinary effects of absorption against a continuous background."

We may recall that there is a progressive decrease in the intensity of the hydrogen emission bands, without a corresponding failing in the absorption lines, as we approach the ultra-violet. This is a phenomenon that was first noted in some of the bright-

* *Ann. Solar Phys. Obs.*, **4**, 32.
† *Ap. Jour.*, **36**, 310, 1912.

line stars by Campbell, and has been found to be very generally characteristic of stellar spectra which show both absorptions and emissions. In substantiation of this statement in its relation to the spectrum under discussion I am able to refer to the excellent reproduction of one of the Allegheny spectrograms for the date March 22 in Plate II. of Stratton's *Memoir*. The emission for $H\theta$ is extremely faint, and I think that any influence of the emission bands lying beyond may be regarded as negligible at least in their bearing on the present discussion. But if we admit, for the sake of argument, that these ultra-violet emission bands are present in strength, in what way are the absorption lines that are scattered among them worse off than those of various origins situated in other parts of the spectrum, which are involved with related and unrelated emission bands, notably the lines lying between $H\gamma$ and $H\beta$? In that region we have a tangle of iron, titanium, and other emissions more complex by far than anything in the ultra-violet, which probably affect the positions of the absorption lines involved with them. Is it not justifiable under such circumstances to seek to mitigate the effect of this haphazard displacement by extending the observations over the greatest possible range in wave-length, even though by so doing we may be led into an equally disturbed region? But whatever the validity of the objection under discussion, it is of little consequence, and I am unable to understand why it should have been advanced, since the observations to which it relates are not vital and may be omitted without seriously affecting any of the conclusions. In the diagrams of fig. 2, to be described later, they are entered as broken circles in their positions on the left of the figure, so that they can be disregarded, or not, as the reader chooses.

4. "These separate hydrogen absorptions are themselves sometimes divided by a narrow bright centre."

However that may be, they were not so divided at the time the observations were made. Whether at the later time referred to by Stratton they became physically double, or were divided through double reversal as he suggests, is a matter of interpretation which there is no occasion to discuss here. But if later misbehaviour of a line is to reflect upon evidence given in the days of its good conduct, is the testimony of the hydrogen lines to be regarded as more seriously impaired than that of the others? Whatever the nature of the disturbance, the iron, titanium, and other lines of the spectrum appear from Stratton's description to have been quite as much affected as those of hydrogen. For instance, the splitting of the hydrogen lines into two components "*a*" and "*b*" on March 30 was followed on March 31 and later by the passing of one group of lines (Ti, Sr, Sc) to position "*b*," and the iron lines to "*a*," with occasional interchanges of position. The lines of these other groups were, therefore, obviously more displaced than the mean position of the hydrogen lines. This is, at least, my interpretation of the text of Stratton's *Memoir* on pages 16 and 45, and of Table xxi. Furthermore, the doubling of

the general dark-line spectrum (absorption I.) is regarded by Stratton as possible (*Memoir*, pp. 40, 50, 52). In view of these observations I think we must conclude that, so far as objection (4) is concerned, the danger from disturbance is no greater for the hydrogen lines than for any of the other lines found in the spectrum of the star.

But since the hydrogen lines have been objected to, let us inquire into the competency of the others to establish the nature of the displacement relation. There is a simple way in which conformability of a group of displacements to the relation

$$\Delta\lambda = A\lambda + B\lambda^2$$

can be tested, and that is by platting the displacement factor $\left(\frac{\Delta\lambda}{\lambda}\right)$ against wave-length. Calling this factor κ, we have

$$\kappa = A + B\lambda,$$

which is the equation of a straight line. If the line determined by the plats is horizontal, the law of direct proportionality is established; if it passes through the origin, the law of squares is indicated; if, on the other hand, the direction of the line is indeterminate, the character of the law is equally in doubt.

Fig. 2*b* is a plat of the values of κ derived from observations of H III. published in my previous note. The things to be noted are whether the platted positions are aligned in a definite direction, and, if so, whether the line they determine is horizontal or inclined.

In discussing the data which Colonel Stratton has provided it will be convenient to distinguish between that published in his *Memoir*, and the measurements of the hydrogen series given in his recent note.

Data from Annals of the Solar Physics Observatory, Vol. IV.—Tables 9, 11, and 14 contain the measured positions of numerous stellar lines to which origins are ascribed, and should therefore provide the basis of an inquiry into the displacement law obeyed by the general absorption spectrum. In selecting lines from these tables I have omitted all blends, including those due to the superposition of two spectra. For example, the lines of normal wave-length 4396 and 4415 recorded in Table 14 have not been used.

In fig. 3*a* are platted the displacement factors derived from Table 9 for March 15. Here the displacements are small and the conditions are consequently unfavourable for the determination of a displacement relation. The several marks or characters designate the chemical origins of the lines as explained in the key accompanying the figure. λλ 4924 and 5018, indicated by broken circles, are near the edge of the field and are of small weight. The line OO′ indicates the direction of the origin. If that line were allowable as within the range of possible solutions, it would determine a relation of the form $\Delta\lambda = B\lambda^2$. The line QQ′ represents the quadratic expression suggested for hydrogen on March 23, reduced by a constant factor to suit the scale of these

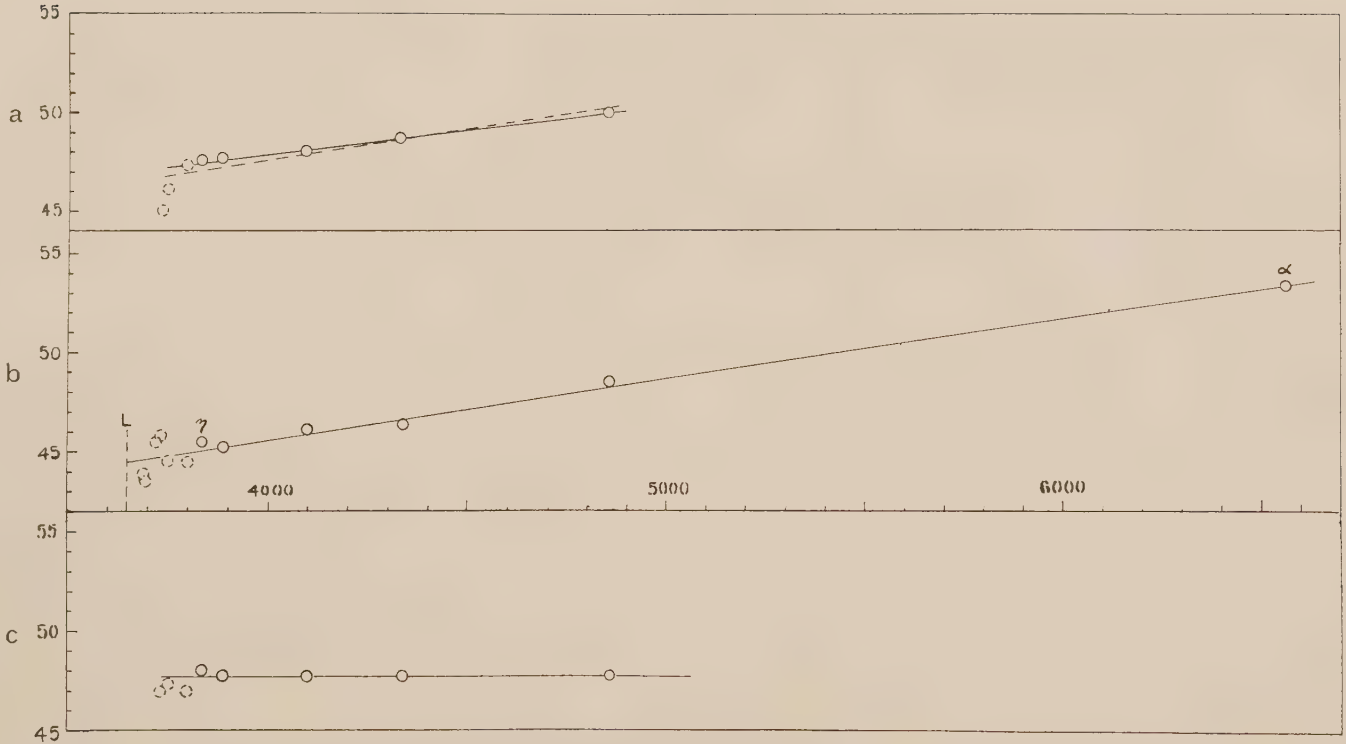

Fig. 2.—Displacement Factors for Hydrogen, 1912 March. a. March 22; b. March 23; c. March 25.
L Indicates the Limit of the Balmer Series.

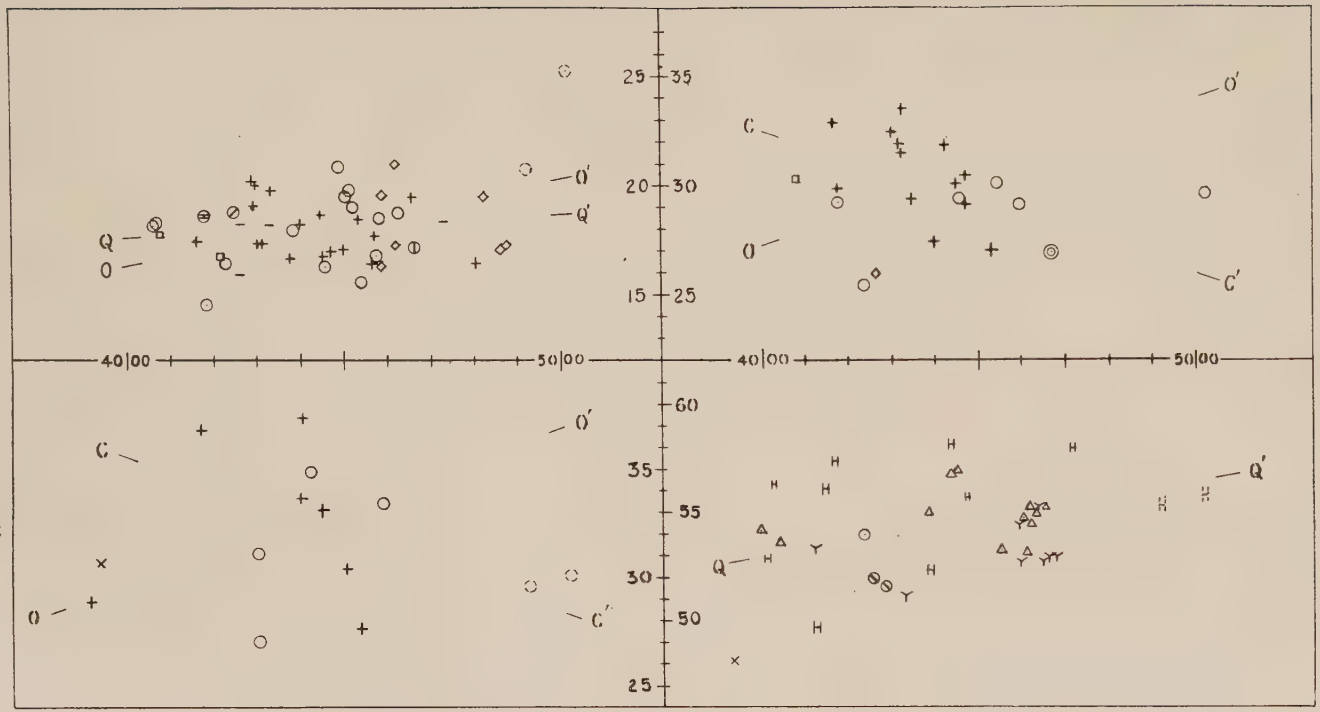

Fig. 3.—Displacement Factors for General Absorption Spectrum, 1912 March. a. Absorption I. March 15; b. Absorption II. March 20; c. Absorption II. March 30; d. Absorption III. March 30.

displacements. It does not seem certain that a horizontal line is determined as against QQ′ or possibly OO′.

Fig. 3*b* is based on Table 11 and represents absorption II. for March 20. The lines CC′ and OO′ represent respectively constant displacement and displacement proportional to the wave-length squared. Both of these, as possible solutions, give residuals of considerable size for 5018, which are, however, no greater than that for the same line in the diagram just considered, nor are they larger than the residual of the good iron line at 4233 of the plat before us, if we assume, with Stratton, that $\kappa = 30$. The plat proves no more, I think, than that the law of displacement for this group of lines lies somewhere between $\Delta\lambda =$ constant and $\Delta\lambda = B\lambda^2$. If we take the lines of titanium alone it happens, as a result of the restricted range of spectrum through which they occur and their chance distribution, that a reciprocal relation would serve as well as any other.

Fig. 3*c* shows the factors for absorption II. of March 30, taken from Table 14. OO′ again represents the law of squares, and CC′ constancy of displacement. It is not certain that the rule of proportionality is established as against either one of these. Fig. 3*d* refers to absorption III. for the same day. Here the law of squares would hardly be admissible as a solution, but there is no determination of a horizontal line as against QQ′, which represents the quadratic law of March 23 multiplied by a factor to bring it to the scale of the displacements for the date.

My opinion of the plats of fig. 3 is that they do not establish any general law of displacement in terms of wave-length other than that there is a general increase of one with the other. This is no reflection on the observations. They are, I have no doubt, as good as can be made. The difficulty lies with the character and environment of the lines and the limited range of spectrum available for measurement. It will be recalled that I questioned the fitness of the word *decisive* in its application to a conclusion which from the context was apparently based on the law of direct proportionality. In his recent note Colonel Stratton casts his conclusion in a somewhat different, and, I believe, in a preferable, form. Referring to the lines of the several elements represented in fig. 3 of the present note, he states that "there is a good general agreement, *suggesting* that for each element the displacement varies with the wave-length." The italics are mine. Had this been the original statement I should not have taken occasion to comment upon it.

I may suggest that the simple plan of platting the displacement factors may find an application beyond the limits of the present discussion. It has lately become somewhat the fashion to state, on the basis of measures of a limited region of the spectrum, that displacements in the spectrum of one or another nova are proportional to the wave-lengths. If that is an assumption made merely for the purpose of correcting measured wave-lengths within limited regions of the spectrum, it is probably

unobjectionable; but if the statement is regarded as the expression of a physical law, it requires to be justified by a somewhat critical analysis of the data on which it is based.

Observations supplied in Colonel Stratton's Note. — Turning now to the later evidence given out by Stratton in response to my note, it is refreshing to deal with observations that appear able to support a conclusion. I refer to the measurements of the hydrogen absorption lines for March 25, the factors for which are platted in fig. 2*c*. In making the chart I have combined with Stratton's observations the published results of Jordan * (which were probably made on the same plates that Stratton used) and those of Plaskett.† These additional observations have been systematically corrected for their mean departure from Stratton's positions, in conformity with the plan adopted on page 196 of my former paper. The plat proves Stratton's statement that on March 25 the displacements were nearly, if not exactly, proportional to wave-length. 2*a* is a plat of the hydrogen lines for March 22, from measures given in my former paper with which, after a small systematic correction, Stratton's measures supplied in his recent note have been combined. The two observations at the extreme left of this diagram depend on Stratton's measures alone. Lines on the more refrangible side of Hη have been indicated by broken circles, as explained in an earlier paragraph. I think that a comparison of fig. 2, referring to the lines of hydrogen, and fig. 3, referring to other lines, will establish that the hydrogen lines of *Nova Geminorum* are not unsuitable for investigations of this character, but rather that they furnish, when they are well measurable, the only group of lines on which any law whatever can be based.

The data at present available appear then to show that on March 22nd and 23rd the displacements of hydrogen III. were subject to a quadratic law, while on the 25th the relation was linear. The publication by Stratton of measures for the latter date justify, I believe, the writing of my earlier note, since they constitute the only published proof within my knowledge that the displacement was at any time proportional to the wave-length.‡

Let us now inquire into the significance of the measures of the hydrogen absorption lines for March 23. Stratton offers the explanation that the lines at the lower end of the Balmer series were broadened toward the violet. If we assume his displacement factor of 46 as best suited to the lines above Hβ, the proportional displacement at Hα would be 30·2A., which would place the centre of the line at $6563{\cdot}0 - 30{\cdot}2 = 6532{\cdot}8$A. The line is at $6527{\cdot}8 \pm$ according to my measures, and $6527{\cdot}0 \pm$ according to those of Miss Hobe. Taking the larger value and adding to it half the width of the line (2·6A.) we obtain 6530·4 as the red edge of the actually

* *Publ. Allegheny Obs.*, **3**, 17.

† *Publ. Dom. Obs., Ottawa*, **1**, 159, 1912.

‡ The Mount Wilson observations of hydrogen absorption II., already referred to, were unfortunately not all made on the same day and are on that account not sufficiently critical to serve the purposes of such a proof.

observed line. The centre of the hypothetical line computed on the basis of proportionality falls more than 2A. to the red of this red edge. I cannot understand how a "broadening toward the violet" of the absorption line could have such an effect, that is to say, how it could displace the red edge of the line to the violetward of the true position of the centre. It might be assumed by one who had not seen the plate that what we actually see is the violet edge of a broad absorption band which is nearly covered by the faint and inconspicuous wing extending from the Hα emission band. Such an absorption would have to be 15 angstroms wide, and the covered 10 angstroms would require to be exactly matched in intensity by the conflicting wing. Against such a contention I should urge the following considerations:—(1) there is nothing in the appearance of the band to substantiate it, (2) the width of the actually observed absorption line is what we should expect it to be from a consideration of the widths of the other hydrogen lines, (3) the general consistency of the observations platted in fig. 2*b*. I am therefore forced to regard the departure from the law of proportionality as real, whatever its cause may be, and not the result of unsymmetrical broadening in the ordinary sense.

If we accept the displacement as primarily a Doppler effect, we must assume that the hydrogen producing the blue lines is inoperative in its effect at Hα, and that the body of gas which absorbs that line is moving 350 kilometres faster than the hydrogen effective at Hη, or that there is an equivalent falling off of pressure in the region where Hα is absorbed, with the possibility that both of these effects contribute to the observed results. These implications are of course not fatal to the velocity hypothesis, in fact they may serve as the starting-point of rather obvious speculations respecting conditions at different levels in the atmosphere of an exploding star; but adjustments on the basis of such uncertain speculations constitute, after all, forced adaptations of a theory to the results of observations. No one, to the best of my knowledge, denies the possibility of nova displacements being due to velocity, many, unquestionably, regard that explanation as probable; but it is quite another matter to close the door to all other interpretations by pronouncing it to be final. The purpose of this note is not, however, to discuss the bearing of spectrum measurements on the theories of novæ, but to attempt to justify the use of the hydrogen lines as a basis for studying the displacement law, and to describe more explicitly the actual nature of the observations in relation to what appears to me their inadequate interpretation as an effect of unsymmetrical broadening.

Radiative Equilibrium: The Effect of a Strong Absorption Line. By E. A. Milne, B.A.

(*Communicated by the Director, Solar Physics Observatory, Cambridge.*)

The approximate form of the equations of transfer of radiant energy when for simplicity the flow of radiation is taken to be "linear" or "tubular" is

$$\frac{dI_\lambda}{dx} = \kappa_\lambda \rho (I_\lambda - B_\lambda), \qquad \frac{dI_\lambda'}{dx} = \kappa_\lambda \rho (B_\lambda - I_\lambda') \quad . \quad (1)$$

$$2\int_0^\infty \kappa_\lambda B_\lambda d\lambda = \int_0^\infty \kappa_\lambda (I_\lambda + I_\lambda') d\lambda \quad . \quad . \quad (2)$$

where I_λ and I_λ' are the outward and inward intensities at the point x, B_λ is the intensity of black-body radiation at the temperature at the point x, and κ_λ is a mean coefficient of absorption, between λ and $\lambda + d\lambda$, for radiation crossing a plane perpendicular to the direction of x; κ_λ is related to the ordinary coefficient k_λ by the approximate relation $\kappa_\lambda = 2k_\lambda$.

The solution of these equations when κ_λ is an arbitrary function of λ would be difficult; the attempt to solve them would hardly be profitable, and their discussion is usually confined to the case where κ_λ is independent of λ. In this note it is proposed to consider briefly the case of a spectrum containing a single absorption line, in the neighbourhood of λ_1, due to a large absorption coefficient κ_{λ_1}; for all other values of λ the absorption is supposed to be constant, given by $\kappa_\lambda = \kappa$.

Now the presence of the dark line in the spectrum means that each layer of gas absorbs much more radiation of wave-length λ_1 than it emits. But in radiative equilibrium the total energy absorbed, of all wave-lengths, is equal to that emitted. Consequently the radiation which the gas fails to emit in wave-length λ_1 must be emitted as extra radiation in the rest of the spectrum, and thus the general distribution of energy in the spectrum is altered. In fact, the total flow of energy being constant, the energy dammed back in the region of the Fraunhofer line must break through elsewhere. The course of events by which this occurs is easily seen. When there is no selective absorption the temperature gradient is, roughly speaking, proportional to the coefficient of absorption κ and to the total flow of energy; when there is selective absorption in the region of $\lambda_1 (\kappa_{\lambda_1} > \kappa)$ the existing temperature gradient* is not sufficient to drive the amount of energy appropriate to λ_1 against the increased resistance given by κ_{λ_1}, and hence the energy accumulates, increasing the temperature gradient until a new steady state is obtained in which the excess gradient in the rest of the spectrum compensates for the deficiency in the neighbourhood of λ_1. A further consequence is that the boundary temperature is slightly decreased in virtue of the cooling

* *Cf.* Schuster, *Astrophys. Jour.*, **21**, 16 (1905).

caused by the increased radiation of the boundary layers in the neighbourhood of λ_1. We shall see later that the combined result of these two effects—increased gradient and decreased boundary temperature—is to increase the intensity on the violet side of the maximum, and to decrease or increase the intensity on the red side according as the absorption line is or is not sufficiently far towards the red.

Let the symbols I_λ, I_λ', B_λ denote the solutions of equations (1) and (2) in the case when there is no selective absorption, *i.e.* when $\kappa_\lambda = \kappa$ for all λ; and let i_λ, i_λ', b_λ denote the solutions in the case when there is a single absorption line, $\kappa_\lambda = \kappa(\lambda \neq \lambda_1)$, *the total flux F being the same in the two cases.* Thus

$$F = \int_0^\infty (I_\lambda - I_\lambda')d\lambda = \int_0^\infty (i_\lambda - i_\lambda')d\lambda.$$

Put $\kappa_{\lambda_1}/\kappa = n$, $\kappa\rho dx = d\tau$. Differentiating (2) and using (1) we have *

$$2\frac{db}{dx}\int_0^\infty \kappa_\lambda \frac{db_\lambda}{db}d\lambda = \rho\int_0^\infty \kappa^2\lambda(i_\lambda - i_\lambda')d\lambda \quad . \quad . \quad (3)$$

but

$$\int_0^\infty \kappa_\lambda \frac{db_\lambda}{db}d\lambda = \int_0^\infty \kappa\frac{db_\lambda}{db}d\lambda + \int_{\lambda_1}^{\lambda_1+d\lambda_1}(\kappa_{\lambda_1}-\kappa)\frac{db_\lambda}{db}d\lambda$$

$$= \kappa\left[1 + (n-1)\frac{db_{\lambda_1}}{db}d\lambda_1\right],$$

and similarly

$$\int_0^\infty \kappa^2\lambda(i_\lambda - i_\lambda')d\lambda = \kappa^2[F + (n^2-1)(i_{\lambda_1} - i_{\lambda_1}')d\lambda_1].$$

Hence (3) becomes

$$\frac{db}{d\tau} = \tfrac{1}{2}\frac{F + (n^2-1)(i_{\lambda_1} - i_{\lambda_1}')d\lambda_1}{1 + (n-1)\dfrac{db_{\lambda_1}}{db}d\lambda_1} \quad . \quad . \quad . \quad (4)$$

Expanding this (assuming $(n-1)d\lambda_1$ is small) and putting

$$b = B + \delta B,$$

we find

$$\frac{d(\delta B)}{d\tau} = \tfrac{1}{2}(n-1)d\lambda_1\left[(n+1)(i_{\lambda_1} - i_{\lambda_1}') - F\frac{dB_{\lambda_1}}{db}\right] \quad . \quad (5)$$

to the first order. This equation determines the *increase in the temperature gradient* due to the absorption line. Further, equation (2) becomes

$$2b - i - i' + (n-1)d\lambda_1(2b_{\lambda_1} - i_{\lambda_1} - i_{\lambda_1}') = 0.$$

At the boundary $i = F$, $i' = i_{\lambda_1}' = 0$, $b_0 = B_0 + \delta B_0$, and thus

$$2\delta B_0 = -(n-1)d\lambda_1(2B_{\lambda_1} - i_{\lambda_1})_0 \quad . \quad . \quad . \quad (6)$$

* The symbols i, b, etc., without suffix denote the corresponding integrated radiation of all wave-lengths.

to the order considered. This equation determines the *decrease in the boundary temperature.*

Except when $\lambda=\lambda_1$, the intensities i_λ and i_λ' will differ only slightly from I_λ and I_λ'. Put then

$$i_\lambda = I_\lambda + \delta I_\lambda, \qquad i_\lambda' = I_\lambda' + \delta I_\lambda' \quad (\lambda \neq \lambda_1).$$

The equation for δI_λ is readily found to be

$$\frac{d(\delta I_\lambda)}{d\tau} = \delta I_\lambda - \delta B_\lambda = \delta I_\lambda - \frac{dB_\lambda}{dB}\delta B \quad . \quad . \quad (7)$$

whence

$$\delta I_\lambda = e^\tau \int_\tau^\infty \frac{dB_\lambda}{dB}\delta B e^{-\tau} d\tau$$

$$= \tfrac{1}{2}(n-1)d\lambda_1 e^\tau \int_\tau^\infty \left[(i_{\lambda_1} - B_{\lambda_1})_0 + \int_0^\tau \left\{ (n+1)(i_{\lambda_1} - i_{\lambda_1}') - 2B_0 \frac{dB_{\lambda_1}}{dB} \right\} d\tau \right] \frac{dB_\lambda}{dB} e^{-\tau} d\tau \quad (8)$$

on inserting the value of δB calculated from (5) and (6). To evaluate this we require the values of i_{λ_1} and i_{λ_1}'; it is clearly sufficient, to the order considered, to neglect the change in the temperature distribution in calculating i_{λ_1} and i_{λ_1}'. The equations are

$$\frac{di_{\lambda_1}}{d\tau} = n(i_{\lambda_1} - B_{\lambda_1}), \qquad \frac{di_{\lambda_1}'}{d\tau} = n(B_{\lambda_1} - i_{\lambda_1}'),$$

yielding

$$i_{\lambda_1} = e^{n\tau} \int_\tau^\infty n B_{\lambda_1} e^{-n\tau} d\tau, \qquad i_{\lambda_1}' = e^{-n\tau} \int_0^\tau n B_{\lambda_1} e^{n\tau} d\tau \quad . \quad (9)$$

Using these values in (8) and putting $\tau = 0$, we obtain after some reduction

$$(\delta I_\lambda)_0 = \frac{(n-1)d\lambda_1}{n} \left[\tfrac{1}{2}(n+1) \int_0^\infty (i_{\lambda_1} + i_{\lambda_1}' - 2B_{\lambda_1}) \frac{dB_\lambda}{dB} e^{-\tau} d\tau \right.$$

$$\left. + \int_0^\infty B_{\lambda_1} \frac{dB_\lambda}{dB} e^{-\tau} d\tau - \tfrac{1}{2}(i_{\lambda_1})_0 \frac{(I_\lambda - B_\lambda)_0}{B_0} \right] \quad (10)$$

This gives the redistribution over the rest of the spectrum of the energy missing in $(\lambda_1, \lambda_1 + d\lambda_1)$. It may be verified that the result of integrating this over all wave-lengths is precisely $(I_{\lambda_1} - i_{\lambda_1})_0 d\lambda_1$, as it should be.

Were the intensity in the line itself, $(i_{\lambda_1})_0$, small compared with that of the neighbouring continuous spectrum, $(I_{\lambda_1})_0$, the only appreciable term in (10) would be the second. But however intense the absorption, the intensity in the line itself can never be less than that corresponding to the boundary temperature. This is obvious physically, and from (9) it can be seen that as $n \to \infty$, $(i_{\lambda_1})_0 \to (B_{\lambda_1})_0$. Thus in strict radiative equilibrium the intensity of radiation in the darkest possible line cannot fall much below that corresponding to a temperature of about $2^{-\frac{1}{4}} T_1$, T_1

being the effective temperature. Instead of approximating to (10) as it stands, we shall consider its limit as $n\to\infty$, *i.e.* we consider the redistribution of energy corresponding to an absorption line as dark as possible.* Detailed analysis which we here omit shows that

$$\lim_{n\to\infty}(\delta I_\lambda)_0 = d\lambda_1\left[\int_0^\infty B_{\lambda_1}\frac{dB_\lambda}{dB}e^{-\tau}d\tau - \tfrac{1}{2}(B_{\lambda_1})_0\left\{\frac{I_\lambda - B_\lambda}{B}+\frac{dB_\lambda}{dB}\right\}_0\right] \quad (11)$$

We shall take this as our approximation. Now we know from the usual theory that $(I_\lambda)_0$ is very nearly the radiation corresponding to the temperature given by $B = 2B_0$. Thus approximately

$$(I_\lambda - B_\lambda)_0 = B_0\left(\frac{dB_\lambda}{dB}\right)_0,$$

and hence approximately from (11)

$$\begin{aligned}(\delta I_\lambda)_0 &= d\lambda_1\left[\int_0^\infty B_{\lambda_1}\frac{dB_\lambda}{dB}e^{-\tau}d\tau - \left(B_{\lambda_1}\frac{dB_\lambda}{dB}\right)_0\right]\\ &= d\lambda_1\int_0^\infty \frac{d}{d\tau}\left(B_{\lambda_1}\frac{dB_\lambda}{dB}\right)e^{-\tau}d\tau \quad . \quad . \quad . \quad (12)\end{aligned}$$

On substituting the explicit value for the temperature distribution, $B = B_0(1+\tau)$, and putting $B/B_0 = y$, we have

$$(\delta I_\lambda)_0 = C\lambda^{-5}\lambda_1^{-5}d_1\lambda_1\int_1^\infty \frac{d}{dy}\left\{\frac{\frac{1}{4}\alpha y^{-\frac{5}{4}}e^{\alpha y^{-\frac{1}{4}}}}{(e^{\alpha_1 y^{-\frac{1}{4}}}-1)(e^{\alpha y^{-\frac{1}{4}}}-1)^2}\right\}e^{-y}dy \quad (13)$$

where we have put

$$\alpha = hc/\lambda RT_0, \qquad \alpha_1 = hc/\lambda_1 RT_0.$$

We know that $\int_0^\infty(\delta I_\lambda)_0 d\lambda$ is positive, being in fact the missing energy. But our expression (13) teaches us the interesting fact that $(\delta I_\lambda)_0$ *may be negative for certain values of* λ *and* λ_1. For on performing the differentiation it appears that so long as $e^{-\alpha y^{-\frac{1}{4}}}$ and $e^{-\alpha_1 y^{-\frac{1}{4}}}$ are small compared with unity, the integrand in (13) is negative when

$$y > \left(\frac{\alpha+\alpha_1}{5}\right)^4 \quad . \quad . \quad . \quad . \quad (14)$$

The value of (13) depends principally on the values of the integrand for small values of y; by analogy with other cases we may expect it to be equal roughly † to the value of the integrand (without the

* It must be remembered that $nd\lambda_1$ must always be so small that terms such as $nI_{\lambda_1}d\lambda_1/I$, etc., are small compared with unity. Thus as $n\to\infty$, we must suppose that $d\lambda_1\to 0$. But our results will hold approximately (for a non-zero $d\lambda_1$) however large n may be, provided the total disturbance due to the line is small. Equation (4) appears to require that $n^2 d\lambda_1$ should be small too, but analysis shows that this is not the case.

† *M.N.*, **81**, 384 (March 1921).

exponential weighting factor) for $y = 2$. We shall thus be fairly safe in saying that $(\delta I_\lambda)_0$ is negative or positive according as

$$\alpha + \alpha_1 \lessgtr 5 \times 2^{\frac{1}{2}} = 5{\cdot}9.$$

We know that the position of maximum intensity (λ_{max}) is given by $\alpha = 6$ approximately.* If now we express λ and λ_1 as multiples of λ_{max},

$$\lambda = r\lambda_{max}, \qquad \lambda_1 = r_1\lambda_{max},$$

these conditions become roughly

$$\frac{1}{r} + \frac{1}{r_1} \lessgtr 1 \quad . \quad . \quad . \quad . \quad (15)$$

If $r_1 < 1$, $(\delta I_\lambda)_0$ will be positive for all values of λ; but if $r_1 > 1$, $(\delta I_\lambda)_0$ will be negative for all wave-lengths to the red side of that given by

$$\lambda = \frac{r_1}{r_1 - 1}\lambda_{max} \quad . \quad . \quad . \quad . \quad (16)$$

and positive for all wave-lengths to the violet side of this. This wave-length is itself on the red side of the maximum. Thus *the effect of an absorption line which lies on the violet side of the maximum is to brighten the continuous spectrum, slightly, everywhere; but if the absorption line lies to the red side of the maximum, there is a certain wave-length also lying to the red side of the maximum such that on the violet side of this wave-length the spectrum is brightened, on the red side darkened.* The region of darkening, when it occurs, begins at a point which is closer to the position of maximum the further the absorption line is to the red, as is seen from (16). It appears probable from a rough investigation of (13) that the position of maximum brightening is always some way to the violet of the ordinary maximum, and near $\alpha = 8$, and that when darkening occurs in the red due to a line far in the red there is a position of maximum darkening near $\alpha = 4$.

For a number of lines these effects must be superimposed. Thus *in strict radiative equilibrium the presence of intense absorption lines necessitates a redistribution of the missing energy over the rest of the spectrum, the consequent distortion of the spectrum consisting in general of a strengthening of the violet with a possible weakening of the red, with a slight shift of the maximum towards the violet.* It is difficult to estimate the practical importance of this effect in actual stars or in the sun; it is probably slight—a detailed bolograph of the spectrum would be required showing exactly the breadths and troughs of the lines. It is important to recognise, however, that assuming radiative equilibrium the general distribution of energy in the continuous spectrum is liable to be seriously changed if there is considerable selective absorption.

* *M.N.*, **81**, 384 (March 1921).

This investigation applies only to the case in which the lines are due to selective absorption ($\kappa_\lambda = \text{const.}$) throughout the whole of that depth of the star from which the "photospheric" light is radiated and not merely to selective absorption in a thin layer near the boundary. Further, it is assumed that in the radiating matter the mechanism of radiation and absorption is adequate for the free transformation, when necessary, of energy absorbed in a particular wave-length into heat energy or into energy of radiation in other wave-lengths.

Solar Physics Observatory, Cambridge:
1921 *May* 23.

The Sun-Spot Group and the Magnetic Disturbances, 1921 *May* 8–21. By the Rev. A. L. Cortie, S.J. (Plate 17.)

The sun-spot which appeared on the sun's E. limb, 1921 May 8, developed into a very large and active group. At first it was a single spot with scattered umbræ in very dark penumbræ. Spots of this type are not unfrequently connected with magnetic disturbance.* It appeared in a region of the sun which had not been disturbed for some time. When it appeared on the sun's E. limb it would have been about five days old. By May 13 it had separated into two large spots. Their maximum area 16·5, in units 1/5000 of the sun's visible disc, was attained on May 14. The leader spot was a composite spot containing two umbræ, the mean heliographic co-ordinates of which were latitude + 1·4° and longitude 6·4°. The following spot was a large single spot, latitude + 0·2°, longitude 358·8°. The type was II_b.† The whole group extended over about 12° in longitude, and 6° in latitude, so that a very considerable area of the sun's surface was disturbed.

Not only was the spot large and active, but it was also an equatorial spot. Moreover, the mean heliographic latitude of the earth being − 2·4°, it was placed very favourably relatively to the spot-outburst. These are conditions under which a great magnetic storm is most likely to occur.

A detailed description of the chief phases of the series of magnetic disturbances which accompanied the passage of the spot-group across the sun, as recorded at this observatory, was communicated to *Nature.*‡ Briefly, after minor yet well-marked preparatory movements of the needles on May 11–12, the first phase in the greater activity of disturbance began abruptly on May 13 at $13^h\ 10^m$. A second and more intense phase of the storm commenced on May 14, $16^h\ 8^m$. The speed and amplitude of the oscillations of the needles grew gradually greater, until May 15, $0^h\ 45^m$, when the beginning of the greatest intensity of

* *M.N.*, 73, 151. † *Memoirs B.A.A.*, 23, 2, 79.
‡ *Nature,* 1921 June 2.

the storm or third phase took place, which lasted until May 15, $7^h\ 30^m$. The magnets continued in a disturbed state throughout May 16, but a lull occurred on May 17, which was comparatively, though not really, a quiet day magnetically, the next day, May 18, being even quieter. Activity was resumed May 19, $20^h\ 0^m$, which persisted throughout May 20. The protracted storm had not completely subsided until May 21, 20^h.

The following table contains the statistics both magnetical and solar, concerning the series of disturbances :—

TABLE.

Day.	Magnetic Range in Minutes of Arc.				Sun-Spots.			Heliographic Co-ordinates.		
	Dn.	H.	V.	Character.	Mean Daily Disc-area.	Mean Co-ordinates. Centre of Group. Lat.	Long.	Centre Sun's Disc. D.	L.	Angular Distance. Spot from Central Meridian.
May 12	21′	34	5	2	14·9	+0°·8	2°·7	−2°·9	32°·2	29°·5
13	40	40	>67	2	15·6	,,	,,	−2·8	19·0	16·3
14	50	64	56	2	16·5	,,	,,	−2·7	5·7	3·0
15	>129	...	>75	2	14·3	,,	,,	−2·5	352·5	10·2
16	47	70	>64	2	13·0	,,	,,	−2·4	339·3	23·4
17	21	29	8	2	11·3	,,	,,	−2·3	326·0	36·7
18	11	19	2	1	7·4	,,	,,	−2·2	312·8	49·9
19	58	30	21	2	...	,,	,,	−2·1	299·6	63·1
20	26	61	27	2	1·6	,,	,,	−2·0	286·4	76·3
21	26	20	11	2	0·3	,,	,,	−1·8	273·1	89·6

In the three columns giving the ranges of the magnetic elements, these ranges, Dn, H, V, are expressed in minutes of arc, in order the more easily to compare the magnitudes of the movements as measured on the curves. To reduce the numbers in the columns under H and V to units of force, γ, where $1\gamma \equiv 1 \cdot 10^{-5}$ C.G.S. unit, the factors are 4·7 for H, and 6·4 for V. The values for V are very notably high. The international character figures for magnetic disturbances are 0 (quiet), 1 (disturbed), 2 (highly disturbed). Every day except one, May 18, is marked by the figure 2. This storm is remarkable for the number of days over which it extended. To find a parallel we must go back to the protracted storm, 1882 November 11–21, which also accompanied the passage of a great spot across the sun's disc. That storm was the greatest recorded up to that date at the Stonyhurst Observatory, where the photographic magnetographs had then been in constant action for fourteen years.*

In the columns concerned with solar data, the first gives the

* *Stonyhurst Observatory Report*, 1882, pp. 64–65.

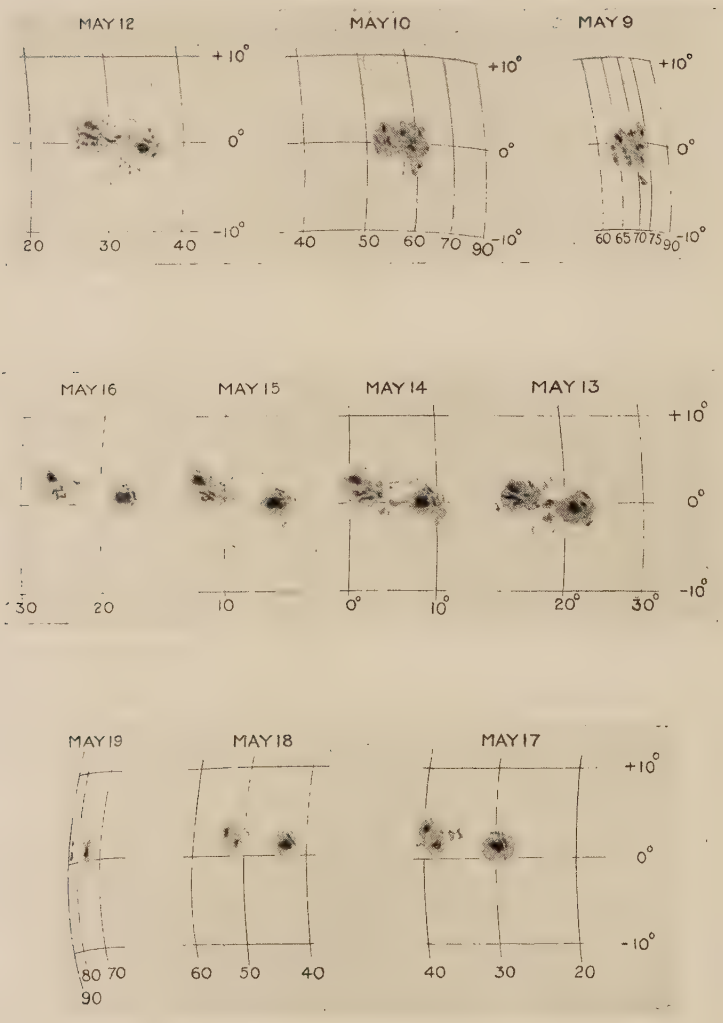

The Sun-spot Group, 1921 May 8–21.

daily disc-area of the spot-group, and the next two the mean latitude and longitude of the centre of the spot-group. The fourth and fifth columns give the heliographic co-ordinates of the centre of the sun's disc, or, what is the same thing, the heliographic position of the earth, when considered as projected on the sun. The last column is important. It gives the angular separation of the centre of the spot-group from the meridian of longitude which faced the earth.

The mean longitude of the centre of the sun-spot group was 2·7°. On May 12 the longitude of the sun's meridian facing the earth was 32·2°, so that there was an angular separation of 29·5°. On May 13–15 the spot was practically opposite the earth. But on May 19–21, when there was a marked revival of magnetic disturbance, the separation of centre of sun-spot group and earth was from 63° to nearly 90°. Although the greatest phase of the magnetic storm was concurrent with the group's passing the central meridian, yet the circumstances of this long-protracted storm are quite out of accord with the idea that streams issuing from spot-disturbed areas of the sun, in an approximately radial direction, are the occasion of magnetic storms. What was coincident in time with the spot's passing the central meridian was the greatest activity of the spot-group itself, which was in evidence on May 12–15, and its greatest disc-area on May 14, or area as viewed from the earth. It seems to be most unlikely that anything resembling radial streamers of cathode-like type, emanating from the region of activity, should have been connected with a series of magnetic disturbances lasting for ten days, especially when the sun-spot, greatly reduced in disc-area, was near the sun's W. limb.

But if we suppose a sheaf of divergent rays of particles of like sign to emanate from the area of disturbance, such particles would by their mutual repulsion be spread out into clouds. These clouds would be extended round a portion of the sun like a belt. It is probably the entry of the earth into clouds of this nature which releases the energy that is responsible for a magnetic storm. If active sun-spots break out in latitudes removed several degrees from the equator, the encircling clouds would be above or below the path of the earth round the sun, and an active spot might appear without any corresponding magnetic disturbance. On the other hand, a region on the sun can remain active even after the sun-spot, as focus of activity, has disappeared. Consequently, after the period of a solar synodic rotation, about twenty-seven days, another magnetic disturbance could be precipitated. But such recurrent magnetic disturbances are never on the scale of activity of the one that accompanied the appearance of the big sun-spot group.

The drawings which accompany this paper, and which illustrate the development of the sun-spot group, are very faithful to nature. They are accurate copies of the drawings made by projection with the 15-inch equatorial by the Rev. H. Macklin, S.J.

Summary.

1. A great sun-spot group, May 8–21, was accompanied by a protracted series of magnetic storms.

2. The magnetic disturbances covered the period May 12–21.

3. The detailed comparison of the solar outburst and the magnetic disturbances favours the theory of divergent streams of particles from the solar focus of activity, which spread into clouds.

Stonyhurst College Observatory:
1921 *June* 3.

Appendix.

The following is a translation from the Spanish of an account of the chief features of the magnetic storm and its relation to the sun-spot, sent by Father Luis Rodès, S.J., Director of the Tortosa Observatory:—

On the 13th of May 1921 at 13 h. 10 min. began the most

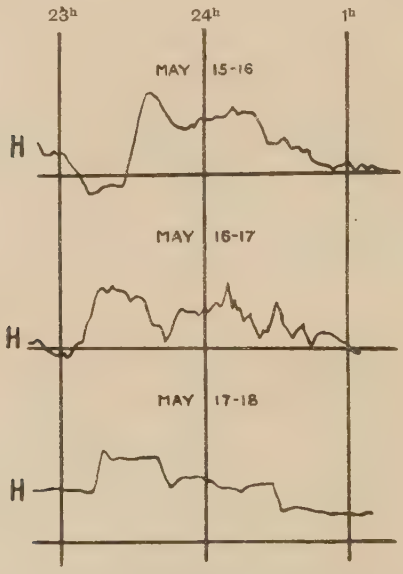

FIG. 1.

violent magnetic storm of all those registered at this observatory since 1910 when the *Bulletin* was first published.

It began with a "sudden commencement" in all three registering instruments, moving the needle of D towards the east, and first diminishing the horizontal component, only to raise it immediately to above normal. The first oscillation of the balance was more rapid, and it is impossible to define exactly the direction of the first deviation.

At 19 h. 18 min. of the same day there was another clearly

marked variation in all three elements; these continued to oscillate rapidly but with little amplitude in the main until the 14th at 16 h. 15 min., when the disturbances of the day before partly reproduced themselves, reaching a period of maximum intensity between 22 h. 15 min. on the 14th and 8 h. on the 15th. During this period all three curves went off the chart several times, making the register incomplete. It is noticeable that the horizontal component remained off the chart for more than seven hours—that is, from 3 h. to 11 h.; this occurred again on the 16th from 8 h. to 10 h., but with less intensity.

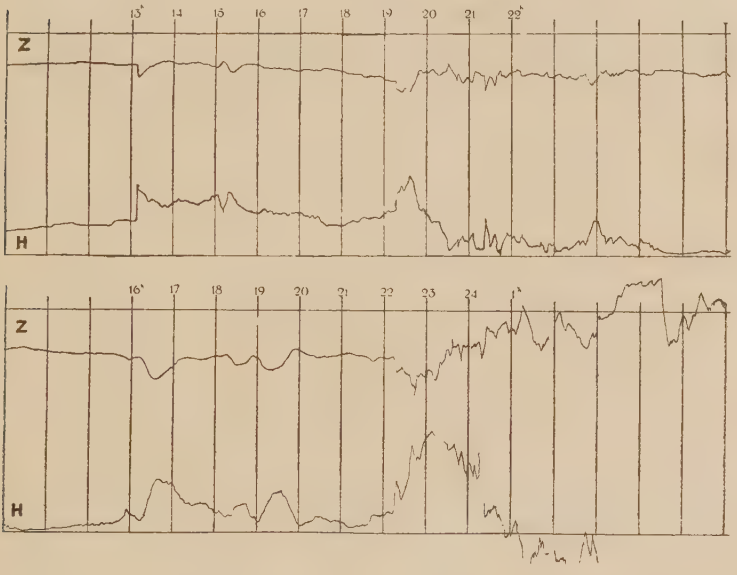

Fig. 2.

The maximum amplitude of the oscillation that is registered on the chart was as follows:—

In D, 47′, which was a deviation of 23′ W. and 24′ E. above the mean value of the curve, which is approximately 11° 47′·5.

In H it was 424γ with 190γ above and 234γ below the mean value, which is of 23·315γ approx.

In V it was 434γ with 147γ above and 287γ below the mean value, which is of 36·768γ approx.

Taking into account that the curve went off the chart several times, the actual amplitude of the oscillation was considerably greater; in H it reached at least 660γ.

Fig. 1 reproduces that portion of the curve included between 23 h. and 1 h. of the days 15–16, 16–17, 17–18, which shows clearly the period of 24 h. due to the rotation of the earth.

Fig. 2 reproduces the curve from 13 h. to 22 h. of the 13th

of May compared with that of the 14th, from 16 h., to 1 h. of the 15th, in which is seen the trace of the same period, although the separation here is of 27 h.

One of the characteristics of this storm has been the general deviation of the curve of the bifilar in a negative direction. D, on the other hand, has oscillated around the normal values.

This time, as in March of last year, the magnetic storm coincided with the appearance of a great sun-spot in the neighbourhood of the central meridian. The spot of the 22nd of March 1920 measured 3223 millionths of the visible hemisphere, and passed through the central meridian at 21 h. 6 min. of the 21st, or 12 h. before the beginning of the magnetic storm; this time the magnetic storm preceded the passage of the spot across the central meridian by 27 h. 35 min.: a difference that is probably due to the different angle at which the sun projects the electrified particles into space.

Results of the Sun-Spots and Faculæ Observations made during the Years 1916, 1917, 1918, 1919, *and* 1920, *at the University Observatory, Rostov-on-Don.* By Professor S. D. Tscherny.

(*Communicated by the Secretaries.*)

(Instrument used—71-mm. Vion refractor, power 71.)

Year.	Number of Days of Observation.	Mean Diurnal Number of Groups of Spots.	Mean Diurnal Number of Individual Spots.	Mean Diurnal Number of Spots.	Maximum of Spots.	Mean Diurnal Relative Number.	Mean Diurnal Number of Faculæ.	Number of Days without Spots.
1916	176	2·8	1·5	15·5	62	58·4	1·9	12
1917	213	4·9	3·6	31·9	101	117·2	4·6	2
1918	240	4·1	3·0	25·9	80	96·8	10·1	0
1919	198	3·9	2·1	23·2	94	83·2	9·7	0
1920	250	2·5	1·4	13·4	71	52·5	10·5	12

University Observatory,
Rostov-on-Don:
1921 *April* 24.

A Remarkable Spot on the South Equatorial Belt of Jupiter.
By F. Sargent.

A surface marking or "spot" on the planet Jupiter of unusual interest has been under observation from here since May 16. It was first noticed on that date as a very dark marking attached to the north edge of the South Equatorial Belt, and gave the impression of being the shadow of a satellite, an idea immediately recognised as being untenable.

As it approached the central meridian of the planet the spot was observed to be of great intensity, elongated, and surrounded by a penumbra-like shading.

The object was on the C.M. at 9 hrs. 30 mins., the longitude derived being 236°·3 according to the Sys. I. On the 18th it was again observed, when it was found to be in longitude 238°·2, the apparent discrepancy being noted.

The spot has been observed on four occasions since that date, and a very marked movement in increasing longitude revealed when compared with that of the Sys. I., to which markings in this region are usually referred.

The series of observations are here given.

1921	May	16	On C.M.	9	hrs. 30	mins. Long.	236°·3 Sys. I.
,,	,,	18	,,	10	46	,,	238·3 ,,
,,	,,	23	,,	9	10	,,	248·5 ,,
,,	,,	25	,,	10	30	,,	252·8 ,,
,,	June	1	,,	10	11	,,	265·5 ,,
,,	,,	3	,,	11	30	,,	269·2 ,,

When plotted these observations show a consistency that is quite satisfactory, and the possibility of wrong identification may be ruled out without hesitation, especially with an object so distinctive in form and intensity.

Forty-four rotations are covered by these observations, and the period derived is 9 hrs. 51 mins. 45 secs., a period almost without parallel in Jovian observation.

During recent years the rotation periods derived for the region in which this spot is situated have ranged between 9 hrs. 50 mins. 10 secs. and 9 hrs. 50 mins. 28 secs., so that the object now under observation is moving slower by 1½ minutes per rotation than is usual for its position.

The abnormal period being recognised, it becomes of interest to examine the observations of the days immediately preceding May 16.

On May 4 I recorded "Angle in N. of S.E.B. (north edge of the South Equatorial Belt), transit time 11 hrs., longitude 197°·5." A small sketch was made, and a covering note added. The "angle" was a position where the dark north edge of the belt bent sharply to the south, at an angle of about forty degrees, the bent portion reaching nearly to the south component of the belt.

On May 9 this angle was again observed. The position of the bend was less definite, but a satisfactory observation of its transit was obtained at 9 hrs. 26 mins., the derived longitude being 209°·3, or nearly twelve degrees greater than for the same feature on the 4th.

A few degrees following, and on the bent portion of the belt, a bright spot had formed in a zone where surface markings usually conform approximately to the Sys. II. rate.

In the present case it will be more convenient to adhere to the Sys. I. as a standard of reference; accordingly, the longitude of the bright spot is found to have been 220°·9, or 11°·6 following the "angle." A position on the sloping belt corresponding to this for the observation of the 4th is therefore 209°·1.

If these positions for the bright spot, the observed and the inferred, are considered in relation to the dark spot found on the 16th, they are seen to be separated from it by from three to five degrees only, and to have probably shared the same abnormal rate of motion. This latter remark also applies to the observed "angle" and the sloping belt.

It therefore appears that we have an instance of an appreciable area rather than a "spot" showing a rate of motion quite out of the ordinary, and in a state of rapid transition, in the course of which a bright spot formed in a few days on the planet's surface, to vanish equally quickly, leaving behind it a mass of non-reflective material probably the product of its activities.

The suggestion seems permissible that the sloping belt was a real deflection southwards of the material of the north component of the South Equatorial Belt, where, becoming involved in a slower-moving mass, its motion was impeded. A bright spot was formed that normally would have appeared on the north edge of the belt, and, postulating volcanic or similar agency, the ejecta are yielding the dark spot.

This spot has taken a position definitely projecting into the Equatorial Zone, and it will be of interest to note whether it maintains its present abnormal period, or ultimately conforms to that more usual for the region in which it exists.

Whilst extremely rare, such a period as here found is not without precedent.

In 1882 Mr. Denning recorded a period practically identical for a bright spot in the Equatorial Regions, observing it over sixty-six rotations.*

In 1779 Sir Wm. Herschel recorded a very similar value for three spots in the same region.†

Schmidt and Trouvelot have also recorded spots in the Equatorial Zones that have exceeded the Sys. I. rate by upwards of half a minute.

* *Monthly Notices*, **44**, 72.
† *Phil. Trans.*, 1781.

Observations of Comets 1921 *a* (*Reid*), 1921 *b* (*Pons-Winnecke*), *and* 1921 *c* (*Dubiago*), *made at the Royal Observatory, Greenwich.*

(*Communicated by the Astronomer Royal.*)

The following observations were made with the Sheepshanks Equatorial (aperture 6·7 inches) by taking transits over two cross-wires, each inclined 45° to the parallel of declination. Magnifying power 55.

G.M.T.	Comet − Star. R.A.	Comet − Star. Decl.	No. of Comps.	Log Factors of Parallax.		Comet's Apparent R.A.	Comet's Apparent Decl.	Star.
				Comet 1921 *a*. (*Obs. A.C.*)				
d h m s	m s	′ ″				h m s	° ′ ″	
May 22 9 44 2·84	+3 45·53	− 4 27·6	3	9·9568	0·4258	7 48 56·39	+66 7 54·1	*a*
,, ,, ,,	+0 41·13	+ 2 59·7	3	,,	,,	7 48 57·47	+66 7 52·8	*b*
,, 23 9 28 58·19	−1 56·30	+ 0 54·8	3	9·9363	0·3982	7 51 9·28	+64 58 39·0	*c*
June 2 9 57 41·17	−0 12·46	− 5 30·3	2	9·8101	0·6606	8 3 45·56	+55 56 44·0	*d*
,, ,, ,,	−0 22·88	+ 0 33·1	2	,,	,,	8 3 46·12	+55 56 39·0	*e*
,, 7 10 7 54·44	+1 7·02	+ 7 23·9	3	9·7645	0·7381	8 7 14·05	+52 41 56·4	*f*
,, ,, 10 10 7·08	−3 3·79	+ 6 50·8	1	9·7633	0·7321	8 7 13·77	+52 41 50·8	*g*
,, 9 11 41 39·25	+5 15·64	− 0 43·9	2	9·6474	0·8509	8 8 27·03	+51 32 0·8	*h*
,, ,, ,,	+1 38·66	− 9 23·1	2	,,	,,			*i*
,, 11 10 19 31·00	−1 50·89	− 9 49·8	1	9·7270	0·7757			*k*
,, ,, 10 22 43·48	−4 25·40	− 1 9·9	2	9·7244	0·7796	8 9 30·14	+50 30 14·7	*l*
,, ,, 10 25 55·96	+0 15·81	+10 8·8	1	9·7218	0·7836	8 9 30·53	+50 29 52·6	*j*
				Comet 1921 *b*. (*Obs. A.C.*)				
May 23 10 33 34·01	+3 13·83	− 0 7·7	5	9·6747*n*	0·4997	18 57 19·60	+45 23 54·5	*q*
June 2 10 55 15·97	+0 39·72	− 2 52·4	6	9·6471*n*	0·6610	20 37 14·86	+37 12 53·9	*s*
,, ,, 11 4 44·83	+2 46·96	− 1 9·4	2	9·6417*n*	0·6483	20 37 18·82	+37 12 21·4	*r*
,, 5 10 33 4·63	+2 6·92	+ 1 49·1	3	9·6362*n*	0·7445	21 9 54·95	+32 25 31·8	*t*
,, ,, ,,	+2 2·68	− 2 4·0	3	,,	,,	21 9 54·73	+32 25 32·6	*u*
,, 7 11 19 9·08	+2 32·12	+ 7 32·4	4	9·6095*n*	0·7367	21 31 53·41	+28 29 52·9	*v*
,, ,, 11 25 35·30	+1 14·54	− 7 2·3	6	9·6066*n*	0·7310	21 31 55·99	+28 29 18·6	*w*
,, ,, 11 38 27·72	+0 41·26	− 2 12.4	2	9·5996*n*	0·7196	21 32 1·50	+28 28 14·5	*x*
,, ,, 11 39 38·53	−1 39·16	− 0 23·5	1	9·5989*n*	0·7185	21 32 2·44	+28 28 10·7	*y*
,, 9 10 44 23·90	−1 3·30	− 3 51·5	3	9·6040*n*	0·7943	21 52 40·44	+24 13 34·7	*z*
,, ,, ,,	−1 38·20	− 8 44·7	3	,,	,,	21 52 40·41	+24 13 36·0	*A*
,, 11 11 4 23·49	−0 27·20	+ 9 59·8	2	9·5893*n*	0·8049	22 12 59·24	+19 30 53·4	*B*
,, ,, ,,	−2 3·01	− 3 12·2	2	,,	,,	22 12 59·48	+19 30 57·1	*C*
				Comet 1921 *c*. (*Obs. A.C.*)				
May 22 10 6 10·92	−1 42·13	− 4 44·6	3	9·6607	0·6469	9 4 30·90	+39 14 51·8	*m*
,, ,, ,,	−2 48·29	+ 6 54·3	3	,,	,,	9 4 32·08	+39 14 55·0	*n*
,, 23 10 10 37·56	+0 14·49	−11 26·9	2	9·6590	0·6551	9 10 15·45	+38 44 32·5	*o*
,, ,, ,,	+0 3·56	+ 4 50·7	2	,,	,,	9 10 15·44	+38 44 32·1	*p*

Comparison Stars.

	Name.	Mag.	Mean Place 1921·0. R.A.	Decl.	Reduction to Apparent Place. s	"	Authority.
			h m s	° ′ ″			
a	B.D. 66° 527	9·5	7 45 10·423	+66 12 21·00	+0·434	+0·72	Greenwich Astrog.
b	B.D. 66° 529	9·5	7 48 15·899	+66 4 52·26	+0·448	+0·78	,, ,,
c	Piazzi VII. 236	7·3	7 53 5·098	+64 57 43·68	+0·478	+0·55	See note.
d	B.D. 56° 1269	7·9	8 3 57·459	+56 2 16·50	+0·557	−2·22	A.G.C., Helsingfors.
e	B.D. 56° 1270	9·1	8 4 8·439	+55 56 8·15	+0·561	−2·25	,, ,,
f	B.D. 52° 1286	9·1	8 6 6·458	+52 34 36·06	+0·573	−3·48	Equat. Comp. with *g*.
g	B.D. 52° 1292	7·7	8 10 16·980	+52 35 3·31	+0·581	−3·36	A.G.C., Harvard.
h	O.A. (N) 8616	8·2	8 3 10·820	+51 32 48·74	+0·571	−4·03	,, ,,
i	B.D. 51° 1395	9·5	8 6 47·8	+51 41 (28)	+0·572	−3·90	
j	O.A. (N) 8731	9·1	8 9 14·136	+50 19 48·17	+0·587	−4·34	,, ,,
k	B.D. 50° 1526	9·5	8 11 20·4	+50 40 (28)	+0·583	−4·20	
l	O.A. (N) 8819	8·1	8 13 54·954	+50 31 28·75	+0·588	−4·14	,, ,,
m	B.D. 39° 2213	9·5	9 6 11·881	+39 19 40·71	+1·148	−4·37	Helsingsfors Astrog.
n	B.D. 39° 2217	8·8	9 7 19·213	+39 8 5·09	+1·153	−4·41	,, ,,
o	W.B. (2) IX. 98	7·3	9 9 59·811	+38 56 3·85	+1·148	−4·44	A.G.C., Lund.
p	W.B. (2) IX. 102–3	8·5	9 10 10·727	+38 39 45·94	+1·151	−4·52	,, ,,
q	Lal. 35466	7·9	18 54 3·237	+45 24 3·07	+2·533	−0·86	See note.
r	B.D. 37° 4003	8·2	20 34 29·359	+37 13 29·07	+2·505	+1·70	A.G.C., Lund.
s	W.B. (2) XX. 1166	8·7	20 36 32·640	+37 15 44·62	+2·498	+1·65	,, ,,
t	W.B. (2) XXI. 90	8·7	21 7 45·573	+32 23 40·72	+2·453	+1·93	,, Leiden.
u	W.B. (2) XXI. 96	8·9	21 7 49·593	+32 27 34·61	+2·455	+1·92	See note.
v	B.D. 28° 4123	9·2	21 29 18·874	+28 22 16·43	+2·411	+4·04	,,
w	B.D. 28° 4128	8·8	21 30 39·044	+28 36 16·90	+2·407	+3·95	Greenwich C., 1910.
x	Anonymous	11·5	21 31 17·836	+28 30 22·99	+2·404	+3·96	Equat. Comp. *w*, *y*.
y	B.D. 28° 4140	8·8	21 33 39·202	+28 28 30·31	+2·395	+3·94	Greenwich C., 1910.
z	B.D. 23° 4432	9·3	21 53 41·388	+24 17 21·07	+2·347	+5·18	Oxford Astrog.
A	W.B. (2) XXI. 1254	8·3	21 54 16·271	+24 22 15·60	+2·345	+5·14	Greenwich C., 1910.
B	B.D. 19° 4894	9·0	22 13 24·148	+19 20 46·84	+2·292	+6·72	Abbadia.
C	Piazzi XXII. 80	6·8	22 15 0·207	+19 34 2·67	+2·288	+6·61	See note.

Notes.

The observations are corrected for the effects of the motion of the comets, but not for parallax or differential refraction.

On most occasions comet *a* had a fairly well-defined nucleus; comet *b* was large and bright on June 7, but appeared decidedly fainter on June 9 and 11; comet *c* was very faint and ill-defined.

The place of star *c* is derived from a combination of Greenwich Astrographic and Greenwich 1900 Catalogues. That of star *q* is derived from Bonn VI., Paris 1875, Bonn A.G.C., with a P.M.

of +″·05 in Decl. That of star *u* from a combination of Bonn VI. with Lund A.G.C. That of star *v* from Cambridge A.G.C., Oxford Astrographic, Bonn X. Star *x* had a nebulous appearance, and was observed to test whether it was a detached fragment of comet *b*. It is not in the Oxford Astrographic, but is shown on the Franklin-Adams Charts. The place of star *C* is derived from Abbadia, with the application of P.M. +ˢ·0033 −″·037 given in Berlin A.G.C.

Photographic Position of Comet 1921 *c* (*Dubiago*).

The following position was derived from a photograph taken with the 30-inch reflector by Mr. Melotte:—

G.M.T. 1921.	Comet's Apparent R.A.	Comet's Apparent Decl.	Log Factors of Parallax.	
d h m s	h m s	° ′ ″		
June 7 11 12 6	10 29 20·75	+29 15 30·5	9·6224	0·7643

The Stellar Magnitude Scales of the Astrographic Catalogue. Sixteenth Note: The Cordoba Magnitudes for −27°, −29°, *and* −31°, *with some remarks on the whole region* −15° *to* −43°. By H. H. Turner, D.Sc., F.R.S., Savilian Professor.

1. The Cordoba counts for −25° were given in the eleventh note (1917 Nov.). The counts for −27°, −29°, and −31° recently received from Mr. Perrine are specially welcome for a number of reasons; they sensibly extend our knowledge of the Southern Hemisphere, and that too in a region where new information was urgently wanted; they give a clear answer to the questions suggested, as will be seen below; and last but not least, they are tangible evidence of the great progress made with the measures of these zones. I have reason to hope that before long we may have the volumes of measures themselves.

2. The counts as supplied by Mr. Perrine are given in Tables I., II., and III.

Table I.

Counts of Zone −27° (*Cordoba*) *for each hour. Numbers of plates,* 7, 8, 7, 8, *etc.*

	50.	40.	30.	20.	10.	All.	Gal. Lat.
h							°
0	6	11	57	161	611	181	−87·5
1	7	13	83	177	537	183	−79·5
2	2	16	55	186	677	203	−65·5
3	14	15	91	198	552	170	−52·5
4	4	10	98	212	653	159	−39·5

TABLE I.—*continued.*

h	50.	40.	30.	20.	10.	All.	Gal. Lat.
5	17	36	130	304	1170	499	−27°·0
6	24	55	227	762	2280	690	−14·5
7	44	66	363	1255	4555	1516	− 2·5
8	16	50	235	893	2676	925	+ 8·5
9	22	37	155	494	1519	289	+18·5
10	7	9	44	182	725	299	+26·5
11	4	21	41	176	682	228	+32·5
12	7	13	55	183	568	59	+35·0
13	2	15	103	303	632	166	+33·5
14	16	17	72	248	1060	453	+29·0
15	14	33	136	358	1051	233	+22·0
16	10	35	164	379	1331	482	+13·0
17	12	23	191	715	2428	1044	+ 2·0
18	19	36	179	766	3419	474	−10·0
19	8	35	127	526	2026	345	−22·0
20	5	15	51	256	1212	345	−34·5
21	12	17	85	253	797	102	−47·5
22	2	14	37	162	546	183	−61·0
23	6	6	34	118	437	254	−74·5

TABLE II.

Counts of Zone −29° (*Cordoba*) *for each hour.*
Numbers of plates, 7, 6, 7 ; 7, 6, 7, *etc.*

h	50.	40.	30.	20.	10.	All.	Gal. Lat.
0	2	9	16	71	388	217	−86°·0
1	0	1	23	69	350	209	−79·5
2	3	1	15	70	339	398	−66·0
3	4	9	24	128	541	387	−53·0
4	3	6	38	154	804	461	−40·0
5	7	0	54	206	1084	566	−27·5
6	12	21	83	361	1978	1571	−15·5
7	12	16	94	330	1692	1222	− 3·5
8	10	11	65	336	1550	1180	+ 7·5
9	1	9	41	204	1163	992	+17·5
10	4	7	27	152	835	436	+25·5
11	6	6	49	186	823	347	+31·0
12	2	6	31	140	980	714	+33·0
13	3	2	24	149	842	812	+32·0

TABLE II.—*continued.*

	50.	40.	30.	20.	10.	All.	Gal. Lat.
h							
14	9	16	38	203	1166	763	+28°0
15	6	10	50	216	1018	709	+20·5
16	5	23	64	246	940	1137	+11·0
17	12	36	149	637	2835	1929	+ 0·5
18	11	29	131	542	2696	1681	−11·0
19	6	11	66	262	1005	711	−23·0
20	6	14	57	148	722	431	−35·5
21	6	10	39	174	583	366	−48·0
22	0	4	18	78	300	268	−61·5
23	5	10	36	100	445	170	−74·5

TABLE III.

Counts of Zone −31° (Cordoba).
Numbers of plates, 7, 6, 7; 7, 6, 7, etc.

	50.	40.	30.	20.	10.	All.	Gal. Lat.
h							
0	4	5	24	102	462	309	−85°0
1	0	1	30	60	378	254	−79·0
2	4	8	29	91	422	294	−66·0
3	3	7	18	77	485	435	−53·5
4	5	6	23	98	454	273	−40·5
5	6	6	23	109	542	521	−28·0
6	14	14	60	227	1339	1035	−16·0
7	17	13	63	213	1432	1147	− 4·5
8	4	5	38	149	2059	2555	+ 6·0
9	3	3	28	209	1489	1261	+15·5
10	4	12	42	189	1532	913	+23·5
11	2	10	31	152	1218	1166	+29·0
12	1	6	49	203	1278	793	+31·0
13	1	4	26	199	1290	1369	+30·0
14	2	1	25	173	1372	1812	+26·0
15	4	7	41	141	1124	950	+19·0
16	7	6	46	198	1470	1854	+10·0
17	18	54	253	1105	4229	1307	− 0·5
18	7	28	142	741	4475	2336	−11·5
19	2	2	23	155	1035	1532	−23·5
20	1	4	21	124	881	760	−36·0
21	3	8	25	97	528	556	−48·5
22	1	2	19	86	506	297	−61·5
23	2	...	26	94	575	434	−74·5

3. These numbers have been treated according to the procedure fully exhibited in *M.N.*, 78, 54 (1917 Nov.), and used in subsequent papers. First the cumulative counts were found by adding the successive members of each row. The heading 50 in Tables I., II., and III. refers to all stars with diameter 51 or greater; the heading 40 to those with diameter 41 to 50; so that on adding this to the former we get all diameters greater than 40; adding the next we get all greater than 30, and so on. Of these cumulative totals the logarithms were taken, and from these was subtracted log 4 (each plate representing 4 square degrees) and log n where n is the number of plates (whether 8 or 7 or 6) in the hour. These reduced logs are considered to be log N_γ as represented on p. 57 (*loc. cit.*), and log N_0 (where N_0 is the corresponding density per square degree on the Galactic Equator) is deduced by the formula there given, viz.—

$$\log N_0 = (1 + \cdot 0025\gamma) \log N_\gamma + K,$$

γ being the galactic latitude as shown in the last column of each table. If the galactic condensation were the only phenomenon affecting star density, and if we have accurately assessed it, the deduced values of log N_0 should all be the same throughout the R.A. circuit. The residual differences from the mean values are shown for the more important columns in Table IV. The residuals for the brighter stars have been formed but are not given here, partly to economise printing, but also because there are difficulties in treating them fully owing to some compartments being blank and thus giving logarithms infinite numerically.

4. We proceed to analyse these columns of residuals harmonically, and in Table V. the harmonics for the brighter stars are also shown (formed on the crude hypothesis that we may supply one star in any blank hour) but not used. They are separated from the utilised results by the first horizontal line. The differential results shown below the second horizontal line of each table are formed by subtracting the sum of the numbers for "30 and 20" from the sum of "10 and All" and then dividing by the difference of sums of log N_0 as in former papers.

TABLE IV.

Cordoba Residuals after Correction for Galactic Latitude.
(*The Unit is* 0·01 *in log* N_0.)

	−27°				−29°				−31°			
h	30.	20.	10.	All.	30.	20.	10.	All.	30.	20.	10.	All.
0	+ 2	+ 5	+15	+16	−17	−17	− 5	− 6	+ 3	+ 6	+ 2	− 1
1	+12	+ 7	+ 4	+ 6	−15	−12	− 4	− 4	+ 8	− 7	− 4	− 7
2	− 1	+ 5	+12	+12	−35	−25	−19	− 5	+14	+ 2	− 9	−12
3	+15	+ 4	− 4	− 4	− 3	+ 2	0	+ 2	− 7	−13	−11	− 9
4	+ 9	+ 2	− 4	− 5	+10	+11	+15	+13	+ 5	− 2	−13	−20
5	+12	0	− 2	+ 1	+ 1	+ 1	+ 4	0	−14	−19	−29	−29

TABLE IV.—*continued.*

	−27°				−29°				−31°			
h	30.	20.	10.	All.	30.	20.	10.	All.	30.	20.	10.	All.
6	+24	+22	+15	+15	+14	+11	+12	+13	+13	0	− 7	−11
7	+25	+24	+22	+22	+13	+ 2	− 2	− 2	+12	− 7	−14	−17
8	+15	+18	+12	+13	− 8	− 6	−11	− 9	−25	−33	− 8	0
9	+ 8	+ 4	− 1	− 5	−20	−16	−11	− 7	−31	−12	− 7	− 7
10	−34	−28	−21	−18	−16	− 9	− 5	− 9	+11	+ 7	+15	+ 9
11	−28	−26	−20	−19	+ 7	+ 3	− 1	− 8	− 4	− 4	+ 5	+ 8
12	−13	−14	−16	−22	−13	−10	+ 5	+ 8	+12	+12	+14	+ 8
13	+ 2	+ 3	−12	−14	−20	− 3	+ 6	+13	−10	+12	+17	+23
14	− 6	− 7	− 1	+ 3	+ 3	+ 2	+ 8	+ 7	−26	− 6	+ 6	+17
15	+ 6	− 2	−11	−13	− 4	− 6	−10	−10	− 6	−17	−13	−13
16	+ 4	− 8	−13	−12	+ 6	− 4	−17	− 9	− 5	−11	− 8	− 2
17	− 8	− 3	− 5	− 3	+25	+20	+11	+10	+57	+51	+27	+11
18	+ 5	+12	+19	+16	+26	+22	+19	+17	+39	+41	+38	+29
19	+ 3	+ 9	+14	+11	+18	+16	+ 5	+ 4	−24	− 7	− 2	+10
20	−18	− 4	+12	+12	+23	+ 5	+ 1	− 2	−18	− 6	+ 1	+ 2
21	+10	+ 8	+ 5	+ 1	+14	+15	+ 3	+ 1	+ 3	+ 5	− 9	− 4
22	−18	− 6	0	+ 2	−20	−11	−15	−10	−10	− 1	+ 4	− 2
23	−30	−23	−13	− 4	+16	+ 4	+ 2	− 6	− 5	0	+ 6	+ 6

TABLE V.

Harmonic Analysis for −27°.

log N_0.	sin θ.	cos θ.	sin 2θ.	cos 2θ.	sin 3θ.	cos 3θ.	sin 4θ.	cos 4θ.
9·66	+·118	−·074	−·077	−·162	−·022	+·085	−·054	+·044
0·25	+·068	−·038	−·036	−·113	−·062	+·038	+·023	−·015
0·93	+·081	+·018	+·036	−·121	−·035	+·045	+·023	−·042
1·51	+·045	+·040	−·015	−·098	−·019	+·036	+·058	−·035
2·09	+·018	+·076	−·052	−·068	+·002	+·025	+·081	−·012
2·18	+·023	+·086	−·048	−·063	−·002	+·041	+·084	−·005
1·83	−·085	+·104	−·121	+·088	+·054	−·015	+·084	+·060
1·00	−·047	+·057	−·066	+·048	+·029	−·008	+·046	+·033

Harmonic Analysis for −29°.

9·40	−·048	−·040	−·012	−·215	−·127	+·001	+·103	+·078
9·88	−·149	−·055	−·102	−·169	−·086	+·024	−·068	+·101
0·59	−·079	+·021	−·045	−·130	−·022	−·030	+·008	+·072
1·27	−·053	+·010	−·023	−·095	−·029	−·045	−·003	+·045
2·00	−·012	−·005	+·010	−·045	−·022	−·057	+·018	+·062
2·20	−·023	−·006	+·029	−·027	−·018	−·049	+·022	+·018
2·34	+·097	−·042	+·107	+·153	+·011	−·031	+·035	−·037
1·00	+·042	−·018	+·046	+·065	+·005	−·013	+·015	−·016

TABLE V.—*continued.*

Harmonic Analysis for $-31°$.

log N_0.	sin θ.	cos θ.	sin 2θ.	cos 2θ.	sin 3θ.	cos 3θ.	sin 4θ.	cos 4θ.
9·25	+·139	+·031	+·025	−·275	+·055	+·140	−·109	+·100
9·71	+·038	−·062	−·023	−·242	+·061	−·023	−·150	+·155
0·49	−·035	+·034	+·040	−·062	+·118	+·008	−·021	+·129
1·20	−·111	+·013	+·008	−·009	+·076	−·035	−·006	+·112
2·03	−·112	−·037	−·012	+·032	+·065	−·024	+·021	+·070
2·28	−·119	−·051	−·010	+·044	+·024	−·022	+·046	+·031
2·62	−·085	−·135	−·070	+·147	−·105	−·019	+·094	−·140
1·00	−·033	−·052	−·027	+·056	−·040	−·007	+·036	−·054

5. In *M.N.*, **79**, 570, the results for a number of zones are assembled; but erroneous figures were given for Zone $-15°$, and there is much new material. In Table VI. below the results to date are given.

TABLE VI.

Zone.	sin θ.	cos θ.	sin 2θ.	cos 2θ.	sin 3θ.	cos 3θ.	sin 4θ.	cos 4θ.
−15°	+·017	−·093	−·095	−·035	+·002	+·034	+·061	−·043
−16	−·069	−·054	−·091	−·029	−·024	+·035	+·057	+·004
−17	−·074	−·104	−·042	−·001	+·096	−·076	+·046	−·053
−18	+·047	−·049	−·129	−·043	+·065	+·019	+·088	+·007
−19	·000	−·084	+·002	−·024	·000	+·032	+·048	−·013
−25	−·024	+·068	−·014	+·027	−·007	−·017	+·022	−·042
−27	−·047	+·057	−·066	+·048	+·029	−·008	+·046	+·033
−29	+·042	−·018	+·046	+·065	+·005	−·013	+·015	−·016
−31	−·033	−·052	−·027	+·056	−·040	−·007	+·036	−·054
−32	−·043	·000	−·008	−·025	−·011	−·013	+·013	−·032
−34	−·061	+·001	−·002	+·063	−·015	+·014	+·057	−·004
−36	−·055	+·020	−·014	−·004	+·005	−·021	+·014	−·004
−38	−·127	+·003	+·048	−·037	−·038	−·015	+·053	+·010
−41	−·113	−·037	−·004	−·025	−·021	−·033	−·009	+·003
−42	−·088	+·026	+·001	−·030	+·036	−·006	−·022	+·012
−43	−·043	−·002	−·006	−·007	−·002	−·066	+·002	+·023
Numl. Mean	·055	·042	·038	·030	·025	·021	·038	·022

6. The gap between $-19°$ and $-25°$ will be presently filled, but already we can see what the general results are likely to be. The mean numerical values of the columns show that the first harmonic is the largest, though the excess is not marked. But the first harmonic undoubtedly dies down near $-29°$, the mean

numerical coefficients for the six zones $-25°$ to $-34°$ being only $\sin\theta = 42$ and $\cos\theta = 33$, and the signs being moreover not consistent. On opposite sides of this weak link in the chain the phase is quite different. The algebraical means are—

$-15°$ to $-19°$ $\quad -\cdot016\sin\theta - \cdot077\cos\theta = -\cdot079\cos(\theta - 12°)$
$-25°$ to $-31°$ $\quad -\cdot016\sin\theta + \cdot013\cos\theta = -\cdot021\cos(\theta - 131°)$
$-32°$ to $-38°$ $\quad -\cdot072\sin\theta + \cdot006\cos\theta = -\cdot072\cos(\theta - 95°)$
$-41°$ to $-43°$ $\quad -\cdot081\sin\theta - \cdot004\cos\theta = -\cdot081\cos(\theta - 87°)$

These figures suggest a very rapid change in the phase near $-22°$, which particular zone has fortunately been selected for special scrutiny at more than one observatory, as explained in the paper by Mr. Bellamy in this same number of the *Notices*. It will be therefore convenient to reserve the final discussion until we have the expected material in this gap.

Summary.

Counts given for the three zones $-27°$, $-29°$, and $-31°$ are analysed by the adopted process. The change in star density with star magnitude shows a weak link in this neighbourhood as compared with adjacent zones.

Note on a Slight Variation of the Linear Scale of Stellar Photographs with the Size of the Star Image. By F. A. Bellamy, M.A.

1. The zone $-22°$ of the Astrographic Survey is included as part of the official programme ($-21°$ to $-23°$) for the Observatory of Santiago de Chile. As the measuring of the plates was not proceeding very fast at Santiago, we undertook to assist in the measurement of one zone ($-22°$) at the University Observatory, Oxford, in 1917, funds being provided by the Government Grant Committee of the Royal Society. The first batch of plates received from Santiago was very satisfactory in point of the number of stars, all being in the Milky Way; these plates were not impressed with the usual form of réseau with continuous lines, but had only small portions of the réseau lines shown. This form of réseau rendered it impossible for the plates to be measured in the usual way with a ruled glass scale; so a copy of our réseau was made on plate-glass and superimposed on the Santiago plate. The réseaued copy was slightly reduced in size, and the two films were placed together in the measuring instrument, this réseau was then adjusted by hand so as to reduce the orientation (b and d) and the constants (c and f) approximately to zero. The two films were not permanently fixed together, but, in order that the réseaued

plate, as cut down, might be used repeatedly, narrow strips of thin plate-glass about half an inch long were cemented to the edges of the negative at certain places by means of celluloid and made to butt against the edges of the réseaued plate as adjusted for orientation. Finally, as a further precaution against any possible movement during measurement, short pieces of lantern-slide binding-strips were fixed to the edges; the united plate could then be freely handled. About 40 of such plates with attached réseaus have been sent from and returned to the observatory by parcel post, in only one instance was the réseau displaced; in that case the package must have received a violent blow, as nearly all the binding and the glass strips were displaced.

The method was first tried here more than twenty years ago. The late Mr. S. A. Saunder was so much impressed with the success then obtained that he adopted it, with suitable precautions, for all the measures made for him by the late Mr. J. A. Hardcastle on the photographs of the moon. Until its use for the Santiago plates an extended trial had never been given, except by Mr. Saunder and Mr. Hardcastle.

In the measurement of the Santiago plates by this method an additional check was applied by making measures of four points near the corners in x and y. These were repeatedly made during the time the plate was under measurement: in no case was any displacement of the réseau detected. The incident referred to above occurred after the plate was completely measured and revised.

The introduction of narrow strips of glass, for butting the cut-down réseaued plate against, was begun for the Santiago plates. These strips serve as important safeguards; if the réseaued plate be removed and these, or essential ones at certain points, be allowed to remain, the same réseaued plate can be replaced at any future time with considerable accuracy.

2. After 37 of the plates received from Santiago had been measured in this way, the other plates in zone $-22°$ which had been received, about 100 in number, were examined before their preparation for measurement and found to be defective in some way, mainly by having too small a number of stars. Ultimately application was made in 1919 to Dr. Hough, at the Cape of Good Hope Observatory, to take the plates required for this zone; through his kind co-operation 48 plates were received in 1920 July and 48 in January of this year. As these plates had the complete réseau the measurement of them was proceeded with at once, in preference to further measures of the Santiago plates, with the superimposed réseau, and 35 of them have been measured and the reductions completed, in addition to 5 improved plates of regions already measured on the Santiago plates—amounting in all to about half the zone.

3. Further, for a reason connected with the magnitudes of the images (*not* their positions, which are the subject of the present note), Professor Turner had suggested that this same zone ($-22°$)

should also be photographed and measured at a northern observatory, in order that the magnitudes as photographed at a northern and a southern observatory might be compared (see *M.N.*, 79, 571): the Nizamiah Observatory, Hyderabad, has undertaken to assist. Hence this zone ($-22°$) is being photographed and dealt with, in whole or in part, at three different observatories; while at a fourth observatory we are utilising some of the valuable material which is being provided.

4. The first circumstance to suggest the present investigation occurred in this way. The measures and reductions of a Cape plate ($-22°\ 10^h\ 56^m$) had just been completed when the measures of the same region were received from Hyderabad; the plate constants of both had been determined from the same 25 reference stars observed on the meridian at the observatory, Bouzaréah, Algiers. (Advance proof-sheets of the Algiers Meridian Catalogue, $-18°$ to $-23°$, have most courteously been sent to us by the Director.)

A direct comparison was easily made between the measures of these 25 stars on photographs taken at Hyderabad and the Cape, thus eliminating any Algiers influence. Using the plate constants thus derived, a general comparison was then made for all the 318 stars measured on both plates. The resulting differences were found to be surprisingly large, indicating some real systematic error. The constants determined from the bright stars were obviously unsuitable for the fainter stars. It may be remarked that the constants c and f merely represent the differences of plate centre, so need no further reference in this note. The values derived from this direct comparison for the constants for scale and orientation are as follows:—

Cape—Hyderabad.

	a.	*b.*	*d.*	*e.*
Catalogue Stars	+·02041	−·00553	+·00554	+·02032
All Stars	+·02075	−·00553	+·00561	+·02070
(All—Cat.)	+·00034	·00000	+·00007	+·00038

5. It will be seen that the differences in b and d (orientation) are small; but there is a sensible difference in a and e (scale value). The inference appears to be that the scale value changes with the magnitude of the star, or, what amounts to the same thing for this purpose, the size of the image of the star on the plate which can be varied by the duration of the exposure. If this be so generally, there is plenty of material already available on the astrographic plates at other observatories for detecting the change, if any, between the 6^m and 20^s exposures, or whatever exposures may have been given that have produced a sufficient relative difference in the size of the images; an equivalent difference of more than two magnitudes is desirable.

As we are concerned primarily with the Oxford O.G. and its results, I first tested the point under discussion by using one of the

plates, $+25^\circ$ 17^h 48^m, plate 2840, which I exposed and measured in 1910. The displacement between the images was made in y (towards the south). When I measured the 20^s images recently I avoided all knowledge of what the difference was between the 7^m and 20^s images, the measures being made without any conscious bias: this applies to any measures used in this note. The results for this Oxford plate were (unit = ″·003):—

Δa.	Δb.	Δd.	Δe.
+·00004	+·00004	·00000	−·00001

which appeared to be reassuring as regards our Oxford plates and seemed to show that for our O.G. this systematic error is small.

6. A comparison of a Santiago plate, with the supplementary réseau, and a Hyderabad plate for the same region (-22° 5^h 52^m) was made with the following results for S—H:—

Santiago—Hyderabad.

	a.	*b*.	*d*.	*e*.
All Stars	+·01486	−·00070	+·00076	+·01516
Bright Stars	+·01467	−·00059	+·00086	+·01483
(All—Bright)	+·00019	−·00011	−·00010	+·00033

Here again a and e seem to indicate something of a systematic character, and turned our thoughts towards the assumption that the cause of these differences was in the Hyderabad O.G., because the O.G.s of the Cape, Oxford, and Santiago astrographic telescopes were of similar construction, size, and focal length, whereas the Hyderabad lens was quite different in every way except the focal length; it is a Taylor photo-visual lens of 8 ins. diameter and a focal length of 133 ins., made by Cooke & Sons (*Hyderabad Astrographic Catalogue*, 1, p. vi), the other three object-glasses being 13 ins. in aperture and approximately 136 ins. focus.

Having three plates at Oxford which had been exposed at Hyderabad, it was possible to test this point further. I accordingly measured the first and third exposures independently in positions D. and R. for plate -17° 12^h 28^m. There were only 43 stars showing measurable third images, some of them excessively faint and one obviously a planet.

The differences between the first and third images did show a variation over the plate of a nature that would explain the discordance noticed, though not large enough. On further scrutiny it was seen that the effect was chiefly restricted to the brighter stars. The material was therefore divided into two parts, viz. (a) stars for which d (for the 20″ exposure) exceeds 9 units (say mag. 10·5), (b) stars with $d < 9$. The value of the scale difference was then determined by "least squares" as follows:—

Hyderabad alone.

	Bright Stars.	Faint Stars.
Change in a	−·00013	+·00001
Change in e	−·00022	−·00006

7. It is not at all surprising that the faintest stars should fail to show the effect. We may presume that it is due to the gradual growth of the image, which takes place not symmetrically round the first impress but more (or less) rapidly in the direction away from the plate centre. [We shall find some evidence of both directions, and will return to this point later.] But it further appears that this unsymmetrical growth takes a little time to develop.

8. In any case, however, the effect as measured in the Hyderabad plates alone is still too small to explain the differences C—H. Hence a Cape plate (-22° 10^h 56^m), which had already been measured in the usual way for the zone, was similarly examined. The stars were again divided into two groups, bright and faint stars, and the results were :—

Cape alone.

	Bright Stars.	Faint Stars.
Change in a	+ ·00010	− ·00003
Change in e	+ ·00017	− ·00005

9. It will be seen that the Cape values are opposite in sign to those for the Hyderabad plate, hence in C—H the two effects are added together. It is difficult to say whether the sum is precisely equivalent to that found in a direct comparison of plates, as the quantities are small and the magnitudes of a number of stars are involved. But they appear to be of about the right order, and the general inference seems to be :—

Summary.

(1) That the Hyderabad O.G. makes the images grow away from the centre.

(2) That the Cape O.G. makes them grow towards the centre.

(3) That although for some O.G.s the effect may be insensible (as it seems to be for the Oxford O.G. from an examination already made), nevertheless the point is worth testing in all cases, especially as the material already exists on the astrographic plates at the various observatories. Measures of the 20^s images on several plates, on which the 6^m images are already measured, would soon settle the question whether such an effect is sensible for any particular O.G. and what is its amount approximately. Whenever such an effect is sensible it is clear that corrections are required to the adopted constants (which are derived from images that are generally large) to make them applicable to the generality of stars.

1921 *June* 9.

Proper Motions of Stars in the Pleiades. By W. M. Smart.

(*Communicated by Professor A. S. Eddington, F.R.S.*)

1. At the beginning of 1920, two plates of the Pleiades (region of Alcyone) were obtained with the photographic film placed outwards, and an experimental reduction of the proper motions of stars in the field was made by placing the plates film to film with plates taken, in the usual way, by A. R. Hinks some years previously. The character of the images obtained through the glass was satisfactory, and the preliminary results appeared to be in good agreement with the proper motions derived by F. J. M. Stratton (*Mem. R.A.S.*, 57, 161). Accordingly, several additional plates were taken when the Pleiades were again suitably placed for observation, and these have been compared with early plates and the proper motions of over 130 stars derived.

2. Table I. gives a list of the plates.

TABLE I.

Plate No.		Date.	Exposure.
9	A	1898 Oct. 21	20 mins.
16	B	Nov. 3	10 ,,
463	C, D	1905 Dec. 30	3, 4 ,,
570	E	1906 Nov. 27	2 hours.
601	F	1907 Jan. 17	2 ,,
1067	G	1920 Feb. 8	2 hours.
1090	H	Nov. 18	2 ,,
1092	K	Dec. 6	2 ,,
1092*a*	L	Dec. 12	3 ,,
1110	M, N	1921 Mar. 10	5, 6 mins.

Plates 463, 1110 contain four images of each star, and of these the measures of two corresponding groups were made (denoted by C, D and M, N). The exposures in 1920 and 1921 were made on Ilford Monarch Plates of specially selected glass, and there is no indication that the passage of the light through the glass has had any serious effect on the quality of the images.

All but the last of the recent plates were obtained in or near the meridian at mid-exposure time. The hour-angle of the Pleiades for plate No. 1110 was $1\frac{1}{2}$ hours W. approximately.

The correction to be applied to the focal setting, when the exposure is made through glass, was determined experimentally and applied for each of the recent plates. For the Sheepshanks telescope of 19·3 feet focal length the correction has an effect just perceptible under the best conditions.

The time-factor (ratio of exposure times in photographing through glass and photographing directly to obtain equal images) seems to be about 3; that is to say, to obtain a plate through

glass with the images of diameter equal to corresponding images on a plate of 1 hour's direct exposure, the exposure requires to be about 3 hours. This high ratio constitutes a rather serious disadvantage in any observing programme of this kind.

3. *Measures.*—An early and a recent plate were placed film to film with corresponding images close together, but not overlapping, and securely held together by means of strong clips. The combination was then placed in the Cambridge measuring machine. The approximate positions of the stars on the plates were obtained from C. Wolf's list of Pleiades stars (*Annales de l'Observatoire de Paris*, 14). The distances between corresponding images, in the X and Y directions, were then measured. All the plates were measured by Dr. M. Hasimoto of the Mizusawa Observatory, H. E. Green, and W. M. Smart, two or three settings being made on each image in each co-ordinate. In cases of discordance in the measures of a star by the three measurers, the images were re-observed and discordant measures rejected. Generally, if any one measure deviated more than 15–20 units (1 unit of the micrometers = 0″·017) from the mean of the three measures, the images were further observed and the mean of all the measures taken. Thus each final measure in the X and Y co-ordinates represents the mean of at least 6 settings, and, in a few instances of difficult images, of as many as 12 settings.

It is important to test the stability of pairs of plates in the measuring machine during the interval necessary for the complete measurement of the images. Two stars, with well-formed images on each plate, were measured several times in the course of the measurement of the plates, and the accordance of the results was uniformly satisfactory. In no pair of plates was there any evidence of a relative shift of the plates during the progress of measurement.

The following table shows the way in which the plates were combined :—

TABLE II.

Plate-pair No.	Combination of Plates.	Interval (in years).
I.	E and K	14·0
II.	F ,, L	14·0
III.	A ,, H	22·0
IV.	B ,, L	22·2
V.	E ,, G	13·2
VI.	C ,, M	15·2
VII.	D ,, N	15·2

4. *Reduction.*—For each star the linear equations

$$\Delta x = p_x + ax + by + c \quad . \quad . \quad . \quad . \quad (1)$$

$$\Delta y = p_y + dx + ey + f \quad . \quad . \quad . \quad . \quad (2)$$

were formed, Δx and Δy being the measured distances between pairs of corresponding images, and p_x and p_y the proper motions (all expressed in terms of the scale-unit).

The method * of determining the plate constants was that first described by Christie and Dyson (*M.N.*, **55**, 61). A selection of 40 stars symmetrically situated, as far as possible, about the centre, 10 in each quadrant, was made after a preliminary reduction of I and V. These stars appeared on all the plates. The visual magnitudes of the selected stars had a range, with one or two exceptions, of two magnitudes (8^m–10^m in Wolf's list). In this way the determination of the proper motions from the pairs of plates I.–VII. was effected in a uniform manner, the derived proper motions of all the stars being relative to the mean motion of the group. Plates I. were reduced by the method of least squares (employed almost universally by investigators on proper motions), and there appeared to be no gain of accuracy over the method adopted.

5. The mean interval between the plate-pairs I., II., V., VI., VII. is 14·3 years, and between III., IV. 22·1 years. In Table III., below, the values of p_x and p_y in III. and IV. are given as $\frac{2}{3}$ of the values actually derived from equations (1) and (2). In forming the means of p_x and p_y derived from all 7 pairs, double weight has been given to III. and IV., and the mean interval has been taken to be 14·5 years. The unit in columns I.–VII. in Right Ascension and Declination is the scale-unit ($1 = 0''{\cdot}017$). The mean relative proper motions per century (in seconds of time in Right Ascension and in seconds of arc in Declination) are simply obtained by applying the factors 0·0085 and 0·117 to the means of p_x and p_y respectively.

The star numbers in the first column of Table III. are those of Wolf.

The stars belonging to the group of 40 are indicated by an asterisk.

TABLE III.

No.	p_x. I.	II.	III	IV.	V.	VI.	VII.	μ_α.	p_y. I.	II.	III.	IV.	V.	VI.	VII.	μ_δ.
								s								″
57		+11						+0·19		+47						+1·5
60		+41						+0·45		+51						+1·9
62	+10	+17	+ 7	− 2	− 7	+20	+11	+0·16	+ 7	+31	+15	+12	+10	−13	+17	−2·6
65	+23	+19						+0·28	+42	+43						+1·0
68	+35	+28	+23	+ 3	+20			+0·26	+36	+21	+46	+ 2	+51			+0·0
69	+19	+27	−14	+14	0			+0·18	+ 7	+16	+25	+ 0	+28			−2·3
72	+ 1	+14	+ 3	+ 3	+ 2	+13	+ 6	+0·14	+ 3	+ 4	+13	− 1	+ 9	− 9	−13	−3·8
*73	+ 6	+11	−20	0	+12	+ 7	− 5	+0·09	+11	+24	+25	+ 5	+24	+16	+25	−2·0
76	+11	+21	+13	+ 2	− 8	+ 6	+13	+0·17	− 5	−48	−10	− 7	− 7	−26	−43	−6·1
77	−29	−23	−30	−28	−22			−0·15	+33	+34	+36	+26	+42			+0·0
79	+ 2	+42	+ 7	+ 5	− 4	+17	+22	+0·19	− 7	+ 6	+19	+ 5	− 4	+ 4	−39	−3·9

* See also H. N. Russell, *Determination of Stellar Parallax*, Washington, 1911.

TABLE III.—*continued.*

o.	p_x I.	II.	III.	IV.	V.	VI.	VII.	μ_α.	p_y I.	II.	III.	IV.	V.	VI.	VII.	μ_δ.
								s								″
86	−17	−32	−32	−30	−27			−0·14	+57	+59	+52	+47	+37			+1·8
87	+16	+14	0	−4	+8	+9	+16	+0·15	−29	−21	+21	−5	−5	−19	−24	−4·9
91	−15	+3	+6	0	−15	+3	−6	+0·08	+17	+16	+12	+8	+4	+2	−10	−2·8
00		−9						+0·02		−20						−6·3
01	+7	+9	+1	+2	+13	+3	−1	+0·13	−20	−6	−4	−17	−15	−18	−20	−6·0
03	+7	+8	+7	+2	+3	+9	+15	+0·16	+2	+11	+8	+10	+15	−2	+9	−3·1
05	+2	−3	+9	−6	−5	+9	+4	+0·12	−15	+4	0	−10	−12	−19	−23	−5·2
06	+8	+5	+4	−3	−7	+10	0	+0·12	−29	−42	+11	−9	−21	−54	−31	−5·9
07	+13		+3	−1	+3	+21	−8	+0·13	−21		+7	−16	+2	−27	−9	−4·9
09	+3	+1	−5	−2	+7	+14	+7	+0·12	−1	+9	+2	−7	+17	−11	+13	−3·8
12		+11						+0·19		+50						+1·8
13		−6						+0·05		+41						+0·8
14	+17	+19	−4	+2	+15	+10	+13	+0·17	+9	+16	+17	+2	+7	+13	+21	−2·6
16	+11	−10						+0·10	+74	+79						+4·9
20	+7	−8	+8	−5	−10	+12	+2	+0·11	0	−3	+3	0	−1	+1	−3	−4·0
21	+2	+1	+4	+4	−3	+2	+11	+0·12	−18	+3	0	−4	−14	−20	−12	−4·8
29	−13	−11	+13	−3	−5	−7	+11	+0·10	−23	−6	−10	−2	−17	−7	−17	−5·3
31		−12						+0·00		+72						+4·4
37	−39	−28	−48	−45	−26			−0·24	+52	+72	+70	+57	+52			+3·2
38		+32						+0·37		+14						−2·4
41	−19	−7	−8		−18	−15	−4	+0·01	+25	+43	+34		+18	+27	+26	−1·0
43	−3	0	+4	+5	−11	−1	−1	+0·10	+4	+3	+5	+4	+7	+3	−11	−3·4
46	+9					+25		+0·24	−45					−21		−7·9
48	+20	+4	+7	−6	+13			+0·14	−9	0	+15	−12	+12			−3·9
51	−6	−4	+10	−4		−11	+14	+0·10	0	−1	−1	−17		+10	+18	−4·1
52	+2	+13	+2		+11			+0·15	−1	−1	−4		+2			−4·2
54	−15	−12	−17	−27	−21	+1	−4	−0·01	+4	−5	+23	+14	+4	+27	−14	−2·8
58	−20	−34	−46	−28	−41			−0·20	−9	+26	+41	+13	+25			−1·4
59		+5						+0·14		+36						+0·2
61	+2	−5	+5		+4	−6	−16	+0·09	−25	−12	−1		−17	+10	−4	−4·7
68	+31	−1	−12	0	+17	0	+3	+0·13	−19	−3	−11	−5	−1	−10	−7	−4·9
69	+3	−9	+2	+6	+9	−3	+14	+0·13	−13	−8	−6	−7	−10	+3	+8	−4·6
72		−13						−0·01		+63						+3·4
75		−41	−1	−12				−0·01		+27	+26	+12				−1·5
79	+15	0	+4	+6	+25			+0·18	−29	−20	−6	−24	−21			−6·2
80		−22						−0·09		+14						−2·4
81	+22	0	+12		+28			+0·20	+4	+4	+30		+30			−1·5
82	0	+5	+10	+6	−7	−10	−4	+0·12	−34	−14	−22	−13	−29	−14	+5	−5·6

TABLE III.—*continued.*

No.	p_x. I.	II.	III.	IV.	V.	VI.	VII.	μ_α.	p_y. I.	II.	III.	IV.	V.	VI.	VII.	μ_δ.
								s								"
183		−37						−0·21		+49						+1·7
184		−57						−0·38		+41						+0·8
186	0	−9	−1	−18	−6			+0·03	+16	+36	+31	+32	+52			−0·1
187		−23						−0·10		+40						+0·7
*188	+6	+1	+8	+5	+3	0		+0·12	−38	−31	−24	−19	−29	−30		−7·0
*189	−16	−1	−8	−10	+2	−8	−4	+0·04	+6	+6	+13	+19	+24	+5	+9	−2·5
*192	+1	+8	+3	+4	+1	+6	−15	+0·12	−22	+2	−7	−6	−13	0	+15	−4·6
*196	+2	−1	0	+4	−1	+10	+4	+0·12	−6	−10	+4	−6	+5	+23	+11	−3·8
198	−15	−31	−26	−30	−29	−33	−19	−0·14	+28	+48	+56	+44	+41	+62	+70	+1·9
*202	+15	−1	+11	+2	+5	0	−10	+0·13	−22	−4	−16	−10	−9	+5	+10	−4·9
204	−26	−45	−40	−37	−21			−0·20	+40	+47	+55	+42	+50			+1·5
205		−15						−0·03		+66						+3·7
207		−1						+0·09		+20						−1·7
208	−69	−49	−23	−43	−42	−43		−0·26	−18	−1	+4	+7	+9	−3		−3·9
*209	−8	−4	+4	+10	−3	−15	−2	+0·10	−16	−2	−14	+2	−15	+3	+10	−4·6
212	−3	−10	+6	+11	−6	−15	+3	+0·10	−17	−3	−8	−3	−12	+5	+19	−4·3
*213	−13	−4	+7	+3	−7	−11	−1	+0·08	−16	−1	−30	0	−21	+4	−7	−5·3
214	−17	−4	+13	+9	−12	+1	+9	+0·13	−31	−11	−25	−19	−31	−7	−9	−6·3
216				−9				+0·02				+15				−2·3
*217	−13	−6	+8	+12	−11	−18	−1	+0·09	−26	−6	−21	−2	−23	−11	−13	−5·6
218		+3	−8	−2				+0·07		+13	−16	+12				−3·9
219	−13	−19	−10	−12	−27	−29	−31	−0·05	+9	+5	+8	+10	+18	+21	+22	−2·6
222	−29	−8						−0·05	−14	+5						−4·4
*225	−12	−5	+3	+1	−14	+9	−7	+0·08	−26	−7	−14	+7	−14	−14	−3	−5·0
226	−8	−3	+6	+9	−5	−15	−16	+0·09	−15	0	−23	−7	−18	−14	−13	−5·5
*233	−29	−7	−18	−20	−32	−20	−22	−0·07	+6	+29	+29	+23	+14	+16	+18	−1·5
235	+41	+37	+25		+33	+30	+15	+0·35	−34	−20	−8		−30	−29	−14	−5·9
*237	+14	+6	+2	+4	+6	+10	+14	+0·16	−24	−1	−11	−16	−10	−13	−18	−5·5
*240	−7	−15	−8	−15	−24	−12	−9	−0·01	+11	+39	+46	+28	+32	+34	+30	−0·1
244		−38			+17			+0·02		+59			+50			+2·3
247	−19	−17		+14				+0·08	−2	+13		−8				−4·1
*249	+10	−8	+4	−3	+2	+4	+6	+0·12	−23	+2	−2	+3	−15	−4	−6	−4·6
258	+7	−5		+21				+0·22	+27	−8		+32				−1·5
262		−38			−43			−0·22		+39			+31			−0·1
*264	−5	−18	−10	−14	−19	−1		+0·01	−4	+19	+15	+4	+21	−1		−3·0
*269	+6	−12	+10	+7	+4	+4	+7	+0·14	+8	+1	+34	+14	+24	+6	+9	−1·9
*275	+1	+3	+6	+11	−6	+16	+19	+0·16	−21	+1	−8	−3	−5	−5	+4	−4·6
*280	−1	+13	+10	+10	−4	−11	−1	+0·13	−28	−8	−25	−17	−27	−23	−7	−6·3

TABLE III.—*continued.*

No.	p_x. I.	II.	III.	IV.	V.	VI.	VII.	μ_α.	p_y. I.	II.	III.	IV.	V.	VI.	VII.	μ_δ.
								s								″
284	−30	−28						−0·15	+42	− 1						−1·7
*286	−14	+23	− 6	+11	− 3	+ 3	0	+0·12	−20	−25	+ 1	−12	− 3	−14	−16	−5·3
*288	− 2	− 1	− 4	− 6	+ 5	− 4	− 1	+0·07	+12	−16	+ 6	+ 1	−10	+ 5	0	−4·0
292	+57	+45	+53	+54	+57			+0·55	−20	−40	− 7	−14	− 8			−5·9
*296	+10	− 3	+ 4	+ 8	+13	+ 6	+12	+0·16	−16	− 4	−12	−10	− 4	−11	−16	−5·2
299		+48						+0·51		+ 6						−4·3
*300	− 6	− 4	+14	+13	− 6	− 8	− 4	+0·13	−31	− 4	−28	−17	−22	−12	−22	−6·3
301		+62						+0·63		+41						+0·8
*307	+ 2	− 4	+ 3	+ 6	+ 9	−10	− 6	+0·11	−13	− 4	−23	− 5	− 8	− 3	−14	−5·3
313		−31						−0·16		+12						−2·6
314		− 9						+0·02		+ 8						−3·1
317		− 2						+0·08		− 1						−4·1
318	−34	−20			− 9			−0·08	+ 5	+21			+12			−2·5
*326	+11	0	−18	−11	0	− 4	0	+0·05	+20	+20	+19	+11	+ 8	+10	+ 7	−2·4
328	+24	+11	+ 7	+18	+ 3			+0·20	−17	− 9	−45	− 5	− 9			−6·2
333	+11	− 2			+ 7			+0·14	+17	+13			+21			−2·0
335		+ 2						+0·12		+25						−1·1
338	+ 8	+23	+40	+30	+ 4	+24	+28	+0·31	−40	−16	−50	−22	−22	−30	−21	−7·5
*347	+ 5	+ 2	+10	+ 8	+13	+ 7	+13	+0·17	+16	−12	− 7	−17	+ 5	− 3	−14	−4·7
350	+11	+24	+24	+19	+24			+0·28	−22	−10	−11	−25	−35			−6·3
354	−25	−22			−16			−0·08	+47	+10			+46			+0·0
*358	− 5	+ 9	+17	− 5	− 2	+ 6	+ 6	+0·13	−31	− 9	−29	−16	−21	−30	−32	−6·8
364		+ 8						+0·17		−19						−6·2
365	+ 6	+ 8	+17	+12	0	0	+11	+0·18	−43	−22	−33	−14	−40	−31	−25	−7·3
370	+ 8	− 1	+21	+19	+ 3	− 4	+ 6	+0·14	−33	−15	−39	− 7	−20	−26	−35	−6·9
376	− 4	+ 8	+21	+11	− 8	+11	− 6	+0·16	−44	−23	−37	−15	−13	−11	−37	−7·0
378	+ 5	+20			+15			+0·21	−22	−32			−29			−7·3
384	+14	+ 5	− 1	+ 1	0			+0·13	+18	+ 2	+31	− 3	+32			−2·2
*393	+11	+20	+ 9	+18	+24	+15	+17	+0·23	−12	−20	−18	− 9	−13	−13	−21	−5·8
400	−22	−21			− 3			−0·02	+12	+35			+48			−0·3
406	+ 8	0	+17	+14	+12	+ 4	+ 4	+0·19	−39	−40	−46	− 7	−30	−26	−59	−7·8
407	− 8	−11	−21	− 4	−16			+0·01	+26	+25	+20	+15	+12			−1·8
408		+24						+0·30		−19						−6·2
*415	− 1	+ 1	− 1	+ 3	+ 1	+ 1	+ 3	+0·11	−17	+ 3	+ 2	+10	− 2	− 4	−13	−4·1
418	− 4	+ 7	+10	+ 7	0	+11	+28	+0·17	−44	−37	−44	−17	−33	−21	−20	−7·6
*420	+ 6	− 7	−17	−13	− 2	0	+ 1	+0·04	−12	+ 6	− 5	+12	+ 8	0	− 9	−3·9
422	+30	+34	+11	+10				+0·24	−32	− 7	−32	−14				−6·2
423	− 2	− 2	+14	+10	+ 9	+ 7	+21	+0·18	−67	−51	−54	−30	−36	−25	−45	−8·0

TABLE III.—*continued.*

No.	p_x. I.	II.	III.	IV.	V.	VI.	VII.	μ_α.	p_y. I.	II.	III.	IV.	V.	VI.	VII.	μ_δ.
								s								"
429		− 2						+0·08		+ 9						− 3·0
430		− 8						+0·03		− 6						− 4·7
432		−19						−0·06		+15						− 2·2
433		−29						−0·14		−21						− 6·5
*436	− 1	− 5	+ 5	− 4	+11	+10	−14	+0·10	− 9	− 5	+ 4	+14	+13	+17	− 8	− 3·4
441	− 3	+21	−14					+0·08	−25	−38	−24					− 7·3
447	+11	+29	+24	+13	+13	+23	+36	+0·28	−46	−17	−22	− 9	−22	+10	+ 5	− 5·6
448	+ 1	+ 1	+22					+0·19	0	+ 1	+22					− 2·8
453			+10					+0·19			+37					+ 0·3
457			+ 5					+0·14			− 8					− 4·9
458			+47					+0·49			+47					+ 1·5

6. *Reduction to Absolute Motions.*—The mean centennial proper motions obtained from columns I.–VII. in Table III. are relative to the group of 40 selected stars. Of these, 7 appear in Boss's *Preliminary General Catalogue*, and the relative proper motions can thus be compared with the absolute proper motions as given by Boss. Kromm's list* of absolute proper motions of 160 Pleiades stars has a much larger number of stars in common with the Cambridge list. As pointed out by Van Maanen,† who compared the absolute proper motions of 14 stars common to Boss and Kromm, there exists a systematic difference in the centennial motions:—

in Right Ascension, $\mu_B - \mu_K = +0^s{\cdot}13$
in Declination, $\mu_B - \mu_K = -0''{\cdot}9$.

I have compared the Cambridge relative proper motions (from at least six determinations) with the proper motions of Boss and Kromm. Table IV. shows the centennial differences.

TABLE IV.

	Remarks.	Right Ascension.	Declination.
(*a*) Boss − Camb.	7 stars	$\mu_B - \mu_C = +0^s{\cdot}08$	$\mu_B - \mu_C = -4''{\cdot}3$
(*b*) Kromm − Camb.	7 stars [as in (*a*)]	$\mu_K - \mu_C = -0^s{\cdot}08$	$\mu_K - \mu_C = -3''{\cdot}8$
(*c*) Kromm − Camb.	24 cluster stars	$\mu_K - \mu_C = -0^s{\cdot}01$	$\mu_K - \mu_C = -2''{\cdot}7$
(*d*) Kromm − Camb.	(*b*) and (*c*) combined	$\mu_K - \mu_C = -0^s{\cdot}03$	$\mu_K - \mu_C = -3''{\cdot}1$

By applying the difference, Boss − Kromm, as found by Van Maanen, the difference Boss − Camb. is formed for (*d*). The results are:—

in Right Ascension, $\mu_B - \mu_C = +0^s{\cdot}10$
in Declination, $\mu_B - \mu_C = -4''{\cdot}0$.

* *Annales de l'Observatoire de Bordeaux*, **14**, 77.
† *Contributions from Mount Wilson Observatory*, No. 167, 10.

For the 7 stars common to Boss and Cambridge, the results are, from (*a*), $+0^s\cdot08$ and $-4''\cdot3$, which are in good agreement with the values just found. Regarding Boss's proper motions as accurate absolute motions, we convert the Cambridge proper motions (relative to the mean of the group of 40 stars) to absolute motions by applying the following corrections to the relative motions:—

in Right Ascension, $+0^s\cdot10$
in Declination, $-4''\cdot0$.

The absolute centennial motions so derived (μ_α, μ_δ) are shown in columns 9 and 17 of Table III.

The proper motion of Alcyone (Boss 869) is given by Boss as $+0^s\cdot14$ and $-4''\cdot8$, and the mean motion of the cluster is given by approximately the same figures. The magnitude of the correction required to reduce the relative motions to absolute motions shows that the majority of the group of 40 stars (probably about 30) belong to the cluster proper. This is confirmed by the absolute proper motions of the individual stars as shown in Table III.

7. *Comparisons.*—I have compared the results given in Table III. with the proper motions derived by F. J. M. Stratton (*Mem. R.A.S.*, 57), F. Kromm and Lagrula (*Travaux de l'Observatoire de Lyon*, 3, 1901). The proper motions derived by Stratton and Lagrula are relative to Alcyone, and I have reduced these to absolute motions by applying the proper motion of Alcyone ($+0^s\cdot14$ and $-4''\cdot8$). Kromm's results are absolute proper motions with the systematic difference, with respect to Boss's proper motions, of $+0^s\cdot13$ and $-0''\cdot9$. These corrections have, accordingly, been applied to Kromm's results. The comparison is shown in Table V., stars with less than three observations being excluded.

TABLE V.

	Right Ascension.				Declination.			
No.	Camb.	Str.	Lag.	Kr.	Camb.	Str.	Lag.	Kr.
	s	s			″	″		
68	+0·26	+0·27			+0·0	−5·6		
69	+0·15	+0·18			−2·3	−6·2		
72	+0·14	−0·01	−0·01	−0·05	−3·8	−4·4	−4·7	−4·8
73	+0·09	+0·05	+0·25	+0·27	−2·0	−4·8	−5·2	−3·5
77	−0·15	+0·07			0·0	−3·6		
91	+0·08	+0·08	+0·10	+0·17	−2·8	−3·2	−6·1	−3·4
101	+0·13	+0·04	+0·10	+0·37	−6·0	−6·8	−6·9	−4·2
105	+0·12	+0·06	+0·00	+0·25	−5·2	−5·8	−5·4	−5·0
109	+0·12	+0·17	+0·01	+0·12	−3·8	−6·4	−5·2	−4·2
114	+0·17	+0·18			−2·6	−6·4		
120	+0·11	+0·02	+0·10	+0·11	−4·0	−3·2	−5·9	−3·7
137	−0·24	−0·21			+3·2	+1·1		
141	+0·01	+0·10	+0·12	+0·26	−1·0	−1·7	−2·3	−0·4

TABLE V.—*continued.*

	Right Ascension.				Declination.			
No.	Camb.	Str.	Lag.	Kr.	Camb.	Str.	Lag.	Kr.
	s	s			″	″		
143	+0·10	+0·07	+0·10	+0·22	−3·4	−4·4	−5·2	−3·7
148	+0·14	+0·21			−3·9	−8·1		
151	+0·10	+0·08	+0·07	+0·10	−4·1	−5·0	−5·0	−4·7
152	+0·15	+0·21			−4·2	−7·1		
158	−0·20	−0·12			−1·4	−5·8		
161	+0·09	+0·05	+0·04	+0·10	−4·7	−3·0	−3·2	−7·4
168	+0·13	+0·06			−4·9	−4·6		
169	+0·13	+0·15	+0·05	+0·13	−4·6	−5·4	−4·6	−4·9
175	−0·01	+0·02			−1·5	−3·8		
182	+0·12	+0·10	+0·08	+0·21	−5·6	−5·0	−4·7	−3·7
186	+0·03	−0·04			−0·1	−2·4		
188	+0·12	+0·24	+0·20	+0·15	−7·0	−6·2	−4·4	−4·7
189	+0·04	+0·05			−2·5	−4·4		
192	+0·12	+0·11	+0·09	−0·01	−4·6	−4·2	−5·5	−3·2
196	+0·12	+0·11	+0·10		−3·8	−3·4	−2·1	
198	−0·14	−0·21	−0·04	−0·01	+1·9	+0·1	+0·2	+0·1
202	+0·13	+0·26	+0·04	+0·18	−4·9	−5·0	−4·1	−3·0
204	−0·20	−0·25	−0·05		+1·5	−1·1	−3·5	
208	−0·26	−0·31	−0·21	−0·30	−3·9	−0·5	−2·2	−3·3
209	+0·10	+0·10	+0·12	+0·15	−4·6	−6·4	−4·6	−1·9
213	+0·08	+0·07	+0·19	+0·09	−5·3	−3·0	−5·5	−2·9
214	+0·13	+0·17	+0·02	+0·16	−6·3	−3·6	−4·5	−3·9
225	+0·08	−0·01	+0·15	−0·03	−5·0	−4·2	−4·6	−3·6
226	+0·09	+0·10	+0·12	+0·13	−5·5	−5·0	−4·8	−4·8
233	−0·07	+0·01			−1·5	−3·0		
235	+0·35	+0·33	+0·37	+0·53	−5·9	−5·4	−6·2	−7·6
237	+0·16	+0·15			−5·5	−3·8		
240	−0·01	+0·07			−0·1	−1·5		
249	+0·12	+0·10	+0·03		−4·6	−6·6	−7·1	
258	+0·22	+0·14			−1·5	−1·7		
264	+0·01	−0·15	−0·10		−3·0	−5·2	−2·1	
275	+0·16	+0·13	−0·05	+0·12	−4·6	−5·0	−4·3	
280	+0·13	+0·13	+0·16	−0·12	−6·3	−4·4	−4·2	−4·6
286	+0·12	+0·05			−5·3	−6·4		
288	+0·07	+0·10			−4·0	−5·6		
296	+0·16	+0·08	+0·14		−5·2	−5·4	−3·2	
300	+0·13	+0·10	+0·05	+0·21	−6·3	−4·4	−4·7	−5·7
307	+0·11	+0·15	−0·10	+0·18	−5·3	−5·4	−5·7	−6·1

TABLE V.—*continued.*

No.	Right Ascension. Camb.	Str.	Lag.	Kr.	Declination. Camb.	Str.	Lag.	Kr.
	s	s			″	″		
313	−0·16	−0·08			−2·6	−3·8		
317	+0·08	+0·02			−4·1	−3·4		
326	+0·05	−0·14			−2·4	−3·8		
328	+0·20	+0·10			−6·2	−5·8		
333	+0·14	−0·08			−2·0	−4·6		
338	+0·31	+0·34	+0·29	+0·32	−7·5	−6·6	−5·9	−5·9
347	+0·17	+0·23			−4·7	−5·4		
350	+0·28	+0·17			−6·2	−6·6		
354	−0·08	−0·06			+0·0	−1·3		
358	+0·13	+0·20	+0·10	+0·12	−6·8	−4·0	−4·4	−4·8
365	+0·18	+0·20	+0·09	+0·25	−7·3	−5·0	−3·7	−5·3
376	+0·16	+0·13	+0·09	+0·24	−7·0	−5·6	−4·3	−4·4
378	+0·21	+0·14			−7·3	−6·8		
384	+0·13	−0·02			−2·2	−0·7		
393	+0·23	+0·13			−5·8	−5·6		
400	−0·02	+0·04			−0·3	−2·1		
407	+0·01	+0·05	−0·04	−0·08	−1·8	−0·7	−0·3	+0·9
415	+0·11	+0·02	−0·06	+0·12	−4·1	−1·5	−1·6	+1·2
418	+0·17	+0·20	+0·12	+0·07	−7·6	−4·0	−3·6	−6·2
420	+0·04	−0·08	+0·12		−3·9	−1·0	−0·5	

8. The centennial absolute proper motions derived from the Cambridge plates are shown diagrammatically. The distinction between the cluster stars and the remainder is fairly well exhibited. The accepted value of the position-angle of the cluster motion is 158°, a value which the diagram seems to confirm. The position-angle of the parallactic motion is 146°, and the non-cluster stars are fairly equally divided on either side of a line drawn in this direction.

9. *Probable Errors of the Results.*—A rough estimate of the probable errors of the results in Table III. has been made by considering the divergence of the individual p_x and p_y from the mean for each star, with not less than three observations. The values of p_x, p_y, however, are not quite independent, as plate E occurs in both I. and V. and plate L in both II. and IV. (Table II.) The resulting probable errors are 6 and 7 in the scale-units, or, per century,

$0^{s}\cdot05$ in Right Ascension
$0''\cdot8$ in Declination.

The figures of Table IV. appear to indicate a probable error of this order of magnitude.

10. I have not made any attempt to discuss the effect of the omission of the quadratic terms from equations (1) and (2). Several investigators, including Lee* and Kapteyn,† conclude that the effect of omitting the quadratic terms in a least-squares solution is in most cases negligible. On the other hand, Van Maanen includes the quadratic terms to obtain the best results

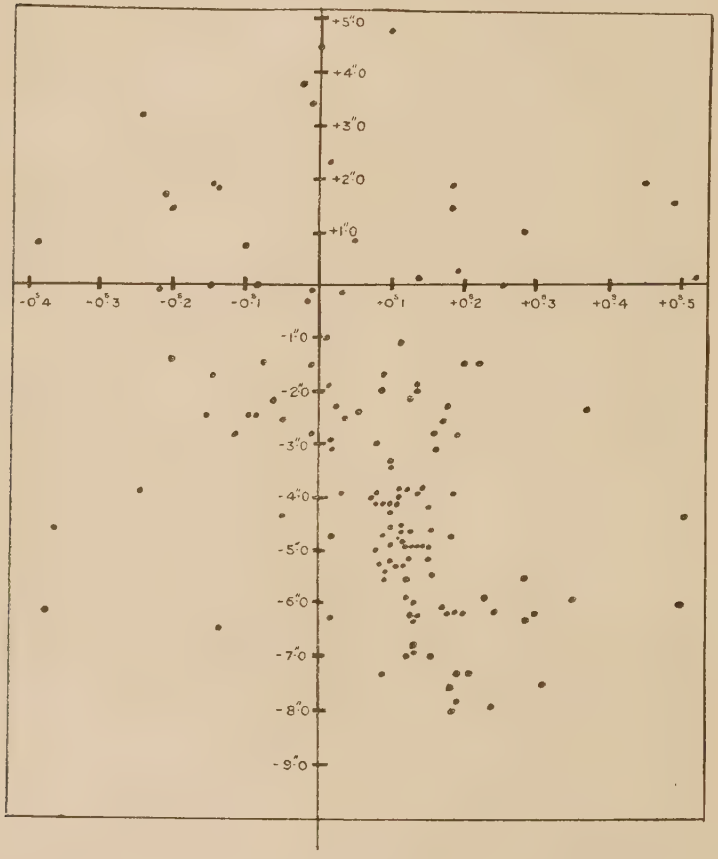

Absolute Proper Motions of Stars in the Neighbourhood of Alcyone.

for the residual proper motions. For a symmetrical distribution of stars, the coefficients of x and y in the linear expressions of (1) and (2) remain unaltered, as shown by Kapteyn, whether the quadratic terms are included or not: but a constant correction is required, in each co-ordinate, for the relative proper motions. On the reduction of the relative to the absolute proper motions,

* *Astronomical Journal*, **29**, 74.
† *Groningen Publications*, **14**, preface, xi.

this constant correction is absorbed in the general correction applied.

11. The general agreement of the results in Table III. with the proper motions derived by other investigators appears to show fairly conclusively that the method of comparing an early plate directly, without the introduction of the intermediary réseau system, with a plate of later date, in which the images are formed through the glass, yields results with an accuracy comparable with that given by the usual method of measuring. The work of measuring is reduced by one-half: in itself this is a considerable advantage. The quality of the images is unimpaired, but the exposure-times require to be increased considerably.

Observatory, Cambridge;
1921 *June* 4.

Star-Discs. By Arnold Buxton, M.A. (Plate 18.)

(*Communicated by Professor A. E. Conrady.*)

I. *Introduction.*

Owing to diffraction phenomena, the image of a star in the ordinary telescope consists of a small circular concentration of light, surrounded by a series of rings of rapidly diminishing intensity. An inquiry has been conducted here into the variation of the intensities of light in the image for ideal, out-of-focus, and out-of-focus together with spherical aberration conditions.

The problem was probably first recorded by Airy in 1834 in the *Cambridge Phil. Trans.* in a paper entitled "On the Diffraction of an Object Glass with Circular Aperture." He confined himself to the investigation of the distribution of light in the ideal focal plane for an object glass of known circular aperture. He tabulated values of the amplitudes by mechanical quadratures covering a range about the same as that given by Professor A. E. Conrady in Table II. of "Star-Discs," *Monthly Notices R.A.S.*, 1919 June. Lord Rayleigh developed the problem by investigating the light distribution in the discs in the presence of spherical aberration. He evaluated the central intensities by developing the integrals into series, and implied that the outer intensities might be calculated by mechanical quadratures. Existing work on the subject, however, has been very much extended by Professor A. E. Conrady in the paper already referred to, where the intensities and positions of the rings have been determined not only for ideal conditions, as in Airy's problem, but also when the image was out of focus and when the other aberrations were present. In the present paper the aim has been to extend Professor Conrady's data, and to provide information strengthening conclusions which were foreshadowed in previous work.

II. *The Determination of the Intensities of the Airy Spurious Disc.*

The intensities have been determined from the usual law, viz. that they are directly proportional to the square of the amplitudes of the vibrations, the determination of which is shown in the following analysis. The method adopted is to investigate, firstly, the amplitudes for a thin circular strip of light with given extreme differences of phase at points close to the optical axis and very near to the focus; secondly, to integrate the results over the whole given aperture.

Consider the elementary strip KPP_0' and let a parallel plane through F_0 represent the focal plane so that OF_0 is the optical axis and F_0 the focus.

Take OF_0 as the axis of x,
„ OP_0' „ „ y,
and „ OK „ „ z.

Let P be a point on the circle such that $\angle^{le} KOP = E$; then co-ordinates of P are $0, -r\sin E, r\cos E$.

Then the disturbance due to an element at P will arrive at a point F_1 in the focal plane and distance y_1 parallel to the y-axis from F_0, with a difference of phase $PF_1 - KF_1$ from that at K. Since the co-ordinates of F_1 are $(f, y_1, 0)$,

$$PF_1 = \{f^2 + (y_1 + r\sin E)^2 + r^2\cos^2 E\}^{\frac{1}{2}}.$$

Also $$KF_1 = \{f^2 + y_1^2 + r^2\}^{\frac{1}{2}} = \sqrt{f^2 + r^2},$$

neglecting terms in y_1^2, etc., as being of second order.

Thus $$PF_1 = \sqrt{f^2 + r^2}\left[\frac{(1 + ry_1\sin E)}{(f^2 + r^2)}\right]$$

or $$PF_1 - KF_1 = \frac{ry_1\sin E}{\sqrt{f^2 + r^2}}.$$

Hence if the vibration reaching F_1 from K is expressed as $a\sin\frac{2\pi t}{T}$, where T is the period of the light, it follows that the equation of the vibration reaching F_1 from P is

$$\eta = a\sin\left(\frac{2\pi t}{T} + W\sin E\right), \text{ where } W = \frac{ry_1}{\sqrt{f^2 + r^2}}.$$

Similarly for point P′ making $-E$ with the vertical OK, we have the vibration expressed as

$$\eta = a\sin\left(\frac{2\pi t}{T} - W\sin E\right).$$

These two vibrations will give a resultant vibration

$$\eta = a\sin\frac{2\pi t}{T}\cos(W\sin E)$$

$$= A\sin\frac{2\pi t}{T}, \text{ where A (the amplitude)} = a\cos(W\sin E).$$

The amplitude (A_1) at F_1 for the whole circular strip is obtained by integrating $a \cos(W \sin E)$ between the limits 0 and π, so that

$$A_1 = a\int_0^{\pi} \cos(W \sin E)dE = 2a\int_0^{\frac{\pi}{2}} \cos(W \sin E)dE$$

$$= 2a\int_0^{\frac{\pi}{2}}\left[1 - \frac{W^2 \sin^2 E}{\underline{|2}} + \frac{W^4 \sin^4 E}{\underline{|4}} - \frac{W^6 \sin^6 E}{\underline{|6}} + \ldots\right]dE$$

$$= 2a \cdot \frac{\pi}{2}\left[1 - \frac{W^2}{2^2(\underline{|1})^2} + \frac{W^4}{2^4(\underline{|2})^2} - \frac{W^6}{2^6(\underline{|3})^2} \cdots (-1)^s \frac{W^{2s}}{2^{2s}(\underline{|s})^2} \cdots\right]$$

$= a\pi J_0(W)$, where $J_0(W)$ is the Bessel Function of zero order.

Choosing a so that A_1 is unity when $W = 0$, or, in other words, making the central intensity unity as the standard, we have

$$a = \frac{1}{\pi},$$

so that

$$A_1 = J_0(W).$$

Consequently, the amplitudes of the vibrations are determined from tables of the Bessel Functions. Table I. was compiled by means of O. Lommel's table of $J_0(W)$ at the end of his *Studien über die Bessel'schen Functionem* (Leipzig, 1868); the values of W taken are 600°, 610°, 620°, etc., up to 1040°, the corresponding values up to 600° being already given in Table I., "Star-Discs," *Monthly Notices R.A.S.*, 1919 June. The amplitudes are seen to change sign between 670° and 680°, 850° and 860°, 1030° and 1040°; or, in other words, the intensities pass through zero values. Hence the roots of $J_0(W) = 0$ will correspond to the positions of the dark patches in the image, and the maximum and minimum values of $J_0(W)$ to the surrounding bright rings in the image. Now

$$W \text{ (in radians)} = \frac{2\pi}{\lambda} \frac{ry_1}{\sqrt{f^2 + r^2}},$$

where λ is the wave-length of the light (taken below as $5{\cdot}3 \times 10^{-5}$ cms.). A usual value of the ratio of the semi-aperture to the focal length $\left(\frac{r}{f}\right)$ is about $\frac{1}{30}$, so that

$$W = \frac{2\pi}{\lambda} \frac{ry_1}{f} \text{ approx.};$$

i.e.

$$y_1 = \frac{30 \times W \times \lambda}{2\pi} = \left[10^{-3} \times \frac{W}{4}\right] \text{ cms. approx.},$$

thus expressing the radii of the rings in terms of W.

The first root of $J_0(W) = 0$ corresponds to $W = 137\frac{3}{4}°$ approx., so that the radius of the first dark ring is ·0006 cm. The follow-

ing results give the radii of the dark rings corresponding to the first ten roots :—

W.	No. of Ring.	Rad. of Ring.
°		cms.
$137\frac{3}{4}$	1	·0006
$316\frac{1}{4}$	2	·0014
$495\frac{3}{4}$	3	·0022
675	4	·0029
855	5	·0037
1035	6	·0045
1215	7	·0053
1375	8	·0061
1575	9	·0069
1755	10	·0077

The radii of the first seven bright rings are given in the following table :—

W.	No. of Ring.	Rad. of Ring (y_1).
°		cms.
$219\frac{1}{2}$	1	·0009
402	2	·0017
583	3	·0025
$763\frac{1}{2}$	4	·0033
943	5	·0041
1124	6	·0049
1305	7	·0057

It has been shown that the amplitude for a thin circular strip of light is $J_0(W)$. If we now integrate this expression multiplied by $2\pi r dr$, the area of the strip, between the limits 0 and the radius of the circular aperture (say unity, in this case), we shall obtain the resulting amplitude over the whole aperture. Let A_2 be this amplitude, then

$$A_2 = 2\pi \int_0^1 J_0(W) r dr$$

$$= \pi \int_0^1 J_0\left(\frac{r y_1}{f}\right) dr^2$$

$$= \pi \int_0^1 \left[1 - \frac{b^2 r^2}{2^2(\underline{|}\,1)^2} + \frac{b^4 r^4}{2^4(\underline{|}\,2)^2} - \frac{b^6 r^6}{2^6(\underline{|}\,3)^2} \cdots (-1)^s \frac{b^{2s} r^{2s}}{2^{2s}(\underline{|}\,s)^2} \cdots \right] dr^2,$$

where $b = \frac{y_1}{f}$

$$= \pi \left[r^2 - \frac{b^2 r^4}{2 \cdot 2^2(\underline{|}\,1)^2} + \frac{b^4 r^6}{3 \cdot 2^4(\underline{|}\,2)^2} - \cdots \frac{(-1)^s b^{2s} r^{2s+2}}{2^{2s}(\underline{|}\,s)^2(s+1)} \cdots \right]_2^1$$

$$= \pi \left[1 - \frac{b^2}{2 \cdot 2^2(\underline{|}\,1)^2} + \frac{b^4}{3 \cdot 2^4(\underline{|}\,2)^2} - \cdots (-1)^s \frac{b^{2s}}{2^{2s}(\underline{|}\,s)^2(s+1)} \cdots \right]$$

$$= \pi \left[1 - \frac{c^2}{2(\underline{|}\,1)^2} + \frac{c^4}{3(\underline{|}\,2)^2} \cdots \frac{(-1)^s c^{2s}}{(s+1)(\underline{|}\,s)^2} \cdots \right], \text{ where } b = 2c,$$

$$\text{or } A_2 c = \pi\left[c - \frac{c^3}{2(\underline{|}\,1)^2} + \frac{c^5}{3(\underline{|}\,2)^2} \cdots \frac{(-1)^s c^{2s+1}}{(s+1)(\underline{|}\,s)^2} \cdots\right]$$

$$= \pi\left[\frac{b}{2} - \frac{b^3}{2^4(\underline{|}\,1)^2} + \frac{b^5}{3 \cdot 2^5(\underline{|}\,2)^2} \cdots \frac{(-1)^s b^{2s+1}}{2^{2s+1}(s+1)(\underline{|}\,s)^2} \cdots\right]$$

$$= -\pi \frac{dJ_0(b)}{db}$$

$$= \pi J_1(b),$$

so that

$$A_2 = \frac{\pi}{2b} J_1(b) = \frac{\pi f}{2y_1} J_1\left(\frac{y_1}{f}\right), \text{ where } J_1 \text{ is the Bessel Function of first order.}$$

The dark patches are again given where $J_1\left(\frac{y_1}{f}\right) = 0$, *i.e.* where $J_0\left(\frac{y_1}{f}\right)$ is a maximum or minimum, so that the radii of the dark rings are given by the same table as those for the bright rings in the case of the thin circular strip. Similarly, by taking the maxima and minima values of $\frac{\pi f}{2y_1} J_1\left(\frac{y_1}{f}\right)$, which occur where $J_2\left(\frac{y_1}{f}\right) = 0$, it can be shown on the above assumptions as to f-ratio and wave-length that the radii of the first seven bright rings are ·0013 cm., ·0021 cm., ·0029 cm., ·0037 cm., ·0045 cm., ·0053 cm., and ·0061 cm. It will have been noticed that the rings are practically equidistant in all cases, and for other f-ratios and wave-lengths the radii will be proportional to both. Table II. is an extension of Professor Conrady's table from 600° to 1000° at 40° intervals. Since, in his table, the central intensity was chosen as the standard for comparison and taken as unity, it follows that, as $A_2 = \frac{\pi}{4}$ when $\frac{y_1}{f} = 0$, the amplitudes given in Table II. are $\frac{4}{\pi}$ times the corresponding amplitudes given by the expression $\frac{\pi f}{2y_1} J_1\left(\frac{y_1}{f}\right)$.

III. *The Determination of the Amplitudes and Intensities under Out-of-focus Conditions.*

This problem differs from that considered in the last section in that the disturbances considered will be out of phase by an extra amount due to the image being out of focus. It can easily be shown that the difference of length between the optical path of the marginal and axial rays is altered by a term proportional to the square of the aperture. Hence the disturbance

arrives out of phase at the point in the new focal plane corresponding to F_1 (fig. 1) by an extra amount c_1r^2 where c_1 is a constant. The new vibration for an element of the thin circular strip is

$$\eta = a \sin\left(\frac{2\pi t}{T} + W \sin E + c_1 r^2\right).$$

Compounding this vibration with that for the element equidistant from the z-axis, the new vibration is

$$\eta' = a \cos W \sin E \sin\left(\frac{2\pi t}{T} + c_1 r^2\right).$$

The latter is clearly composed of two vibrations at right angles to each other and amplitudes $a \cos W \sin E \cos c_1 r^2$ and $a \cos W$

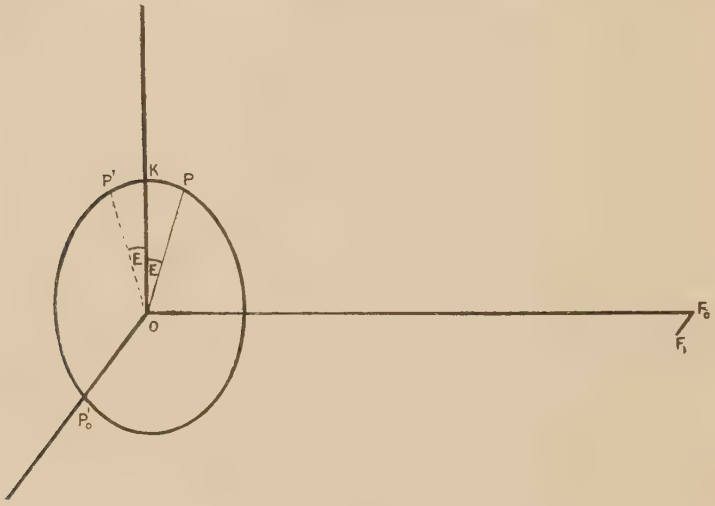

FIG. 1.

$\sin E \sin c_1 r^2$ respectively. Integrating these expressions over the circular strip and then over the whole aperture, we have the resulting amplitudes as

$$A_3 = a\pi \int_0^1 J_0\left(\frac{ry_1}{f}\right) \cos c_1 r^2 dr^2$$

and

$$A_4 = a\pi \int_0^1 J_0\left(\frac{ry_1}{f}\right) \sin c_1 r^2 dr^2.$$

Choosing a as before and noting that the required intensity is equal to the sum of the squares of A_3 and A_4, it follows that the

$$\text{Intensity} = \left[\left\{ \int_0^1 J_0\left(\frac{ry_1}{f}\right) \cos c_1 r^2 dr^2 \right\}^2 + \left\{ \int_0^1 J_0\left(\frac{ry_1}{f}\right) \sin c_1 r^2 dr^2 \right\}^2 \right].$$

Both the above integrals have been discussed elsewhere,* but the solutions have been left in terms of functions which have yet to be evaluated. Hence the integrals were computed by mechanical quadratures, the assumption being that the graphs of the integrands approximate to polynomials of the fourth degree. In Table III. the squares of the amplitudes A_3 and A_4 are tabulated and written as $A^2\cos^2\psi$ and $A^2\sin^2\psi$. Professor Conrady's results for the intensities when the marginal zone is $\frac{1}{2}\lambda$ out of focus have been extended from 600° to 1000°. Also the intensities are shown for the cases when the marginal zone is $\frac{3}{4}\lambda$, 1λ, $1\frac{1}{2}\lambda$, 2λ, and 4λ out of focus. The linear changes of focus corresponding to these amounts are, for F/15, ·028″, ·038″, ·056″, ·076″, ·152″ on either side of the perfect focus.

The general tendency of the intensities is shown in the graphs. After the marginal zone is half a wave-length out of focus the central intensities diminish rapidly and the light is scattered into the outer part of the diffraction pattern, thus deteriorating the image. For $\phi = \frac{1}{2}\lambda r^2$ the central intensity is down to 40 per cent. of the Airy spurious disc; for $\frac{3}{4}\lambda r^2$ it is at 9 per cent., then becomes zero for $1\lambda r^2$, 4·5 per cent. for $1\frac{1}{2}\lambda r^2$, and again zero for $2\lambda r^2$ and $4\lambda r^2$. In fact, for a central intensity $J_0\left(\frac{ry_1}{f}\right) = 1$, and therefore its value can be shown to be $\frac{\sin^2 c_1/2}{c_1^2/4}$. Hence it follows that, when c_1 is an even multiple of π, or when the image is out of focus by one, two, three, four, etc., whole wave-lengths, the central intensity is zero and therefore useless for star observation. On the other hand, when c_1 is an odd multiple of π, then the value of the central intensity is $\frac{4}{c_1^2}$, so that it is practically zero after $c_1 = 5\pi$.

The intensity curves for $\phi = 2\lambda r^2$ and $\phi = 4\lambda r^2$ are plotted on five and ten times respectively the scale of the other curves.

IV. *The Intensities when Spherical Aberration is Present.*

Hitherto it has been assumed that the system has been perfectly corrected or is free from spherical aberration, coma, and astigmatism. Even when the intensities were studied under out-of-focus conditions, it was tacitly assumed that the shifts of focus were not accompanied by the introduction of the various optical aberrations. The intensities will now be found, firstly, when spherical aberration alone is present; secondly, when it is present under out-of-focus conditions; coma and astigmatism will be assumed to be absent in both cases. If ϕ be the extra difference of phase due to the introduction of spherical aberration, it may be shown that ϕ can be expressed as a series of even powers of the aperture with constant coefficients, beginning at the fourth power when

* See Gray and Matthews, *Treatise on the Bessel Functions and their Application to Mathematical Physics.*

there are no out-of-focus conditions. Neglecting the terms involving sixth and higher powers of the aperture, $\phi = c_2 r^4$, where c_2 is a constant. Hence for simple spherical aberration the intensity can be expressed as

$$\left[\left\{ \int_0^1 J_0\left(\frac{ry_1}{f}\right) \cos c_2 r^4 dr^2 \right\}^2 + \left\{ \int_0^1 J_0\left(\frac{ry_1}{f}\right) \sin c_2 r^4 dr^2 \right\} \right].$$

These integrals were evaluated by the same method of mechanical quadratures as was used in the case of out-of-focus conditions; the results are tabulated in Table IV. for $\frac{1}{4}$ wave-length of primary spherical aberration. It is interesting to note that the central intensity is given by

$$\left[\int_0^1 \cos c_2 r^4 dr^2 \right]^2 + \left[\int_0^1 \sin c_2 r^4 dr^2 \right]^2.$$

By the simple substitution $z = c_2 r^4$, the first integral can be transformed into

$$\frac{1}{2\sqrt{c_2}} \int_0^{c_2} \frac{\cos z}{\sqrt{z}} dz = \frac{1}{2}\sqrt{\frac{\pi}{2c_2}} \int_0^{c_2} J_{-\frac{1}{2}}(z) dz,$$

and similarly the second integral becomes

$$\frac{1}{2}\sqrt{\frac{\pi}{2c_2}} \int_0^{c_2} J_{\frac{1}{2}}(z) dz.$$

Both integrals * without the factor $\sqrt{\frac{\pi}{2c_2}}$ have been tabulated by Lommel (*Abhandl. Münch. Ak.*, (2), **15**, 120, 1886) for different values of the upper limit, so that the central intensities for varying amounts of primary spherical aberration can readily be found.

The question now arises as to how the intensities will be affected by combining out-of-focus conditions with spherical aberration. The intensity is now determined by the expression

$$\left[\int_0^1 J_0\left(\frac{ry_1}{f}\right) \cos (c_2 r^4 + c_1 r^2) dr^2 \right]^2 + \left[\int_0^1 J_0\left(\frac{ry_1}{f}\right) \sin (c_2 r^4 + c_1 r^2) dr^2 \right]^2,$$

where c_1 represents the number of wave-lengths out of focus admitted in addition to c_2 wave-lengths of primary spherical aberration. The computation was effected as before, and the results shown in Table IV. and graphically in figs. 2 and 3, where the relative merits of different combinations of c_2 and c_1 can be noticed. Much guidance can, however, be obtained in this respect by the consideration of the values of the central intensities. These are now determinable in the form

$$\left[\int_0^1 \cos (c_2 r^4 + c_1 r^2) dr^2 \right]^2 + \left[\int_0^1 \sin (c_2 r^4 + c_1 r^2) dr^2 \right]^2.$$

* A good table is given on p. 25 in *Funktionentafeln mit Formeln und Kurven*, by Jahnke and Emde.

Making the substitution $c_2 z = \left(c_2 r^2 + \frac{c_1}{2}\right)^2$, the first integral reduces to

$$\frac{1}{2\sqrt{c_2}} \cos \frac{c_1^2}{4c_2}\left[\int_0^{\frac{1}{c_2}\left(c_2+\frac{c_1}{2}\right)^2} \frac{\cos z dz}{\sqrt{z}} - \int_0^{\frac{c_1^2}{4c_2}} \frac{\cos z dz}{\sqrt{z}}\right]$$

$$+ \frac{1}{2\sqrt{c_2}} \sin \frac{c_1^2}{4c_2}\left[\int_0^{\frac{1}{c_2}\left(c_2+\frac{c_1}{2}\right)^2} \frac{\sin z}{\sqrt{z}} dz - \int_0^{\frac{c_1^2}{4c_2}} \frac{\sin z dz}{\sqrt{z}}\right]$$

and the second becomes equivalent to a similar expression with the coefficients

$$\frac{1}{2\sqrt{c_2}} \cos \frac{c_1^2}{4c_2}, \quad \frac{1}{2\sqrt{c_2}} \sin \frac{c_1^2}{4c_2} \quad \text{changed to} \quad -\frac{1}{2\sqrt{c_2}} \sin \frac{c_1^2}{4c_2}, \quad \frac{1}{2\sqrt{c_2}} \cos \frac{c_1^2}{4c_2}$$

respectively. Squaring and adding, the central intensity

$$= \frac{\pi}{2c_2}\{[c_1(z) - c_2(z)]^2 + [s_1(z) - s_2(z)]^2\},$$

where $c_1(z)$, $c_2(z)$, $s_1(z)$, and $s_2(z)$ are written for the integrals

$$\frac{1}{\sqrt{2\pi}} \int_0^{\frac{1}{c_2}\left(c_2+\frac{c_1}{2}\right)^2} \frac{\cos z dz}{\sqrt{z}}, \text{ etc.,}$$

tabulated values of which were referred to above. There are two cases to be noted. (i) When $c_2 = -c_1$, the central intensity formula takes a slightly different form, viz.

$$\text{C.I.} = \frac{2\pi}{c_2}[c(z) + s(z)]^2,$$

where

$$c(z) = \frac{1}{\sqrt{2\pi}} \int_0^{\frac{c_2}{4}} \frac{\cos z}{\sqrt{z}} dz = \tfrac{1}{2} \int_0^{\frac{c_2}{4}} \mathrm{J}_{-\frac{1}{2}}(z) dz$$

and

$$s(z) = \tfrac{1}{2} \int_0^{c_2} \mathrm{J}_{\frac{1}{2}}(z) dz.$$

For example, taking $c_2 = -c_1$ and giving c_2 values $\frac{\lambda}{4}$, $\frac{\lambda}{2}$, λ, 2λ, 4λ, 8λ in succession, the central intensities are 98·5 per cent., 94 per cent., 79 per cent., 37 per cent., 10 per cent., 5 per cent. of the ideal Airy disc. Remembering that the central intensity is zero for one wave-length out of focus, it seems very curious that one wave-length spherical aberration balanced by the same amount of out of focus should increase the central intensity by about 80 per cent. (ii) When c_1 is negative and less in magnitude than $2c_2$ the central-intensity formula becomes

$$\text{C.I.} = \frac{\pi}{2c_2}[\{c_1(z) + c_2(z)\}^2 + \{s_1(z) + s_2(z)\}^2],$$

and when $c_1 > 2c_2$ in magnitude the first formula given has to be used.

To determine where the foci corresponding to the above combinations of c_2 and c_1 occur on the optical axis, it is convenient to compare them with respect to the paraxial and marginal foci. If the optical axis be taken as the axis of x, and the tangent plane to the wave surface as the plane of yz, the section of the ideal wave surface converging to the paraxial focus by the plane $y=0$ may be written

$$x=\tfrac{1}{2}\frac{r^2}{f}+\tfrac{1}{8}\frac{r^4}{f^3},$$

neglecting higher powers of $\frac{1}{f}$, as introducing quantities too small to be taken into account, since the range of r is from 0 to 1. The actual wave surface is distorted by simple spherical aberration (say c_2r^4), so that its equation is, in the case of under correction,

$$x=\tfrac{1}{2}\frac{r^2}{f}+\left(\frac{1}{8f^3}-c_2\right)r^4.$$

The ideal wave for the marginal focus is similarly

$$\begin{aligned}x&=\tfrac{1}{2}\frac{r^2}{(f+df)}+\tfrac{1}{8}\frac{r^4}{(f+df)^3}\\&=\tfrac{1}{2}\frac{r^2}{f}+\tfrac{1}{8}\frac{r^4}{f^3}-df\left(\tfrac{1}{2}\frac{r^2}{f^2}\right).\end{aligned}$$

At the margin, where $r=1$, the slopes of the two latter curves are the same, so that $df=4f^2c_2$. Hence the lead of the third over the second is $c_2r^4-2c_2r^2$, so that we may take this combination of c_2 and c_1, *i.e.* where $c_1=-2c_2$ as defining the marginal focus. So far as the central intensities are concerned, it is clear that these are equal at the paraxial and marginal foci for all values of c_2. Further, it can easily be shown that they are also equal at points equidistant from the paraxial and marginal foci, and that the maximum central intensity is reached halfway between these two foci, for a given value of c_2. Taking $c_2=\frac{\lambda}{4}$, the central intensity at the geometrical focus is 6 per cent. lower than that at the best focus. A comparison of the intensities for the latter focus as given in Table IV. with those for the ideal Airy disc in Table II. (figs. 2 and 3) shows a diminution of central intensity for the former of about $1\frac{1}{2}$ per cent. The light lost in the central part reappears to a large extent in the first three rings, so that detail will be obscured slightly by the extra light around the centre of the diffraction pattern. However, there is no doubt that the presence of $\frac{1}{4}\lambda$ of primary spherical aberration greatly improves the intensities and resolving power in every way over the results obtained for $\frac{1}{4}\lambda$ out of focus. In fact, the data show that four times this classical limit may be tolerated without undue loss of contrast or resolving power, provided it

is balanced by an equal amount of spherical aberration. In figs. 3 and 4 the intensity values are plotted against the W values. The curves show the intensities for the best foci when c_2 is taken as $\frac{1}{4}\lambda$ in fig. 3 and λ in fig. 4. They also show the results of going out of focus from the best focus by equal amounts on either side. In both cases the light distribution rapidly deteriorates beyond the paraxial focus on one side and the marginal focus on the other. When $c_2 = \frac{\lambda}{4}$, for example, the central intensity has fallen to about ·6 per cent. at foci 1λ on either side of the best focus. When $c_2 = \lambda$, the central intensity is not so sensitive to out-of-focus movement, but at foci 2λ on either side of the best focus the central intensity is again below 1 per cent. The linear positions of the different foci are given in the tables.

Fig. 3 also shows the distribution of light over the width of the pattern considered, of approximately ·044 millimetre radius, with an increased spherical aberration of two wave-lengths balanced by three wave-lengths out of focus. The central intensity has decreased to 25 per cent., while the first and second rings have maximum intensities which are comparatively close to the central intensity, so that the light is fairly evenly distributed over the pattern. Hence there is a loss of contrast and loss of resolving power.

Another interesting feature of the computation for this combination of c_2 and c_1 is that the first dark ring occurs for a value of W of about 160° as compared with about 220° in the case of the Airy spurious disc, or when $\frac{1}{4}\lambda$ of spherical aberration is balanced by $\frac{1}{4}\lambda$ out of focus. Further, the falling off of the intensities in the central concentration of light for the former is much more rapid than in either of the latter cases. For example, when $W = 120°$ the intensity for $\frac{1}{4}\lambda$ spherical aberration balanced by $\frac{1}{4}\lambda$ out of focus is 30 per cent. of its central intensity, whereas for this case of 2λ spherical aberration balanced by 3λ out of focus the corresponding intensity is only about 10 per cent. of its central intensity. Hence it follows that with this combination of c_2 and c_1 the central concentration of light is becoming decidedly smaller in diameter than with a perfect image. If we can obtain a focus in this neighbourhood where the intensities in the first ring are comparatively negligible, we shall most probably have an explanation of the freak resolutions which have been obtained from time to time. The central intensities for two wave-lengths of spherical aberration are as follows:—

(i)	2λ primary spherical aberration . . .	·05 per cent.
(ii)	,, balanced by 2λ out of focus .	37 ,,
(iii)	,, ,, 4λ ,, ,, . .	·05 ,,
(iv)	,, ,, 6λ ,, ,, . .	·002 ,,
(v)	,, together with 2λ ,, ,, . .	·002 ,,

In conclusion, it is hoped that the fundamental importance of this problem for optical designers has been made clear. A knowledge of the effect of residuals of the optical aberrations in a

telescopic system on the light distribution in star discs must be regarded as essential. The results seem to indicate that the best optical system for star observation does not necessarily give the best results on more extended objects, for residuals well above the classical limits may in certain cases be permitted. Professor Conrady has shown this to be especially true in the case of the higher spherical aberrations in the paper already referred to. A more complete solution of the problem and practical applications of the results will be accompanied by higher double-star resolutions.

TABLE I.

Amplitude of Vibration produced by a narrow plane Circular Zone of a Light-wave at Points where the extreme difference of Phase is equal to 2 W Degrees, the amplitude in the axis of the Zone being taken as Unity.

(Extension of Table I., "Star-Discs," *Monthly Notices R.A.S.*, 1919 June.)

W.	600°.	700°.	800°.	900°.	1000°.
0°	−·239	+·094	+·176	−·141	−·111
10	−·222	+·128	+·151	−·163	−·081
20	−·200	+·157	+·122	−·179	−·050
30	−·172	+·182	+·090	−·191	−·018
40	−·139	+·200	+·056	−·196	+·015
50	−·102	+·212	+·020	−·195	
60	−·063	+·218	−·016	−·188	
70	−·023	+·217	−·051	−·176	
80	+·018	+·209	−·084	−·159	
90	+·057	+·195	−·110	−·136	
100	+·094	+·176	−·141	−·111	

TABLE II.

Values of Amplitudes and Intensities contributed by narrow Circular Zones taken over the whole aperture.

(Extension of Table II., "Star-Discs.")

W. of Marginal Zone.	Amplitude.		Intensity.
600°	−·129		·0002
640	−·378		·0014
680	−·387	3rd ring	·0015
720	−·245		·0006
760	−·019		·0000
800	+·182		·0003
840	+·275	4th ring	·0008
880	+·246		·0006
920	+·216		0005
960	−·056		·0000
1000	−·164		·0003

Table III.

Light Distribution when Star is out of focus.

(Extension of Table III., "Star-Discs.")

W. of marginal zone.		600°.	640°.	680°.	720°.	760°.	800°.	840°.	880°.	920°.	960°.	1000°.
Marginal zone	$A^2 \cos^2 \psi$	·0010	·0028	·0024	·0007	·0000	·0006	·0011	·0007	·0001	·0001	·0005
$\frac{1}{2}\lambda$	$A^2 \sin^2 \psi$	·0008	·0000	·0001	·0004	·0004	·0001	·0000	·0000	·0001	·0000	·0000
out of focus *	Intensity	·0018	·0028	·0025	·0011	·0004	·0007	·0011	·0007	·0002	·0001	·0005

Table III.—*continued.*

Light Distribution when Star is out of focus.

W. of marginal zone.		0°.	40°.	80°.	120°.	160°.	200°.	240°.	280°.	320°.	360°.	400°.	440°.	480°.
Marginal zone	$A^2 \cos^2 \psi$	·0450	·0330	·0097	·0003	·0176	·0485	·0681	·0429	·0350	·0102	·0002	·0033	·0089
$\frac{3}{4}\lambda$	$A^2 \sin^2 \psi$	·0450	·0472	·0520	·0539	·0478	·0275	·0113	·0004	·0043	·0167	·0238	·0176	·0091
out of focus †	Intensity	·0900	·0802	·0617	·0542	·0654	·0760	·0794	·0433	·0393	·0269	·0240	·0209	·0180

		520°.	560°.	600°.	640°.	680°.	720°.	760°.	800°.	840°.	880°.	920°.	960°.	1000°.
	$A^2 \cos^2 \psi$	·0097	·0051	·0010	·0001	·0011	·0017	·0010	·0006	·0000	·0004	·0006	·0002	·0000
	$A^2 \sin^2 \psi$	·0139	·0006	·0021	·0054	·0033	·0006	·0002	·0015	·0020	·0011	·0001	·0001	·0006
	Intensity	·0236	·0057	·0031	·0055	·0044	·0023	·0012	·0021	·0020	·0015	·0007	·0003	·0006

W. of marginal zone.		0°.	40°.	80°.	120°.	160°.	200°.	240°.	280°.	320°.	360°.	400°.	440°.	480°.
Marginal zone	$A^2 \cos^2 \psi$	·0000	·0004	·0047	·0002	·0012	·0048	·0125	·0231	·0313	·0306	·0203	·0071	·0002
1λ	$A^2 \sin^2 \psi$	·0000	·0000	·0000	·0172	·0341	·0427	·0349	·0162	·0017	·0024	·0146	·0249	·0236
out of focus ‡	Intensity	·0000	·0004	·0047	·0174	·0353	·0475	·0474	·0393	·0330	·0330	·0349	·0320	·0238

		520°.	560°.	600°.	640°.	680°.	720°	760°.	800°.	840°.	880°.	920°.	960°.	1000°.
	$A^2 \cos^2 \psi$	·0007	·0094	·0120	·0060	·0024	·0000	·0016	·0034	·0030	·0010	·0000	·0008	·0013
	$A^2 \sin^2 \psi$	·0137	·0030	·0001	·0030	·0053	·0045	·0017	·0001	·0003	·0013	·0013	·0001	·0008
	Intensity	·0144	·0124	·0121	·0090	·0077	·0045	·0033	·0035	·0033	·0023	·0013	·0009	·0021

* This represents a focus with a linear distance of ·019″ from the ideal focus for F/15.
† A focus with linear distance ·028″ from the ideal focus for F/15.
‡ This represents a focus distant ·038″ from the ideal focus for F/15.

TABLE III.—*continued.*

W. of marginal zone.		0°.	40°.	80°.	120°.	160°.	200°.	240°.	280°.	320°.	360°.	400°.	440°.	480°.
Marginal zone $1\frac{1}{2}\lambda$ out of focus *	$A^2\cos^2\psi$	·0000	·0000	·0001	·0004	·0008	·0016	·0019	·0028	·0046	·0092	·0105	·0134	·0138
	$A^2\sin^2\psi$	·0453	·0097	·0276	·0151	·0057	·0036	·0029	·0039	·0058	·0064	·0038	·0004	·0005
	Intensity	·0453	·0097	·0277	·0155	·0065	·0052	·0048	·0067	·0104	·0156	·0143	·0138	·0143

		520°.	560°.	600°.	640°.	680°.	720°.	760°.	800°.	840°.	880°.	920°.	960°.	1000°.
	$A^2\cos^2\psi$	·0091	·0034	·0002	·0017	·0066	·0109	·0102	·0053	·0047	·0003	·0013	·0016	·0018
	$A^2\sin^2\psi$	·0055	·0145	·0160	·0047	·0062	·0005	·0011	·0053	·0073	·0047	·0017	·0000	·0014
	Intensity	·0146	·0179	·0162	·0064	·0128	·0114	·0113	·0106	·0120	·0050	·0030	·0016	·0032

W. of marginal zone.		0°.	40°.	80°.	120°.	160°.	200°.	240°.	280°.	320°.	360°.	400°.	440°.	480°.
Marginal zone 2λ out of focus †	$A^2\cos^2\psi$	·0000	·0000	·0000	·0000	·0001	·0003	·0009	·0017	·0027	·0037	·0043	·0046	·0049
	$A^2\sin^2\psi$	·0000	·0001	·0012	·0043	·0089	·0117	·0110	·0078	·0040	·0022	·0004	·0001	·0001
	Intensity	·0000	·0001	·0012	·0043	·0090	·0120	·0119	·0095	·0067	·0059	·0047	·0047	·0050

		520°.	560°.	600°.	640°.	680°.	720°.	760°.	800°.	840°.	880°.	920°.	960°.	1000°.
	$A^2\cos^2\psi$	·0061	·0051	·0046	·0034	·0012	·0000	·0010	·0049	·0079	·0088	·0059	·0018	·0000
	$A^2\sin^2\psi$	·0000	·0001	·0005	·0028	·0061	·0095	·0098	·0063	·0018	·0000	·0023	·0056	·0068
	Intensity	·0061	·0052	·0051	·0062	0073	·0095	·0108	·0112	·0097	·0088	·0082	·0074	·0068

W. of marginal zone.		0°.	40°.	80°.	120°.	160°.	200°.	240°.	280°.	320°.	360°.	400°.	440°.	480°.
Marginal zone 4λ out of focus ‡	$A^2\cos^2\psi$	·0005	·0005	·0003	·0002	·0001	·0000	·0000	·0000	·0001	·0001	·0002	·0002	·0004
	$A^2\sin^2\psi$	·0000	·0000	·0004	·0013	·0027	·0038	·0037	·0028	·0016	·0009	·0012	·0006	·0008
	Intensity	·0005	·0005	·0007	·0015	·0028	·0038	·0037	·0028	·0017	·0010	·0014	·0008	·0012

		520°.	560°.	600°.	640°.	680°.	720°.	760°.	800°.	840°.	880°.	920°.	960°.	1000°.
	$A^2\cos^2\psi$	·0004	·0006	·0007	·0009	·0010	·0011	·0011	·0010	·0009	·0009	·0007	·0005	·0004
	$A^2\sin^2\psi$	·0007	·0010	·0003	·0002	·0000	·0003	·0009	·0014	·0017	·0018	·0021	·0025	·0031
	Intensity	·0011	·0016	·0010	·0011	·0010	·0014	·0020	·0024	·0026	·0027	·0028	·0030	·0035

* This represents a focus distant ·056″ from the ideal focus for F/15.

† ,, ,, ,, ·075″ ,, ,, ,,

‡ ,, ,, ,, ·152″ ,, ,, ,,

Table IV.

Light Distribution when Spherical Aberration is present.

(This table is supplementary to Table III., "Star-Discs," etc.)

W. of marginal zone.		64°.	68°.	72°.	76°.	80°.	84°.	88°.	92°.	96°.	100°.
¼ λ spherical aberration *	$A^2 \cos^2 \psi$	·0000	·0002	·0003	·0002	·0000	·0000	·0001	·0001	·0000	·0000
	$A^2 \sin^2 \psi$	·0019	·0017	·0005	·0000	·0009	·0012	·0007	·0001	·0000	·0002
	Intensity	·0019	·0019	·0008	·0002	·0009	·0012	·0008	·0202	·0000	·0002

Table IV.—*continued.*

Light Distribution when Spherical Aberration is present and combined with Out-of-focus Conditions.

W. of marginal zone.		0°.	40°.	80°.	120°.	160°.	200°.	240°.	280°.	320°.	360°.	400°.	440°.	480°.
¼ λ spherical aberration balanced by ¼ λ out of focus †	$A^2 \cos^2 \psi$	·9199	·8141	·5544	·2728	·0888	·0065	·0033	·0137	·0221	·0096	·0014	·0023	·0039
	$A^2 \sin^2 \psi$	·0662	·0585	·0196	·0189	·0070	·0001	·0013	·0034	·0037	·0023	·0007	·0000	·0001
	Intensity	·9861	·8726	·5740	·2917	·0958	·0066	·0046	·0171	·0258	·0119	·0021	·0023	·0040

	520°.	560°.	600°.	640°.	680°.	720°.	760°.	800°.	840°.	880°.	920°.	960°.	1000°.
$A^2 \cos^2 \psi$	·0029	·0003	·0003	·0015	·0015	·0005	·0001	·0004	·0008	·0006	·0001	·0000	·0003
$A^2 \sin^2 \psi$	·0003	·0002	·0001	·0000	·0000	·0001	·0000	·0000	·0000	·0000	·0000	·0000	·0000
Intensity	·0032	·0005	·0004	·0015	·0015	·0006	·0001	·0004	·0008	·0006	·0001	·0000	·0003

* This represents a longitudinal spherical aberration of ·019″ at the paraxial focus for F/15.

† This represents a focus halfway between the paraxial and marginal foci and distant ·009″ from the paraxial focus for F/15.

TABLE IV.—*continued*.

W. of marginal zone.		0°.	40°.	80°.	120°.	160°.	200°.	240°.	280°.	320°.	360°.	400°.	440°.	480°.
$\frac{\lambda}{4}$ spherical aberration balanced by $\frac{5\lambda}{4}$ out of focus *	$A^2\cos^2\psi$	·0004	·0002	·0000	·0001	·0000	·0004	·0041	·0135	·0264	·0264	·0301	·0164	·0035
	$A^2\sin^2\psi$	·0061	·0031	·0000	·0075	·0262	·0430	·0436	·0269	·0073	·0078	·0079	·0201	·0245
	Intensity	·0065	·0033	·0000	·0076	·0262	·0434	·0477	·0404	·0337	·0342	·0380	·0365	·0280
		520°.	560°.	600°.	640°.	680°.	720°.	760°.	800°.	840°.	880°.	920°.	960°.	1000°.
	$A^2\cos^2\psi$	·0001	·0058	·0115	·0106	·0053	·0007	·0003	·0022	·0028	·0015	·0001	·0001	·0007
	$A^2\sin^2\psi$	·0184	·0071	·0007	·0007	·0028	·0041	·0023	·0005	·0000	·0001	·0009	·0006	·0002
	Intensity	·0185	·0129	·0122	·0113	·0081	·0048	·0026	·0027	·0028	·0016	·0010	·0007	·0009

W. of marginal zone.		0°.	40°.	80°.	120°.	160°.	200°.	240°.	280°.	320°.	360°.	400°.	440°.	480°.
$\frac{\lambda}{4}$ spherical aberration together with $\frac{3\lambda}{4}$ out of focus. $\phi=\frac{\lambda}{4}r^4+\frac{3\lambda}{4}r^2$ †	$A^2\cos^2\psi$	·0004	·0005	·0012	·0028	·0067	·0136	·0225	·0297	·0305	·0229	·0107	·0014	·0008
	$A^2\sin^2\psi$	·0057	·0080	·0155	·0275	·0377	·0371	·0235	·0068	·0000	·0075	·0204	·0259	·0189
	Intensity	·0061	·0085	·0167	·0303	·0444	·0506	·0460	·0365	·0305	·0304	·0311	·0273	·0197
		520°.	560°.	600°.	640°.	680°.	720°.	760°.	800°.	840°.	880°.	920°.	960°.	1000°.
	$A^2\cos^2\psi$	·0056	·0085	·0100	·0043	·0004	·0007	·0032	·0041	·0025	·0004	·0001	·0011	·0016
	$A^2\sin^2\psi$	·0078	·0004	·0018	·0060	·0068	·0040	·0007	·0001	·0013	·0021	·0015	·0004	·0000
	Intensity	·0134	·0089	·0118	·0103	·0072	·0047	·0039	·0042	·0038	·0025	·0016	·0015	·0016

W. of marginal zone.		0°.	40°.	80°.	120°.	160°.	200°.	240°.	280°.	320°.	360°.	400°.	440°.	480°.
1 λ spherical aberration balanced by 1 λ out of focus ‡	$A^2\cos^2\psi$	·1922	·1698	·1181	·0597	·0216	·0049	·0008	·0004	·0013	·0036	·0052	·0043	·0015
	$A^2\sin^2\psi$	·6079	·5379	·3641	·1754	·0467	·0013	·0092	·0261	·0277	·0161	·0045	·0001	·0008
	Intensity	·8001	·7077	·4822	·2351	·0683	·0062	·0100	·0265	·0290	·0197	·0097	·0044	·0023
		520°.	560°.	600°.	640°.	680°.	720°.	760°.	800°.	840°.	880°.	920°.	960°.	1000°.
	$A^2\cos^2\psi$	·0001	·0012	·0031	·0032	·0015	·0001	·0002	·0012	·0012	·0001	·0001	·0003	·0006
	$A^2\sin^2\psi$	·0017	·0013	·0001	·0003	·0012	·0008	·0003	·0000	·0001	·0004	·0002	·0000	·0000
	Intensity	·0018	·0025	·0032	·0035	·0027	·0009	·0005	·0012	·0013	·0005	·0003	·0003	·0006

* This represents a focus distant ·047″ from the paraxial focus and ·028″ from the marginal focus for F/15.

† ,, ,, ,, ·028″ ,, ,, ,, ·047″ ,, ,, ,,

‡ This represents the intensities at a point midway between paraxial and marginal focus with a longitudinal spherical aberration of ·076″ at the paraxial focus for F/15.

TABLE IV.—*continued.*

		0°.	40°.	80°.	120°.	160°.	200°.	240°.	280°.	320°.	360°.	400°.	440°.	480°.
W. of marginal zone.														
1 λ of spherical aberration balanced by $\frac{3\lambda}{4}$ out of focus *	$A^2 \cos^2 \psi$	·0656	·0643	·0622	·0500	·0344	·0071	·0033	·0003	·0062	·0136	·0149	·0093	·0024
	$A^2 \sin^2 \psi$	·5650	·5007	·3626	·1870	·0609	·0166	·0009	·0066	·0281	·0015	·0001	·0026	·0048
	Intensity	·6306	·5650	·4248	·2370	·0953	·0237	·0042	·0069	·0343	·0151	·0150	·0119	·0072

	520°.	560°.	600°.	640°.	680°.	720°.	760°.	800°.	840°.	880°.	920°.	960°.	1000°.
$A^2 \cos^2 \psi$	·0001	·0017	·0035	·0027	·0008	·0000	·0009	·0018	·0014	·0004	·0000	·0005	·0008
$A^2 \sin^2 \psi$	·0034	·0007	·0001	·0015	·0022	·0016	·0005	·0000	·0004	·0008	·0005	·0005	·0004
Intensity	·0035	·0024	·0036	·0042	·0030	·0016	·0014	·0018	·0018	·0012	·0005	·0010	·0012

		0°.	40°.	80°.	120°.	160°.	200°.	240°.	280°.	320°.	360°.	400°.	440°.	480°.
W. of marginal zone.														
λ spherical aberration balanced by $\frac{5\lambda}{4}$ out of focus †	$A^2 \cos^2 \psi$	·0654	·0518	·0221	·0016	·0055	·0276	·0478	·0261	·0277	·0161	·0044	·0001	·0008
	$A^2 \sin^2 \psi$	·5946	·5228	·3641	·1752	·0467	·0013	·0092	·0500	·0348	·0150	·0026	·0001	·0026
	Intensity	·6600	·5746	·3862	·1768	·0522	·0289	·0570	·0761	·0625	·0311	·0070	·0002	·0034

	520°.	560°.	600°.	640°.	680°.	720°.	760°.	800°.	840°.	880°.	920°.	960°.	1000°.
$A^2 \cos^2 \psi$	·0018	·0013	·0001	·0003	·0012	·0008	·0003	·0000	·0002	·0003	·0003	·0001	·0000
$A^2 \sin^2 \psi$	·0040	·0027	·0008	·0000	·0001	·0004	·0002	·0000	·0000	·0002	·0001	·0000	·0000
Intensity	·0058	·0040	·0009	·0003	·0013	·0012	·0005	·0000	·0000	·0005	·0004	·0001	·0000

		0°.	40°.	80°.	120°.	160°.	200°.	240°.	280°.	320°.	360°.	400°.	440°.	480°.
W. of marginal zone.														
1 λ spherical aberration together with 1 λ out of focus ‡	$A^2 \cos^2 \psi$	·0002	·0007	·0010	·0019	·0030	·0051	·0073	·0093	·0106	·0110	·0093	·0065	·0038
	$A^2 \sin^2 \psi$	·0058	·0101	·0126	·0156	·0174	·0158	·0123	·0065	·0020	·0001	·0005	·0012	·0034
	Intensity	·0060	·0108	·0136	·0175	·0204	·0209	·0196	·0158	·0126	·0171	·0098	·0077	·0072

	520°.	560°.	600°.	640°.	680°.	720°.	760°.	800°.	840°.	880°.	920°.	960°.	1000°.
$A^2 \cos^2 \psi$	·0018	·0002	·0001	·0010	·0029	·0052	·0042	·0032	·0017	·0001	·0004	·0020	·0037
$A^2 \sin^2 \psi$	·0050	·0045	·0043	·0039	·0023	·0008	·0000	·0007	·0027	·0044	·0034	·0020	·0002
Intensity	·0068	·0047	·0044	·0049	·0052	·0060	·0042	·0039	·0044	·0045	·0038	·0040	·0039

* This represents a focus between the marginal and paraxial foci and distant ·047″ from the paraxial focus for F/15.
† This represents a focus between the paraxial and marginal foci and distant ·047″ from the marginal focus for F/15.
‡ This represents a focus distant ·038″ from the paraxial focus on the side away from the marginal focus for F/15.

TABLE IV.—*continued.*

W. of marginal zone.		0°.	40°.	80°.	120°.	160°.	200°.	240°.	280°.	320°.	360°.	400°.	440°.	480°.
1 λ spherical aberration balanced by 3 λ out of focus *	$A^2\cos^2\psi$	·0069	·0046	·0008	·0006	·0055	·0110	·0122	·0082	·0033	·0005	·0000	·0000	·0001
	$A^2\sin^2\psi$	·0014	·0011	·0004	·0000	·0001	·0000	·0000	·0005	·0016	·0026	·0026	·0025	·0007
	Intensity	·0083	·0057	·0012	·0006	·0056	·0110	·0122	·0087	·0049	·0031	·0026	·0025	·0008

		520°.	560°.	600°.	640°.	680°.	720°.	760°.	800°.	840°.	880°.	920°.	960°.	1000°.
	$A^2\cos^2\psi$	·0017	·0029	·0034	·0018	·0000	·0021	·0086	·0153	·0168	·0120	·0034	·0004	·0008
	$A^2\sin^2\psi$	·0005	·0005	·0021	·0041	·0067	·0080	·0059	·0019	·0000	·0031	·0090	·0113	·0087
	Intensity	·0022	·0034	·0055	·0059	·0067	·0101	·0145	·0172	·0168	·0151	·0124	·0117	·0095

W. of marginal zone.		0°.	40°.	80°.	120°.	160°.	200°.	240°.	280°.	320°.	360°.	400°.	440°.	480°.
2 λ spherical aberration balanced by 3 λ out of focus †	$A^2\cos^2\psi$	·2077	·1726	·0922	·0233	·0015	·0238	·0327	·0281	·0082	·0001	·0028	·0120	·0174
	$A^2\sin^2\psi$	·0505	·0419	·0225	·0062	·0001	·0008	·0020	·0001	·0021	·0102	·0193	·0215	·0140
	Intensity	·2582	·2145	·1147	·0295	·0016	·0246	·0347	·0282	·0103	·0103	·0221	·0335	·0314

		520°.	560°.	600°.	640°.	680°.	720°.	760°.	800°.	840°.	880°.	920°.	960°.	1000°.
	$A^2\cos^2\psi$	·0149	·0128	·0041	·0004	·0001	·0005	·0006	·0006	·0006	·0008	·0010	·0011	·0007
	$A^2\sin^2\psi$	·0042	·0001	·0053	·0138	·0171	·0137	·0069	·0017	·0000	·0002	·0004	·0005	·0000
	Intensity	·0191	·0129	·0094	·0142	·0172	·0142	·0075	·0023	·0006	·0010	·0014	·0016	·0007

* This represents a focus distant ·038″ from the marginal focus on the side away from the paraxial focus for F/15.

† This represents a focus between the marginal and paraxial foci and distant ·114″ from the paraxial focus. (Spherical aberration ·152″ at paraxial focus for F/15.)

Mathematics and Mechanics Department,
City and Guilds Engineering College,
Imperial College of Science and Technology,
London, S.W. 7.

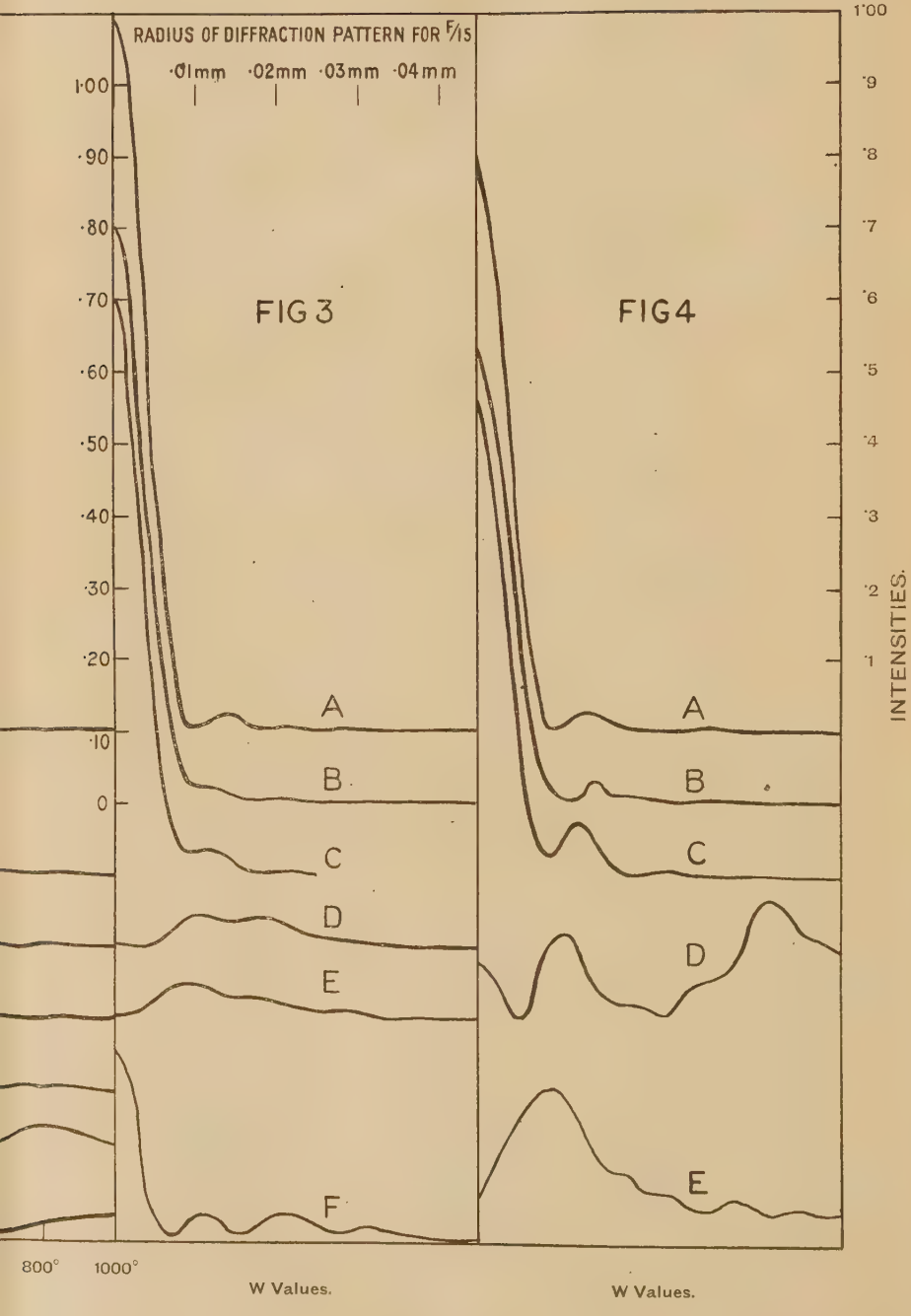
RADIUS OF DIFFRACTION PATTERN FOR F/15
·01mm ·02mm ·03mm ·04mm
1·00
·90
·80
·70
·60
·50
·40
·30
·20
·10
0
FIG 3
FIG 4
A
B
C
D
E
F
1·00
·9
·8
·7
·6
·5
·4
·3
·2
·1
INTENSITIES.
800°
1000°
W Values.
W Values.

KEY TO PLATE.

Fig. 2.

A. Airy spurious disc curve.
B. $\frac{1}{4}$ wave-length out of focus.
C. $\frac{1}{2}$ wave-length out of focus.
D. $\frac{3}{4}$ wave-length out of focus.
E. 1 wave-length out of focus.
F. $1\frac{1}{2}$ wave-length out of focus.
G. 2 wave-lengths out of focus. [Scale 5 times.]
H. 4 wave-lengths out of focus. [Scale 10 times.]

Fig. 3.

A. $\frac{1}{4}$ wave-length of spherical aberration balanced by $\frac{1}{4}$ wave-length out of focus.
B. $\frac{1}{4}$ wave-length spherical aberration.
C. $\frac{1}{4}$ wave-length spherical aberration balanced by $\frac{1}{2}$ wave-length out of focus.
D. $\frac{1}{4}$ wave-length spherical aberration balanced by $\frac{5}{4}$ wave-length out of focus.
E. $\frac{1}{4}$ wave-length spherical aberration together with $\frac{3}{4}$ wave-length out of focus.
F. 2 wave-lengths spherical aberration balanced by 3 wave-lengths out of focus.

Fig. 4.

A. 1 wave-length spherical aberration balanced by 1 wave-length out of focus.
B. 1 wave-length spherical aberration balanced by $\frac{3}{4}$ wave-length out of focus.
C. 1 wave-length spherical aberration balanced by $\frac{5}{4}$ wave-length out focus.
D. 1 wave-length spherical aberration balanced by 3 wave-lengths out of focus. [Scale 10 times.]
E. 1 wave-length spherical aberration together with 1 wave-length out of focus. [Scale 10 times.]

Micrometrical Measures of Double Stars.

By Rev. T. E. R. Phillips, M.A.

The following measures were made in the year 1920 with the 8-inch refractor belonging to the Society:—

Star.	1920. R.A.	1920. Dec.	Mags.	Position Angle	Distance.	No. of Nights.	Date.
	h m	° ′		°	″		
OΣ 12 (λ Cassiop.)	0 2·7	+54 5	5·6, 5·9	158·6	0·68	2	1920·847
Σ 60 (η Cassiop.)	0 44·0	57 24	4·0, 7·6	258·9	7·26	4	·777
73 (36 Androm.)	0 50·7	23 12	6·2, 6·8	52·2	0·78	3	·745
113 (42 Ceti)	1 15·2	− 0 58	6·2, 7·2	358·5	1·47	3	·843
186	1 51·7	+ 1 27	7·2, 7·2	40·4	1·01	3	·846
OΣ 38 (γ^2 Androm.)	1 59·0	41 57	5·0, 6·2	109·5	0·55	6	·759
Σ 228	2 8·9	47 6	6·7, 7·6	119·3	0·56	3	·824
305	2 42·9	19 2	7·3, 8·2	314·6	3·22	3	·825
OΣ 98 (14 Orionis)	5 3·5	8 24	6·0, 6·8	137·5	0·91	3	·844
Σ 1110 (Castor)	7 29·5	32 4	2·7, 3·7	215·1	4·66	6	·867
1130	7 37·3	9 54	8·4, 8·9	176·9	0·79	3	·825
1196 (ζ Cancri)	8 7·6	17 54	5·5, 6·2	277·2	0·84	5	·512
1670 (γ Virginis)	12 37·7	− 1 0	3·6, 3·6	322·9	5·64	4	·422
1687 (35 Comæ Ber.)	12 49·4	+21 41	5·2, 8·0	96·9	0·95	3	·503
1768 (25 Can. Ven.)	13 33·9	36 42	5·7, 7·6	119·9	1·52	3	·349
1785	13 45·5	27 23	7·2, 7·5	9·5	1·30	3	·375
1865 (ζ Boötis)	14 37·3	14 4	3·5, 3·9	136·4	0·85	4	·368
1888 (ξ Boötis)	14 47·7	19 26	4·7, 6·6	64·0	2·58	20	·486
1937 (η Coronæ)	15 19·9	30 34	5·5, 6·0	91·5	0·63	4	·543
1938 (μ^2 Boötis)	15 21·5	37 37	6·7, 7·3	47·7	1·65	3	·526
OΣ 298	15 33·2	40 4	7·0, 7·3	204·2	0·89	3	·537
Σ 2272 (70 Ophiuchi)	18 1·4	2 31	4·1, 6·1	133·2	5·44	15	·613
OΣ 358	18 32·3	16 35	6·8, 7·2	185·7	2·18	4	·610
371	19 12·7	27 19	6·8, 6·9	156·5	0·87	3	·797
Σ 2525	19 23·3	27 10	7·4, 7·6	302·9	0·83	5	·691
2579 (δ Cygni)	19 42·5	44 53	3·0, 7·9	275·4	1·71	3	·833
OΣ 387	19 47·8	35 0	7·2, 8·2	305·2	0·55	3	·626
Σ 2624	20 0·5	35 48	7·2, 7·8	173·6	2·03	3	·820
2695	20 28·5	25 32	6·2, 8·0	78·5	0·89	3	·835
OΣ 413 (λ Cygni)	20 44·3	36 12	5·0, 6·3	47·5	0·68	3	·554
Σ 2758 (61 Cygni)	21 3·3	38 21	5·3, 5·9	132·2	24·11	5	·714
2799	21 25·6	10 44	6·6, 6·6	289·6	1·41	3	·838

Headley, Epsom.

Results of Micrometric Measures of Double Stars made with the 15-inch Refractor of the Royal Observatory, Edinburgh.

(*Communicated by the Astronomer Royal for Scotland.*)

The following observations of double stars comprise observations made in the years 1911, 12, 13, 14, 15, 19, and 20, and are in continuation of those published in *M.N.*, vols. **70**, p. 466, and **71**, p. 479.

The initials in the last column are those of the observers, viz. Messrs. Storey, Wrigley, Jameson, and Baker, denoted by S., W., J., and B. respectively.

Name of Star.	1910. R.A.	1910. Dec.	Position Angle.	Dist.	No. of Nights.	Mags.	Epoch 1900+.	Obs.
	h m	° ′	°	″				
β 997	0 0·3	45 11	337·4	4·27	2	7·9, 8·9	11·900	S.
			338·7	4·22	1		12·865	S.
			337·6	4·23	1		14·821	S.
OΣ 547 ...	0·7	45 19	138·4	4·88	2	8·3, 8·3	11·900	S.
			138·5	4·95	1		12·865	S.
			140·2	5·07	1		14·821	S.
Aitken 110 ...	1·1	42 9	125·3	1·99	1	9·2, 9·3	12·882	S.
			122·2	2·09	1		14·824	S.
			123·9	2·14	1		,,	B.
			123·5	2·06	2		19·871	S.
Hussey 502	1·3	49 7	110·7	2·26	1	7·2, 10·5	12·882	S.
			112·6	2·03	1		14·824	B.
			111·3	2·17	1		,,	S.
Krueger 67 ...	1·3	60 22	159·2	3·15	1	9·0, 9·2	14·936	S.
			162·0	3·00	1		20·019	S.
Σ 3062... ...	1·5	57 56	3·7	1·83	4	6·9, 8·0	12·882	S.
			6·3	1·85	2		14·904	S.
			12·6	1·71	1		20·019	S.
Espin 114 ...	4·6	66 39	162·8	4·53	1	8·7, 11·2	12·882	J.
Hussey 1003 ...	5·4	66 47	28·8	1·96	1	8·5, 11·2	12·882	J.
β 253	5·7	58 1	38·4	0·73	1	8·3, 8·5	19·868	S.
Aitken 801 ...	6·2	75 1	234·4	1·94	2	9·1, 9·5	12 930	S.
Krueger 1 ...	6·2	57 20	188·5	2·15	1	9·2, 9·5	12·879	J.
			192·6	2·07	1		12·882	S.
Σ 7	6·9	55 28	215·2	1·38	1	8·0, 8·5	12·879	J.
			215·8	1·35	1		12·977	S.
OΣ 1	7·0	65 38	206·5	1·47	2	7·2, 9·9	12·930	S.
Σ 10	10·0	62 20	176·7	17·91	2	7·5, 8·2	19·889	S.

Name of Star.	1910. R.A.	1910. Dec.	Position Angle.	Dist.	No. of Nights.	Mags.	Epoch 1900+.	Obs.
	h m	° ′	°	″				
Krueger 3 ...	0 10·2	55 12	44·7	3·40	1	9·0, 9·0	13·966	S.
			44·2	3·44	1		14·936	S.
Aitken 904 ...	12·4	57 6	359·8	3·46	1	8·9, 10·0	12·882	J.
β 776	12·5	50 5	200·5	1·23	1	8·8, 9·0	14·824	S.
Hussey 1006 ...	16·7	65 18	197·6	3·22	2	9·0, 9·4	12·933	S.
Holden 2 ...	20·5	51 4	334·8	3·13	1	8·8, 8·8	12·879	J.
			335·5	2·49	1		12·882	S.
			331·8	2·74	1		14·936	S.
β 107	26·2	62 51	354·4	6·25	1	8·0, 9·6	19·887	S.
Σ 43	31·7	60 1	166·9	4·90	1	8·5, 9·0	12·885	S.
			165·8	4·92	1		14·936	S.
Σ 52	39·2	45 45	13·6	1·47	1	8·0, 9·0	12·977	S.
Holden 3 ...	40·1	53 4	53·1	2·83	1	8·5, 8·6	13·966	S.
			51·0	2·83	1		14·936	S.
Σ 59	42·8	50 57	147·8	2·49	1	7·2, 8·1	12·879	J.
			147·1	2·17	1		13·966	S.
Σ 60	43·6	57 20	246·8	6·64	1	4·0, 7·6	12·579	J.
			246·4	6·73	2		12·925	S.
			248·2	6·83	1		13·966	S.
			249·8	6·86	1		14·915	B.
			250·0	6·96	1		14·915	S.
			258·5	7·49	1		19·887	S.
β 781	45·9	63 30	29·0	...	1	8·1, 8·6	12·879	J.
Σ 65	0 47·0	68 23	38·0	3·12	1	8·0, 8·0	12·879	J.
			37·5	3·10	1		14·915	B.
			34·1	3·25	1		14·915	S.
Σ 97	1 6·9	51 3	99·5	4·60	1	8·5, 8·7	14·915	S.
			99·5	4·58	2		14·925	B.
Hussey 1023 ...	7·7	65 8	2·0	3·71	1	8·7, 10·2	12·885	S.
			2·7	3·89	1		14·936	S.
Aitken 813 ...	10·4	75 25	50·7	1·83	1	9·0, 10·2	12·882	J.
β 3	11·5	56 2	29·4	4·57	1	7·8, 10·2	12·901	S.
			26·8	4·55	1		13·966	S.
Krueger 11 ...	13·8	61 7	235·9	1·89	1	9·3, 9·3	12·882	S.
			237·3	1·95	1		20·019	S.
β 782	15·2	55 45	81·8	3·22	1	8·0, 9·6	12·885	S.
			81·2	3·05	1		12·901	J.
Σ 114	17·3	72 22	351·7	3·70	1	7·2, 10·4	12·882	J.
Espin 4 ...	25·8	43 9	104·0	3·17	1	7·7, 9·7	12·901	S.
			104·4	3·03	1		14·936	B.
β 870	38·3	57 5	43·5	1·07	1	6·9, 8·3	20·019	S.

Name of Star.	1910. R.A.	1910. Dec.	Position Angle.	Dist.	No. of Nights.	Mags.	Epoch 1900+.	Obs.
	h m	° ′	°	″				
Σ 158	1 41·6	32 43	258·8	2·11	1	8·3, 8·8	13·966	S.
			257·8	2·20	2		14·894	S.
			257·9	2·15	2		14·894	B.
Σ 156	41·9	59 55	96·6	5·80	1	8·3, 11·0	12·901	S.
Σ 170	47·1	75 47	247·6	3·28	1	6·7, 7·5	12·964	S.
			243·3	3·09	1		14·936	S.
Σ 183 AC ...	50·0	28 22	162·2	5·43	1	7·5, 8·7	12·901	J.
			166·1	5·95	1		13·966	S.
AB ...			356	elong.	1	7·5, 8·2	13·966	S.
Σ 192	54·4	58 6	178·7	4·69	1	8·2, 10·8	12·901	J.
Σ 202	1 57·4	2 20	315·1	2·60	1	2·8, 3·9	13·966	S.
			309·6	2·73	2		14·893	S.
			311·6	2·57	2		14·893	B.
Holden 7 ...	2 19·0	57 47	183·8	2·26	1	8·1, 10·4	11·112	S.
Σ 262 AB ...	21·6	67 0	251·2	2·76	1	4·2, 7·1	11·014	S.
AC ...			109·9	7·08	1	4·2, 8·1	11·014	S.
Σ 268	23·1	55 8	127·4	2·41	1	6·9, 8·2	11·022	S.
			131·4	3·08	1		14·936	S.
Σ 284	33·8	60 54	194·0	5·89	1	8·0, 10·0	11·022	S.
			197·7	5·64	1		12·912	S.
Arg. 9	40·8	49 45	145·7	2·74	2	8·4, 8·4	11·067	S.
			146·8	3·12	1		13·047	J.
Σ 306 AB ...	44·1	60 3	92·7	2·23	1	7·1, 9·0	11·022	S.
Σ 314	46·5	52 38	303·2	1·40	1	6·9, 7·1	11·085	S.
Σ 312	47·1	72 32	20·5	2·98	1	7·1, 8·0	11·085	S.
			23·3	3·10	1		14·936	S.
			23·8	3·35	1		15·011	S.
			44·0	2·94	1		20·049	S.
Krueger 17 ...	56·2	60 29	222·6	3·49	1	9·0, 9·1	15·011	S.
			219·8	3·62	1		20·049	S.
Krueger 18 ...	2 58·8	57 23	279·5	1·51	1	9·2, 9·3	11·085	S.
Σ 349	3 3·2	63 27	322 0	6·34	1	7·4, 8·1	20·049	S.
OΣ 50 AB ...	3·7	71 13	198·7	1·34	2	7·5, 7·5	11·103	S.
Σ 345	4·9	78 10	81·2	6·34	1	8·0, 9·8	13·047	J.
OΣ 51	6·9	43 57	312·3	1·33	1	7·9, 8·1	12·049	S.
			307·7	1·17	1		12·912	J.
OΣ 52	9·6	65 20	114·3	0·64	1	6·4, 7·0	11·112	S.
Hussey 545 ...	11·8	48 56	77·0	3·58	1	8·5, 9·3	13·047	J.
Σ 386	21·2	54 51	61·1	2·86	1	8·8, 8·8	11·014	S.
Σ 385	21·7	59 37	162·4		1	4·7, 9·0	11·085	S
Σ 419	33·7	69 33	73·6	3·00	3	7·2, 7·2	11·114	S.

Name of Star.	1910. R.A.	1910. Dec.	Position Angle.	Dist.	No. of Nights.	Mags.	Epoch 1900+.	Obs.
	h m	° ′	°	″				
Hussey 103 ...	3 38·8	49 35	206·6	1·06	1	8·1, 8·4	12·912	J.
Hussey 209 ...	42·6	50 7	93·1	1·25	1	8·7, 9·7	13·142	S.
Σ 445	43·1	59 51	256·3	3·10	2	8·2, 9·2	11·084	S.
Σ 461	48·2	56 15	117·6	1·10	1	8·0, 10·6	13·142	S.
β 743	48·8	52 0	250·7	0·69	1	8·5, 9·0	13·142	S.
OΣ 67	49·4	60 51	45·8	1·83	2	5·0, 8·2	11·096	S.
Σ 460	54·8	80 27	57·0	1·10	1	5·2, 6·1	11·112	S.
			59·5	0·91	1		13·142	S.
Σ 480	3 57·3	55 30	328·7	3·17	1	8·3, 8·5	11·014	S.
Hussey 1074 ...	4 0·1	61 26	263·8	4·53	2	9·0, 10·2	11·096	S.
Σ 490	2·8	59 55	57·3	4·67	2	8·5, 9·0	11·071	S.
Σ 503	8·8	63 56	226·1	4·98	1	8·8, 8·8	11·022	S.
			225·9	4·85	1		20·049	S.
Krueger 22 ...	10·8	60 37	183·9	3·96	1	9·3, 9·4	11·134	S.
OΣ 75	10·8	60 17	170·2	0·68	1	7·6, 8·0	11·112	S.
Σ 521	15·0	49 50	258·1	2·05	1	7·2, 9·3	12·049	S.
Σ 522	15·6	51 24	214·0	1·50	1	8·5, 8·5	11·112	S.
			215·3	1·80	1		12·049	S.
			215·2	1·13	1		13·142	J.
OΣ 80	17·3	42 13	174·0	0·70	1	6·5, 7·0	12·049	S.
Σ 535	18·3	11 10	322·1	1·53	1	6·7, 8·2	13·137	J.
Σ 531	19·5	55 26	307·0	0·91	1	7·4, 8·6	11·112	S.
Σ 553	26·5	50 52	134·2	3·28	1	8·0, 8·5	11·159	S.
Krueger 24 ...	31·2	56 45	238·8	3·76	1	9·5, 9·5	11·079	S.
Σ 566	32·8	53 18	282·0	1·49	1	5·1, 7·4	11·159	S.
Aitken 1013 ...	35·5	59 21	308·2	0·57	1	7·2, 7·2	11·112	S.
			311·7	...	1		13·137	J.
Hussey 552 ...	39·2	54 57	237·6	1·33	1	8·8, 9·5	13·137	J.
OΣ 88	49·1	61 36	303·7	0·78	1	6·5, 8·2	13·137	S.
Σ 604	49·1	69 55	38·5	2·25	2	8·1, 8·9	11·151	S.
Σ 608	49·2	51 57	116·5	4·14	2	7·8, 9·2	11·070	S.
Krueger 25 ...	49·9	56 30	125·7	2·92	1	9·0, 9·5	11·153	S.
A. G. 84 ...	4 55·1	54 42	158·9	4·16	1	8·8, 9·2	11·047	S.
Σ 635	5 0·5	54 53	311·5	0·72	1	8·3, 8·3	12·049	S.
Σ 638	4·4	69 44	222·1	5·22	3	7·5, 8·5	11·070	S.
			220·5	5·61	1		20·049	S.
Σ 657	11·6	52 45	286·4	1·38	1	7·5, 8·0	11·153	S.
			290·6	1·02	1		12·049	S.
Σ 656	12·2	63 4	214·8	2·96	1	8·3, 10·0	11·153	S.
Σ 659	13·0	64 49	317·1	6·14	1	8·7, 9·7	11·151	S.
Σ 676	16·0	64 39	274·6	0·96	1	7·5, 8·5	13·107	J.

Name of Star.	1910. R.A.	1910. Dec.	Position Angle.	Dist.	No. of Nights.	Mags.	Epoch 1900+.	Obs
	h m	° ′	°	″				
Σ 677	5 16·2	63 18	240·3	1·38	2	7·7, 8·0	11·080	S.
Σ 685	16·4	50 23	317·7	2·15	1	8·2, 10·0	13·107	J.
Σ 689	19·4	67 50	326·5	6·14	2	8·0, 10·0	11·152	S.
Hussey 1105 ...	21·3	62 38	242·0	3·07	1	8·5, 10·0	11·153	S.
Σ 723	27·4	51 52	103·1	4·05	1	8·4, 10·5	13 107	J.
			102·2	4·57	1		14·178	S.
Σ 720	28·0	63 27	167·1	5·75	2	8·2, 9·3	11·111	S.
OΣ 109 ...	30·0	71 35	128·9	11·00	1	7·7, 9·0	11·151	S.
Σ 739	34·4	66 30	249·4	2·24	1	8·3, 9·3	11·079	S.
			249·6	2·08	1		13·107	J.
Σ 769	38·2	53 17	175·1	4·41	1	8·0, 10·2	11·151	S.
			171·4	4·07	1		13·167	S.
			172·4	4·35	1		13·167	J.
Σ 3115 ...	39·8	62 47	14·7	1·21	3	6·7, 7·8	11·111	S.
Σ 780 AB ...	42·0	65 44	102·2	3·97	1	6·7, 7·9	11·110	S.
AC ...			151·5	11·56	1	10·2	11·110	S.
Σ 810	5 49·4	52 55	245·3	2·63	2	8·8, 9 5	11·108	S.
			245·8	2·76	1		13·167	J.
			243·2	2·78	1		14·178	S.
Σ 824	6 2·1	76 32	207·1	1·36	1	8·0, 10·0	13·167	S.
Σ 865	7·3	51 12	66·6	5·59	1	8·2, 10·3	14·178	S.
Σ 868	12·7	73 57	42·6	3·55	2	8·5, 9·0	11·075	S.
OΣ 136 ...	18·0	70 35	79·5	5·53	1	6·5, 10·3	13·167	S.
Espin 66 ...	23·3	58 31	275·7	2·58	1	9·1, 9·3	13·167	J.
Σ 916	26·4	56 43	253·5	9·42	1	8·5, 9·8	13·197	J.
Σ 918	26·8	52 32	328·7	4·10	2	6·7, 7·7	11·096	S.
			334·2	3·85	1		14·178	S.
Σ 925	30·8	67 25	88·9	3·20	2	7·8, 10·3	13·182	J.
Σ 935	31·4	52 23	323·6	3·49	2	8·2, 9·0	11·096	S.
Σ 934	31·6	55 7	331·5	4·22	2	8 7, 9·5	11·116	S.
Σ 946	36·9	59 33	130·3	3·95	3	7·2, 9·0	11·108	S.
Σ 948 AB ...	38·3	59 32	116·5	1·83	2	5·2, 6·1	11·171	S.
AC ...			306·5	8·68	2	7·4	11·171	S.
Σ 958	40·7	55 48	256·9	5·07	1	6·0, 6·0	11·159	S.
Σ 977	48·6	48 41	128·7	1·84	2	8·0, 9·5	13·158	J.
Σ 982	49·6	13 18	159·5	6·56	2	5·4, 7·7	13·143	J.
Krueger 29 .	53·0	56 59	355·2	7·93	1	9·0, 9·1	11·183	S.
			357·3	6·72	1		13·167	S.
Σ 980	54·1	72 48	190·0	3·86	1	8·6, 10·1	13·186	J.
Σ 1001 AB ...	55·8	54 19	59·1	9·32	1	7·1, 8 7	11·183	S.
Σ 1009 ...	6 58·5	52 54	152·5	3·62	2	6·7, 6·8	11·119	S.

Name of Star.	1910. R.A.	1910. Dec.	Position Angle.	Dist.	No. of Nights.	Mags.	Epoch 1900+.	Obs.
	h m	° ′	°	″				
Σ 1038 ...	7 9·0	68 42	96·5	12·54	1	7·3, 9·7	13·118	J.
Σ 1039 ...	10·3	63 41	208·3	3·08	1	8·8, 9·5	11·137	S.
			206·3	3·30	1		13·118	J.
			209·7	3·05	1		13·189	S.
Σ 1051 AB ...	15·8	73 16	282·7	1·35	3	6·5, 8·6	11·123	S.
AC ...			82·5	31·92	3	6·7	11·123	S.
Σ 1092 ...	23·1	49 18	71·9	2·72	2	8·0, 9·8	13·178	S.
			68·6	2·64	1		13·203	J.
Σ 1110 ...	28·9	32 5	219·4	5·59	1	2·7, 3·7	14·178	S.
Σ 1127 AB ...	38·0	64 19	341·2	5·49	2	6·2, 8·0	11·148	S.
AC ...			176·2	11·41	2	9·2	11·148	S.
Σ 1131 ...	42·1	71 41	177·1	2·89	1	9·3, 9·5	11·137	S.
A.G. 146 ...	51·6	50 30	281·1	3·33	1	9·1, 9·1	11·159	S.
			285·1	3·47	1		13·118	S.
Σ 1151 ...	53·4	77 2	220·2	4·03	1	8·7, 10·2	11·137	S.
Hussey 713 ...	57·5	49 33	128·8	4·93	1	9·0, 9·0	13·118	S.
			129·9	5·02	2		13·162	J.
Σ 1175 ...	7 57·7	4 24	229·4	1·38	1	7·8, 9·7	13·206	J.
			233·1	1·58	1		13·228	S.
Aitken 1075 ...	8 1·9	58 14	65·5	2·09	2	8·7, 11·0	13·200	J.
			70·2	2·35	1		13·206	S.
Espin 71 ...	6·7	53 32	282·4	3·36	1	9·0, 9·1	13·118	S.
Σ 1192 AB ...	8·3	60 40	257·2	2·75	2	6·8, 10·5	13·200	J.
AC ...			223·7	49·16	2	10·2	13·200	J.
Hussey 854 ...	16·5	65 46	209·4	1·32	1	9·2, 9·5	13·225	J.
			212·6	1·46	1		13·228	S.
Aitken 1078 ...	21·8	85 1	57·4	1·09	1	9·1, 9·2	13·242	J.
Σ 1225 ...	23·1	51 30	191·0	3·53	1	8·5, 8·5	11·183	S.
Σ 1235 ...	27·2	57 14	81·1	1·15	1	8·0, 10·0	13·228	S.
			83·1	1·13	1		13·228	J.
Krueger 30 ...	39·9	58 2	117·5	1·85	2	9·5, 9·5	13·214	J.
Σ 1271 ...	43·3	56 33	70·7	1·38	1	8·6, 9·7	13·228	S.
			71·5	1·20	1		13·228	J.
Σ 1279 ...	44·6	39 55	271·9	1·45	2	8·3, 8·3	13·137	S.
Σ 1280 ...	47·4	71 9	46·7	4·78	3	7·5, 7·6	11·171	S.
Σ 1289 ...	48·8	43 56	6·5	3·96	2	7·7, 8·5	13·143	S.
			4·1	4·07	1		14·178	S.
Σ 3120 ...	50·1	44 0	350·4	1·48	1	7·8, 8·8	13·118	J.
			350·2	1·49	1		13·156	S.
			350·4	1·79	1		14·178	S.
β 408	51·5	63 46	342·2	2·88	1	7·8, 10·3	13·242	J.

Name of Star.	1910. R.A.	1910. Dec.	Position Angle.	Dist.	No. of Nights.	Mags.	Epoch 1900+.	Obs.
	h m	° ′	°	″				
Σ 1284 ...	8 54·5	81 24	167·6	2·43	2	8·0, 9·7	13·223	J.
Hussey 721 ...	8 58·7	50 16	160·1	2·97	1	9·1, 11·0	13·203	J.
Σ 1313 ...	9 5·4	70 21	259·1	1·04	1	8·5, 8·7	13·225	S.
Σ 1305 ...	5·5	80 11	0·3	1·63	1	9·3, 10·0	13·242	J.
Σ 1318 ...	7·6	47 22	242·1	2·81	2	7·5, 8·7	13·172	S.
Σ 1321 ...	8·5	53 6	68·2	18·87	1	7·4, 7·4	13·192	J.
Σ 1340 ...	16·4	49 55	320·5	6·49	1	6·5, 8·3	13·189	S.
			318·8	6·68	1		13·192	J
OΣ 200 ...	18·7	51 57	336·1	1·68	2	6·7, 8·4	11·215	S.
Σ 1345 ...	19·7	64 44	85·7	2·92	1	8·5, 10·1	13·192	J.
Σ 1359 ...	26·5	56 39	62·1	7·94	2	8·5, 9·2	11·215	S.
Σ 1362 ..	29·0	73 29	129·1	5·10	1	7·0, 7·0	11·183	S.
Hussey 565 ..	29·6	50 28	184·5	1·71	1	8·8, 8·8	13·192	J.
			186·2	1·81	1		13·225	S.
Σ 1373 ..	36·6	77 8	134·7	1·88	1	8·2, 9·5	13·192	J.
			132·7	2·10	1		13·225	S.
Krueger 33 ...	44·5	58 38	212·4	1·96	1	9·0, 9·0	13·225	S.
Σ 1381 ...	44·7	61 3	208·2	1·31	1	8·5, 8·7	13·228	S.
Σ 1387 ...	47·7	69 22	272·2	8·95	1	9·5, 9·5	13·228	J.
Σ 1398 ...	54·3	69 10	175·4	1·66	3	7·5, 10·7	13·261	S.
			178·4	1·29	1		13·228	J.
Σ 1400 ...	9 55·8	69 13	223·1	2·60	1	7·3, 10·5	13·329	S.
			223·2	2·46	1		13·370,	J.
Σ 1408 ...	10 3·7	73 29	10·8	3·76	2	8·4, 9·2	13·277	J.
Σ 1428 ...	10 20·7	53 5	87·0	3·46	1	7·5, 7·8	13·290	J.
			86·5	3·65	2		20·217	S.
Σ 1510 ..	11 2·8	53 18	334·3	4·72	2	7·1, 8·4	20·216	S.
Σ 1523 ...	13·4	32 3	284·3	3·42	1	4·0, 5·0	20·222	S.
Σ 1553 ...	30·0	56 38	167·7	5·59	1	7·3, 7·8	11·318	W.
			167·6	5·84	2		20·216	S.
Σ 1573 ...	11 42·0	67 50	176·6	11·27	1	6·6, 7·6	11·318	W.
Hussey 1136 ...	12 1·1	63 27	223·8	1·68	1	6·0, 11·4	13·306	J.
Hussey 891 ...	9·6	78 57	10·9	2·53	2	9·0, 9·1	13·318	J.
Σ 1630 ...	13·0	56 51	168·0	2·45	2	8·3, 9·0	20·216	S.
Σ 1695 ...	52·4	54 35	285·3	3·67	1	6·3, 8·2	11·337	W.
			286·5	3·73	1		11·381	S.
			285·5	3·53	1		13·332	J.
Σ 1720 ...	12 58·8	83 25	333·8	1·65	1	8·4, 8·7	13·329	J.
OΣ 263 ...	13 12·8	51 2	130·5	2·25	1	7·7, 8·5	11·381	S.
			133·8	2·17	1		13·370	J.
Σ 1767 ...	31·5	68 13	348·6	4·41	1	8·0, 8·5	11·337	W.

Name of Star.	1910. R.A.	1910. Dec.	Position Angle.	Dist.	No. of Nights.	Mags.	Epoch 1900+.	Obs.
	h m	° ′	°	″				
Σ 1770 ...	13 34·1	51 11	118·9	2·05	2	6·4, 7·9	11·392	S.
Σ 1798 ...	13 55·2	78 50	13·2	7·78	1	7·5, 9·3	11·405	S.
Σ 1820 ...	14 10·1	55 45	82·2	2·33	1	8·2, 8·5	11·381	S.
Σ 1829 ...	12·2	50 52	150·0	5·57	2	7·7, 8·2	11·393	S.
Σ 1830 AB ...	12·8	57 5	293·1	7·02	1	8·5, 9 8	11·405	S.
Σ 1872 ...	38·4	58 21	42·8	7·74	1	7·0, 8·0	11 589	S.
Σ 1871 ...	38·5	51 46	295·9	1·90	1	7·0, 7·0	11·589	S.
Σ 1878 ...	39·8	61 38	326·9	4·07	2	7·0, 9·2	11·497	S.
			326·4	3·79	2		13·376	J.
Krueger 43 ...	45·5	62 31	213·4	2·91	1	9·7, 10·0	13·394	J.
Σ 1905 ...	14 56·2	71 12	159·1	3·40	1	8·3, 8·3	11·589	S.
Σ 1928 ...	15 9·4	72 47	275·5	6·79	1	8·5, 9·2	11·589	S.
OΣ 299 ...	15 32·6	64 12	23·9	3·68	1	7 2, 9·5	11·589	S.
Σ 2180 ...	17 26·8	50 57	263·2	3·18	2	7·0, 7·2	12·785	J.
Σ 2218 ...	17 39·7	63 43	338·0	1·89	1	6·5, 7·7	12·775	J.
Hussey 926 ...	18 9·1	64 13	268·0	4·07	1	9·1, 9·3	12·775	J.
Σ 2382 ...	41·3	39 35	11·8	3·36	2	4·6, 6·3	12·779	S.
			9·6	3·37	2		14·695	S.
			10·6	3·30	2		19·845	S.
Σ 2383 ...	41·4	39 31	122·0	2·31	2	4 9, 5 2	12·779	S.
			121·4	2·25	1		12·786	J.
			121·6	2·37	2		14·695	S.
			120·0	2·39	2		19·845	S.
Σ 2410 ...	18 45·6	59 14	95·0	1·75	1	8·2, 8·7	12·772	S.
			94·7	1·56	1		12·794	J.
Σ 2455	19 3 1	22 2	66·7	4·06	2	7·2, 8·3	12·837	S.
			69·3	3·99	1		12·786	J.
			60·4	4·24	2		19·839	S.
Σ 2461 ...	4·0	32 22	314·0	3·74	2	5·7, 9·8	12·844	S.
Σ 2576 ...	42·1	33 24	285·8	2·10	3	7·8, 7·8	12·741	J.
			286·7	2·43	2		12·735	S.
			285·1	2·21	1		14·824	B.
			279·1	1·92	2		19·845	S.
Σ 2579 ...	42·1	44 54	286·7	1·71	2	3·0, 7·9	12 790	J.
			282·8	1·98	1		12·786	S.
			288·3	1·81	1		13·772	S.
			284·0	1·77	1		14·824	S.
Hussey 684 ...	48·1	48 38	175·6	0·93	1	8·6, 8·6	13·772	S.
Σ 2603 ...	48·5	70 3	7·5	3·29	2	4·0, 7·6	14·657	B.
			9·1	3·41	2		14·657	S.
Σ 2605 ...	19 53·3	52 12	180·9	3·27	3	5·0, 7·5	12·759	J.

Name of Star.	1910. R.A. h m	1910. Dec. ° ′	Position Angle. °	Dist. ″	No. of Nights.	Mags.	Epoch 1900+.	Obs.
			184·7	3·25	2		14·672	S.
			181·9	3·50	1		14·665	B.
OΣ 392 ...	19 54·9	42 1	293·1	3·21	1	7·2, 9·0	12·901	S.
AB & C ...			290·2	3·21	2		19·845	S.
AB ...			292·0		2	7·2, 9·0	16·387	S.
Σ 2640 ...	20 3·6	63 38	20·1	5·60	2	6·0, 9·9	12·792	J.
Krueger 50 ...	15·7	57 1	134·0	2·30	1	9·0, 9·5	14·696	S.
Σ 2671 ...	16·2	55 7	339·6	3·51	2	6·0, 7·4	12·762	J.
			338·8	3·65	2		14·695	S.
Σ 2717 ...	35·9	60 26	267·5	2·09	2	7·2, 9·7	12·782	J.
			266·1	2·15	2		12·840	S.
Σ 2732 ...	46·0	51 35	75·0	4·09	3	6·7, 8·7	12·758	J.
Σ 2741 ...	55·6	50 7	35·1	2·02	1	6·0, 7·3	12·794	J.
			27·2	1·85	2		12·884	S.
			30·7	2·34	2		19 923	S.
Σ 3133 ...	55·7	61 1	101·0	3·54	2	7·4, 8·9	19·923	S.
β 68	56·6	49 52	148·0	2·00	2	8·5, 9·2	12·884	S
β 156	58·7	46 13	244·6	1·13	1	7·1, 9·4	12·882	S.
Σ 2751 ...	20 59·7	56 19	352·6	1·72	1	6·0, 7·0	12·794	S.
			352·9	1·89	1		12·808	J.
Hussey 959 ...	21 0·2	66 21	149·6	1·49	1	7·7, 9·0	12·794	J.
			154·3	1·33	2		12·838	S.
Σ 2771 ...	3·8	70 24	214·2	2·65	2	8·8, 8·8	12·882	S.
			214·7	2·79	1		12·808	J.
			215·4	2·72	2		14·821	S.
Σ 2766 ...	4·7	58 38	249·3	4·41	1	8·3, 8·5	12·775	J.
			250·0	4·82	1		14·821	S.
			249·3	5·10	2		19·923	S.
Aitken 760 ...	5·8	58 45	332·9	3 40	1	9·0, 10·5	19·887	S.
β 159 AB ...	7·4	47 19	317·4	1·25	1	6·1, 9·2	12·882	S.
Doolittle 16 ...	8·6	55 58	31·7	0·97	1	8·6, 9·1	12·882	S.
Σ 2780 ...	9·5	59 37	218·5	1·33	1	6·2, 7·2	12·882	S.
Σ 2789 ...	17·1	52 36	116·4	6·54	1	7·1, 7·1	13·851	S.
			115·7	6·56	2		14·912	S.
			116·5	6·57	1		14·915	B.
Σ 2801 ...	21·2	79 58	270·7	1·84	1	7·3, 8·0	12·813	J.
			269·0	1·89	1		12·882	S.
Σ 2807 ...	22·6	82 8	315·0	2·52	1	8·2, 8·3	12·882	S.
			317·1	2·20	2		14·703	S.
Hussey 593 ...	27·9	49 44	59·0	1·72	1	8·8, 9·0	11·887	S.
			64·8	1·68	1		12·794	J.

Name of Star.	1910. R.A.	1910. Dec.	Position Angle.	Dist.	No. of Nights.	Mags.	Epoch 1900+.	Obs.
	h m	° ′	°	″				
			60·0	1·72	2		12·841	S.
β 370 ...	... 21 29·2	52 21	326·8	3·71	1	8·5, 9·0	12·739	J.
			326·7	3·73	2		12·756	S.
Σ 2837	... 41·5	82 31	292·3	2·81	2	8·5, 9·0	12·875	J.
			291·6	2·87	2		12·884	S.
			289·2	2·83	1		14·709	S.
Σ 2827	... 41·6	63 11	203·7	5·22	2	8·5, 9·0	12·875	J.
			204·4	5·25	1		14·915	S.
			204·6	5·20	2		19·889	S.
Holden 48	... 45·4	51 11	22·3	4·75	1	8·6, 8·9	12·772	S.
			21·8	4·56	1		12·868	J.
Hussey 694	... 47·8	49 58	190·7	1·36	1	9·0, 10·0	12·882	J.
Σ 2843	... 49·4	65 19	141·4	2·08	2	7·0, 7·2	19·889	S.
OΣ 456	... 52·3	52 6	34·9	1·80	1	7·8, 8·0	12·794	S.
			29·1	1·31	1		12·832	J.
Hussey 976	... 21 58·2	62 24	39·9	1·49	1	9·0, 9·0	12·882	J.
Σ 2860	.. 22 0·4	60 25	256·6	7·92	1	7·7, 9·3	13·851	S.
Σ 2863	... 1·2	64 11	282·7	7·13	1	4·7, 6·5	11·876	S.
			280·9	7·08	3		12·759	J.
Hough 614	... 11·5	51 2	175·5	4·84	1	7·5, 10·0	13·851	S.
Σ 2909	... 24·2	−0 29	309·7	3·14	2	4·0, 4·1	12·779	S.
			307·8	3·03	1		12·786	J.
			308·7	3·15	1		13·851	S.
			304·7	3·11	2		19·830	S.
Σ 2947	... 45·9	68 5	66·3	3·87	3	7·2, 7·2	12·765	J.
			62·6	3·93	1		14·906	S.
			64·0	3·92	1		14·906	B.
			63·4	4·05	3		19·907	S.
OΣ 530	... 46·4	67 42	210·7	5·16	3	9·0, 10·0	12·910	S.
Holden 54	... 46·8	50 39	12·7	1·84	1	8·7, 8·9	12·831	J.
			14·3	1·98	2		19·871	S.
β 1332 AB	... 47·1	52 34	130·5	1·85	1	8·4, 8·6	14·887	S.
			132·5	1·56	1		14·887	B.
Σ 2950	... 47·8	61 13	306·3	2·11	3	5·7, 7·0	12·807	J.
			309·2	2·32	1		12·808	S.
OΣ 483	... 54·7	11 15	232·7	1·03	1	6·2, 7·7	19·816	S.
Aitken 193	... 57·3	46 10	178·0	1·68	2	8·9, 9·1	19·871	S.
Hussey 993	... 22 58·3	67 18	222·3	1·98	1	7·9, 10·2	12·832	J.
			220·2	1·65	1		12·832	S.
Aitken 195	... 23 0·0	48 6	20·6	1·41	1	8·5, 11·5	12·832	J.
			28·7	1·80	1		12·832	S.

Name of Star.	1910. R.A.	1910. Dec.	Position Angle.	Dist.	No. of Nights.	Mags.	Epoch 1900+.	Obs.
	h m	° ′	°	″				
Arg. 45 ...	23 0·1	46 8	16·2	3·56	2	8·5, 9·5	12·860	S.
OΣ 490 ...	6·3	56 58	297·5	1·47	1	7·2, 9·2	12·827	J.
			303·7	1·43	1		12·977	S.
Hussey 996 ...	8·3	67 6	209·1	2·59	1	8·5, 9·1	14·821	S.
Σ 2996 ...	9·2	81 20	105·9	5·12	1	8·3, 8·7	12·862	J.
			107·3	5·11	2		19 889	S.
Aitken 787 ...	10·3	68 36	18·5	2·63	1	9·3, 9·4	14·934	S.
			17·1	2·64	1		14·934	B.
Krueger 64 ...	13·6	55 13	235·1	2·07	1	9·4, 9·5	19·873	S.
Σ 3001 ...	14·9	67 37	200·0	3·01	1	5·2, 7·8	11 887	S.
			203·5	2·98	3		12·804	J.
			202·0	3·12	1		12·865	S.
Espin 108 ...	21·5	52 9	245·1	2·91	1	9·1, 9·2	14·934	B.
			245·1	2·74	2		14·935	S.
β 857	36·3	67 3	295·7	1·36	1	8·5, 8·9	12·827	J.
Σ 3049 ...	54·4	55 15	324·8	3·35	1	5·4, 7·5	11·887	S.
			325·5	3·23	3		12·799	J.
Σ 3050 ...	54·9	33 14	221·0	2·78	2	6·0, 6·0	12·822	S.
			218·1	2·29	2		12·849	J.
			220·2	2·04	1		13·851	S.
			224·1	2·37	1		14·821	S.
			223·2	2·26	1		14·821	B.
Aitken 800 ...	23 58·3	46 45	291·9	1·83	1	8·5, 8·5	14·824	B.
			291·7	1·69	1		14·824	S.
			290·5	1·58	2		19·845	S.